CHIRAL ANALYSIS OF AMINO ACIDS IN BACTERIAL SAMPLES USING LC-MS/MS.

By

TARLIKA PERSAUD B.Sc.

A Thesis

Submitted to the School of Graduate Studies

in Partial Fulfillment of the Requirements

for the Degree

Master of Science

McMaster University

© Copyright by Tarlika Persaud, October 2008.

MASTER OF SCIENCE (2008) McMaster University

(Chemistry) Hamilton, Ontario

TITLE: Chiral Analysis of Amino Acids in Bacterial Samples Using LC-MS/MS.

AUTHOR: Tarlika Persaud B.Sc. (University of Guyana)

SUPERVISOR: Dr. Brian E. McCarry

NUMBER OF PAGES: xviiii, 125

ABSTRACT

An optimized method for the chiral resolution of enantiomers of amino acids in bacterial supernatants is reported. This LC-MS/MS method is performed using a chiral Teichoplanin LC column and does not require sample clean up or chemical derivitization. This method allows for the determination of the relative amounts of the D and L enantiomers of 20 proteinogenic amino acids. The detection limits and response factors for the 20 amino acids were determined. Calibrations over three orders of magnitude showed least squares coefficient values (R^2) greater than 0.996 for eighty percent of the amino acids and greater than 0.992 for the remainder.

The amino acids and their enantiomers were identified based on their retention times and their unique Multiple Reaction Monitoring (MRM) transitions for each amino acid. L-Aspartic acid-2,3,3-d_3 was used as the internal standard.

Cultures of *Sinorhizobium meliloti* (a nitrogen-fixing soil bacterium) were grown on minimal media; thus, all amino acids were biosynthesized by the bacterium. After centrifugation, supernatants were freeze dried, reconstituted in a small volume of methanol/water with internal standard and injected onto the LC column. The amino acids detected in the bacterial supernatant and the concentrations of the enantiomers were reported as the L and D isomers respectively: arginine [L, 12.6 ± 3.1 μg/L; D, 10.1 ± 3.2 μg/L], serine [L, 7.2 ± 1.16 μg/L; D, n.d.], threonine [L, n.d.; D, 11.2 ± 2.7 μg/L] and valine [L, 15.5 ± 4.3 μg/L; D, 11.3 ± 3.7 μg/L], where the term n.d. means below detection limit.

The limits for detection for all amino acids ranged from 1.3 μg/L - 5.1 μg/L. In media with no added phosphate, the amino acid profiles changed somewhat under these stress conditions. Arginine was no longer detected while alanine and proline were now observed; the concentrations of the amino acids were: alanine [L, 7.7 ± 1.2 μg/L; D, 13.4 ± 2.5 μg/L], proline [L, n.d.; D, 8.63 ± 1.3 μg/L], serine [L, 7.6 ± 1.2 μg/L; D, n.d.], threonine [L, n.d.; D, 10.2 ± 3.2 μg/L] and valine [L, 11.6 ± 2.3 μg/L; D, 10.1 ± 3.1 μg/L]. These data represent the mean values of three independent bacterial growth experiments conducted over a 3 month period; the data came from the analysis of five separate aliquots from each growth experiment. The percent standard deviation for these data ranged from 15% to 33% and averaged 24%.

Under both the normal and stressed growth conditions of *S. meliloti* produced the L enantiomer of serine, the D enantiomer of threonine and racemic valine. While racemic arginine was observed under normal growth conditions, levels were below detection under stressed conditions; under stress conditions only the D enantiomer of proline was observed while alanine was found in 1:2, L:D ratio.

ACKNOWLEDGEMENTS

For the completion of this thesis and the research for my Masters degree, there are a number of persons to be thanked.

It would be impossible to complete my Masters degree if not for the outstanding guidance of Dr. Brian McCarry. He went much beyond his role as a supervisor and mentor and extended tremendous generosity, kindness and support to me throughout my time at McMaster University. I cannot thank him enough. My co-supervisors, Dr. Kirk Green and Dr. Britz Mc-Kibbin were also tremendously supportive. Dr. Green was always available, tolerant and patient, while working beyond his hours to provide advice and assistance at any time of the day. Dr. Britz Mc Kibbin's understanding, kindness and support was also unfaltering during my research. Dr Rahat Zaheer was of tremendous help in harvesting and preparing my bacterial samples. Without her input, my research would have been a difficult experience.

I wish to express sincere gratitude to my parents; Deoroop and Savetrie who supported me throughout the course of this degree with unwavering faith and patience. Their sacrifices for my success are far beyond that which words can ever express. I would also like to thank my sisters Sushma and Menaka, whose love, kindness and generosity made it possible for me to overcome many difficulties which threatened my degree pursuit, especially Sushma, who endured my tantrums, tears and anxieties and kept me on the path to success. Special thanks to my brother, Avinash Balbahadur whose initial assistance made a world of difference at a crucial time in my studies. I would also like thank Sreedhar Cheekoori for his friendship, guidance, support and especially for lending an ear

and helping hand to my difficulties at any hour. He helped me to keep my sanity in my darkest moments.

I would also like to thank my labmates, David Dam, Britawit Asfaw, Uwayemi Sofowote, Libia Saborido, Sujan Fernando and Catherine Amoateng.

A special note of acknowledgement goes to Mrs. Carol Dada, who opened the door and provided me with the resources I needed to move forward not just in the pursuit of this degree, but also in my life. Like Dr. McCarry, Mrs. Carol Dada went much beyond her duties and responsibilities to lend a much needed helping hand during difficult times.

TABLE OF CONTENTS

ABSTRACT ii

ACKNOWLEDGEMENTS iv

TABLE OF CONTENTS vi

LIST OF FIGURES AND SCHEMES ix

LIST OF TABLES xiii

LIST OF ABBREVIATIONS xv

1. Introduction 1

1.1 Overview 2

1.2 The Metabolome 3

1.2.1 Metabolites 3

1.2.2 Metabolomics 5

1.2.3 Metabolomic Fingerprinting (The Endo-Metabolome) 6

1.2.4 Metabolomic Footprinting (The Exo-Metabolome) 7

1.3 The Significance of Amino Acid Metabolites 9

1.3.1 The Importance of Amino Acids 13

1.4 Challenges of Metabolomic Studies 15

1.4.1 Analytical Techniques used for the Identification and Resolution of Enantiomers of Amino Acids. 18

1.5 Derivitization of Amino Acids 19

1.5.1 Direct Separation of Enantiomers 20

1.6 Chiral LC-Stationary Phase **22**

1.7 Mass Spectrometric Methods **24**

1.7.1 Mass Spectrometers 25

1.7.2 Ion Source 26

1.8 Literature Results based on Studies Done for Amino Acid Analysis by LC-MS/MS. **27**

1.9 Goals **29**

2.0 Experimental **30**

2.1 Chemicals 30

2.2 Gases and Solvents 30

2.3 Samples for Analysis **30**

2.3.1 Preparation of Sample for Analysis 32

2.4 Enantiomer Resolution: Infusions Vs Injections. **34**

2.5 Internal Standards **35**

2.6 Calibration Data **36**

2.6.1 Detection Limits 36

2.6.2 Response Factors 37

2.6.3 Quantitation 38

2.7 LC-MS/MS Analysis: Instrumentation **39**

2.7.1 Analysis Programs 40

2.7.2 Full Scan Method 40

2.7.3 MRM Programs 41

2.7.4 Deconvolution of Co-eluting peaks 43

2.7.5 Monitoring Column Performance 43

2.7.6 Ion Suppression Factors 44

2.7.7 Ion Suppression

2.8 Optimised Methodology **46**

3.0 Analytical Method Development **48**

3.1 LC-MS/MS Analytical Conditions **49**

Parent-Daughter Ion Scan:

Determination of Optimum Collision Energy

3.2 Analysis of Amino Acids Standards as Groups for Sensitive and Selective Analyses. **51**

3.2.1 Parent-Daughter Ion Scan: Verification of MRM Transitions 53

3.3 Dead Volume and Dead Time **55**

3.4 Determination of Isocratic Elution Mobile Phase Composition **59**

3.4.1 Retention Factors and Resolution. 60

3.5 Calibration Data: Detection Limits and Response Factors **62**

3.6 Infusion of Samples **63**

3.6.1 Fragmentation Patterns of Amino Acids 68

4.0 Results and Discussion **72**

4.1 Separation of Enantiomers of Amino Acids **73**

4.2 Identification of Co-eluting Peaks **76**

4.2.1 Determination of Integration Parameters 79

4.2.2 Monitoring Column Performance 83

4.3 Determination of the Degree of Ion Suppression Factor **85**

4.3.2 Ratio of Enantiomers 92

4.3.3 Determination of the Minimum Ratio for Enantiomeric Separation and Resolution of Amino Acids. 93

4.4 Data from the Exo-metabolome of *Sinorhizobium meliloti* **100**

5.0 Conclusion and Future Work **109**

LIST OF FIGURES AND SCHEMES

Scheme 1-1: The protocol followed for sample preparation prior to analysis by LC-MS/MS. 35

Figure 1-1: Genetics Research Schematic. 4

Figure 1-2: General L and D assignment of enantiomers of amino acids. 10

Figure 1-3: Structure of 20 proteinogenic amino acids. 11

Figure 1-4: Reaction of amino acids to produce a pair of diastereomers. 20

Figure 1-5: Examples of derivatizing agents and their derivatized products. 21

Figure 1-6: Structure of the Teichoplanin chiral stationary phase. 24

Table 1-3: Concentrations of amino acids found in bacterial and human samples by LC-MS/MS.

Fig 3-1: Full Scan run of *S.meliloti* grown in P0 medium. 49

Fig 3-2: Full Scan chromatographic run of *S. meliloti* in P0 media between the mass range of 0 and 200. 50

Figure 3-3: Daughter ion scan of Tyrosine, showing the dominant peak of 136 of the MRM transition 182-136. 54

Figure 3-4: Illustration depicting the calculation of dead time and retention time Of eluents. 61

Figure3-5: Calibration standard of L-lysine and internal standard, L-aspartic acid-2,3,3-d_3 64

Figure 3-6: Calibration standard of D-methionine and internal standard, L-aspartic acid-2,3,3-d_3 69

Figure 3-7: Mass Spectrum of lysine showing the fragments produced on collision with 12 eV of collision energy. 69

Figure 3-8: Mass Spectrum of valine showing the fragments produced on collision with 12 eV of collision energy. 69

Figure 4-1: Chromatogram of L/D-serine standard separated with an α value of 1.8. 73

Figure 4-2: Chromatogram showing a L/D valine standard with moderate enantioresolution. 74

Figure 4-3: Chromatogram showing a L/D serine standard showing very poor resolution. 74

Figure 4-4: Total ion chromatogram produced for an LC MS/MS run with an MRM program to identify 6 amino acids 77

Figure 4-5: Chromatogram of the 175>116 MRM transition of which corresponds to phenylalanine. 77

Figure 4-6: Chromatogram of the 166>120 MRM transition of which corresponds to arginine. 78

Figure 4-7: Chromatogram A showing poorly separated D and L enantiomers of threonine compared to Chromatogram B, in which the D and L enantiomers are clearly separated. 78

Figure 4-8: The difference between an automated integration (Chromatogram A) versus a manual integration (Chromatogram B). 80

Figure 4-9: Chromatogram A shows a fully resolved separated pair of D/L enantiomers of arginine under standard LC-MS/MS conditions compared to a partially resolved pair of enantiomers in Chromatogram B. 81

Figure 4-10: Deconvolution of overlapping peaks of the D and L enantiomers of valine. 82

Figure 4-11: Chromatogram showing the resolution of the enantiomers of 2,4-dimethylphenyl hydantoin. 83

Figure 4-12: Changes in column performancedemonstrated by an L-valine standard run under optimal LC-MS/MS conditions. 84

Figure 4-13: Calibration plot of an LC-MS/MS run of L-alanine, a neutral amino acid. 87

Figure 4-14: Calibration plot of an LC-MS/MS run of L-aspartic acid, an acidic amino acid. 88

Figure 4-15: Calibration plot of an LC-MS/MS run of L-phenylalanine, a neutral amino acid. 89

Figure 4-16: Calibration plot of an LC-MS/MS run of L-arginine, a basic amino acid. 89

Fig 4-17: Ratio of five enantiomeric amino acid standards run in a single MRM program. 93

Figure 4-18: Chromatogram of D-valine and L-valine enantiomers run separately before being combined. 94

Figure 4-19: Chromatogram showing a 60:40 ratio of L:D enantiomers of valine 95

Figure 4-20: Chromatogram showing a 70:30 ratio of L:D enantiomers of valine. 96

Figure 4-21: Chromatogram showing a 90:10 ratio of L:D enantiomers of valine. 96

Figure 4-22: Chromatogram showing a 40:60 ratio of L:D enantiomers of valine 96

Figure 4-23: Chromatogram showing a 20:80 ratio of L:D enantiomers of valine. 97

Figure 4-24: Chromatogram showing a 30:70 ratio of L:D enantiomers of valine 97

Figure 4-25: Chromatogram showing a 10:90 ratio of L:D enantiomers of valine 98

Figure 4-26: Chromatogram showing a 5:95 ratio of L:D enantiomers of valine

Figure 4-26': Figure 4-26': Correlation between % L enantiomer injected and percent L enantiomer detected. 98

Figure 4-27: Chromatogram showing only D-threonine in a P0 exo-metabolomic sample of *Sinorhizobium meliloti.* 100

Figure 4-28: Chromatogram showing D/L-valine in a P0 exo-metabolomic sample of *Sinorhizobium meliloti.* 101

Figure 4-29: Chromatogram showing only D-proline resolved from a P0 exo-metabolomic sample of *Sinorhizobium meliloti.* 102

Figure 4-30: Chromatogram showing only D/L-alanine resolved from a P0 exo-metabolomic sample of *Sinorhizobium meliloti.* 102

Figure 4-31: Chromatogram showing only L-serine resolved from a P0 exo-metabolomic sample of *Sinorhizobium meliloti* 102

Figure 4-32: Chromatogram showing the L-aspartic acid-2,3,3-d_3 standard run in a solution of 50:50 methanol/water. 103

Figure 4-33: Chromatogram showing L-serine resolved from a P2 exo-metabolomic sample of *Sinorhizobium meliloti* 103

Figure 4-34: Chromatogram showing L-threonine resolved from a P2 exo-metabolomic sample of *Sinorhizobium meliloti* 104

Figure 4-35: Chromatogram showing D/L-valine resolved from a P2 exo-metabolomic sample of *Sinorhizobium meliloti* 104

Figure 4-36: Chromatogram showing D/L-arginine resolved from a P2 exo-metabolomic sample of *Sinorhizobium meliloti* 105

LIST OF TABLES

Table 1-1: Table showing the essential and non essential amino acids in humans. 9

Table 1-2: Table showing the short term, letter code and polarity of each amino acid 12

Table 1-3: Conc. of amino acids found in bacterial and human samples by LC-MS/MS. 28

Table 2-1: Composition of the growth media 31

Table 2-2: Dry Weight, Reconstitution Volume and Concentration Factor of Growth Media. 33

Table 2-3: Dry Weight of 10ml growth medium, Volume of MeOH/H_2O and volume of internal standard added prior to LC-MS/MS analysis 33

Table 2-4: Chiral column properties used for chiral separation of enantiomeric amino acids in the supernatant of *S. meliloti*. 40

Table 2-5: Mass Spectral transitions for 20 amino acids. 42

Table 3-1: Effect of different collision energies on the peak of the protonated molecular ion of 19 amino acids. 53

Table 3-2: MRMs determined based on literature reports. 55

Table 3-3: MRM transition programs separated into groups and sub groups for sensitivity comparison. 57

Table 3-4: k' and α values for the D and L enantiomers of the 20 amino acids 60

Table 3-5: Detection Limits of 20 enantiomeric amino acids in methanol:water and P0 growth media. 66

Table 3-6: Detection Limits of 20 enantiomeric amino acids in P2 and P40 growth media. 67

Table 3-7: The fragments for each amino acid and the corresponding losses 70

Table 4-1: The effect of changing mobile phase composition of methanol:water on the α values. 75

Table 4-2: Difference in integration areas of peaks in Chromatograms A and B of Figure 4.8. 81

Table 4-3: Ion Suppression Factors of amino acids in three concentrated growth media; $P0_{(40)}$, $P2_{(100)}$ and $P40_{(121)}$. 90

Table 4-4: t-test results growth media P0, P2 and P40. 91

Table 4-5: Ionic strength of three different growth media; P0, P2 and P40. 92

Table 4-6: The mean concentrations of the D and L enantiomers of the amino acids detected in the sample of extracellular supernatant of *Sinorhizobium meliloti* grown in P2 growth medium. 107

Table 4-7: The mean concentrations of the D and L enantiomers of the amino acids detected in the sample of extracellular supernatant of *Sinorhizobium meliloti* grown in P0 growth medium. 107

Table 4.8: Detection limits of amino acids detected in *Sinorhizobium meliloti* *108*

LIST OF ABBREVIATIONS

CE	capillary electrophoresis
Chirobiotic T	Chirobiotic Teichoplanin
k'_L	capacity factor of the levorotatory enantiomer
k'_D	capacity factor of the dextrorotatory enantiomer
LC	liquid chromatography
MOPS	3-(N-morpholino) propanesulfonic acid
MRM	multiple reaction monitoring
MS	mass spectrometry
P0	phosphate starved growth medium (0 mM phosphate)
P2	growth medium with 2 mM phosphate
P40	growth medium with 40 mM phosphate
$P0_{(40),}$	growth medium with 0 mM phosphate concentrated 40 fold
$P2_{(100)}$	growth medium with 2 mM phosphate concentrated 100 fold
$P40_{(121)}$	growth medium with 40 mM phosphate concentrated 121 fold
R^2	least squares correlation coefficient values
RF	response factor
α	selectivity factor
TIC	total ion chromatogram

1. Introduction

Within the human body, there are an estimated 30,000 to 40,000 genes, 99.9% of which are the same for every human being. However, the remaining 0.1% which is different determines the genetic variations of that individual, allowing for the assessment of a person's predisposition to disease, drug treatment and disorders unique to them or their family [1]. There are three main classifications under which research is done for a more comprehensive understanding of genes and the factors related to them. These classifications, all of which had their terms coined as a consequence of the Human Genome Project, are proteomics; where the objective is primarily identifying abnormal protein patterns, genomics, the study of an organism's entire genome including intensive efforts to determine the entire DNA sequence of organisms. The field also includes studies of intragenomic phenomena while metabolomics is aimed at the identification of metabolites and their patterns [2].

Within the study of metabolomics, several different bioinformatics approaches are utilized along with different analytical protocols which include techniques such as NMR, mass spectrometry coupled to GC, HPLC, CE etc. Metabolic studies can be achieved by measuring the biochemical constituents, excretion products, precursor-product relationships, changes which occur as a result of nutrition by way of diet and inhalation; sub-threshold changes of metabolic precursors etc [3]. These measurements allow for an understanding of not only the composition of the metabolome but the effect of different environments (chemical and physical) on these systems. These measurements allows for

the identification of biomarkers and classifications for disease and disorders, functional genomics, identification and understanding of the mechanism of disease and therefore drug development coupled with personalized medicine and preventative nutrition [4, 5].

1.1 Overview

The intra and extra-cellular compositions of bacterial cells can be studied in a multitude of ways, utilising a variety of biochemical and analytical techniques in order to answer an invariable number of questions. One such bacterium is *Sinorhizobium meliloti (S. meliloti). S. meliloti* is quite amenable to genomics research having a multipartite genome with a size of approximately 6.6 Mb [6, 7].

The characteristic feature of *S. meliloti* is its ability to induce the formation of nodules on the roots of leguminous plants, namely *Medicago, Melilotus and Trigonella sp.* Inside of these nodules, bacteroids, which are differentiated bacteria fix atmospheric nitrogen (i.e. reduces N_2 to form NH_3) which is of significant benefit to the plants since it can then be utilised to produce proteins. In return, the plants provide a carbon and energy source for the bacteria. The bacterium enters the root tissue by way of infection threads which then form growths (nodules) on the roots of these plants. There are a number of host plants which enjoy this symbiotic relationship with *S. meliloti*, one of the more popular ones being the diploid and autogamous lucerne *Medicago truncatula* [8]. By harvesting this bacterium, it is possible to probe and examine the contents of its exo and endo metabolome by investigating its extra and intracellular composition [5, 9].

1.2 The Metabolome

The metabolome can be defined as a quantitative set of low molecular weight metabolites or small molecule metabolites such as amino acids, sugars, lipids and carbohydrates in the form of hormones, metabolic intermediates, signalling molecules etc. which exist in a biological sample such as a single cell organism (the cell) under a given set of physiological conditions. The metabolome is dynamic and undergoes continual change with time [10,11].

Within this system, the genome gives rise to the transcriptome, which in turn gives rise to the proteome which acts on the metabolome, comprising endogenous (intracellular) and exogenous (extracellular) molecular subsets of an organism. Within this system, there are feedback interactions at every different level. At all of these levels, especially that of the metabolome, there are perturbations on account of many different factors such as the environment, toxins, nutrition etc, which would give a representation of the physiological status of the organism at that period [11, 12].

1.2.1 Metabolites

Metabolites are the products or intermediates of cellular metabolism and can be classified as either primary metabolites, which are directly involved in growth, development and reproduction, or secondary metabolites, which are indirectly involved in these processes. There are an estimated 3000 identified metabolites which are vital in terms of growth, development and reproduction while there remain thousands of unidentified secondary metabolites which are important in forming defences against

Figure 1.1 Genetics Research Schematic

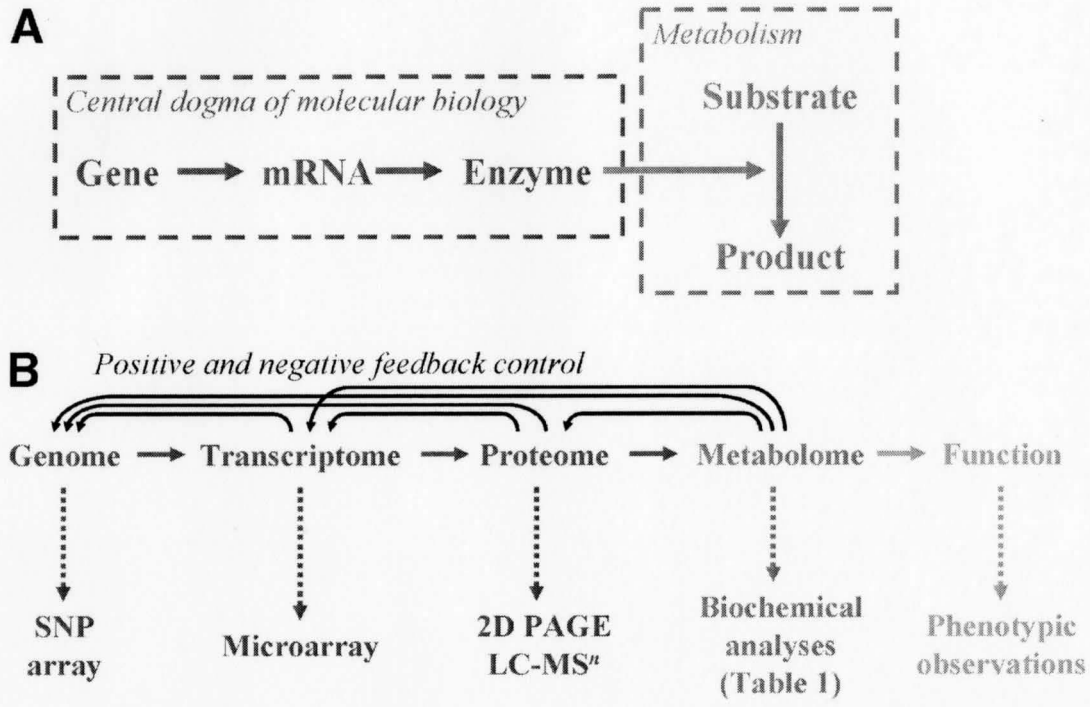

disease, stress and disorders, such as metabolic disorders, which lead to serious, debilitating diseases which are extremely difficult to diagnose [13-15].

Monitoring the way in which metabolites change along with changes in their concentrations can allow unique profiles or patterns to be identified. This can be used directly for monitoring the profile changes that occur during disease, for diagnosis and also during drug treatment [16].

1.2.2 Metabolomics

Metabolomics therefore refers to the quantitative study of the dynamic multi-parametric metabolic response of living systems to genetic modifications or pathophysiological stimuli. In metabolomic studies, there are two main common research characteristics. The first involves the characterization of the relationship which exists between the metabolites, possibly within a certain group or class, while the second involves profiling the metabolites without specific bias towards any particular group(s) [7, 17, 18].

Research in metabolomics is therefore aimed presently at providing a description of metabolic pathways and the ways in which they change. The concentration of intermediary metabolites is a function of the enzymatic reactions which occur and are dependant upon the available substrates, products and modifiers which are present at that instance in time. Consequently, the metabolome is much more sensitive to perturbations than the proteome, genome and transcriptome. Changes which occur in the metabolome are transferred to and over-expressed in the genome, transcriptome and proteome thereby allowing a picture of these three to be available upon the study of the metabolome only [19].

The advantages associated with metabolic studies are of tremendous importance with phenomenal applicability towards disease identification and monitoring as well as for drug treatment and drug discovery. Early detection of diseases can be made possible while the diagnosis of difficult disorders; metabolic disorders, can be effectively identified. There can be a much greater degree of specificity associated with the use of

certain drugs by target patients in order to maximise the benefits derived. Additionally, assessment of treatment procedures can be done in order to understand their suitability towards the patient [20, 21].

1.2.3 Metabolomic Fingerprinting (The Endo-Metabolome)

Metabolic processes can be affected by environmental conditions, mutations, natural variations etc. Metabolite fingerprinting is an approach that attempts to answer questions about what metabolites are present and in what concentration at the time of an analysis. In order to analyse and understand the link between the characteristics of an organism and the link between these intricate factors, there needs to be a large number of analyses which can be achieved by any given technique [22].

Metabolic fingerprinting is based on technology which provides information from the spectra obtained through a particular method, for the determination of total composition and identity. Spectroscopy, NMR and other high throughput methods are usually used. Metabolomic fingerprinting therefore is involved in sorting datasets into categories so that questions about individual samples and their classifications can be answered [12, 23].

Metabolomic fingerprinting analyses are done by examining the 'intracellular' composition of cells (usually bacterial samples such as *E. coli, Sinorhizobium meliloti* etc.). Examining the components of the inside of the cell allows for an understanding of the 'metabolites' present in the 'metabolome'. The advantages of using fingerprinting techniques include the ability for high-throughput, rapid analyses which allow attention to

be focused on that area of the spectra of most relevance to the particular study [24]. However there are several disadvantages on account of the variability of the metabolic composition of the samples. It is also often difficult or even impossible to identify the metabolite(s) responsible for this variability [25].

Performing analyses for the monitoring and measurement of intracellular metabolites can be time consuming and could require rapid quenching of the metabolism as a result of rapid changes of the metabolism in the range of microseconds [26]. The methods for these analyses therefore need to be capable of rapidly quantifying and detecting a tremendous number of metabolites with widely differing concentrations [27]. There is an incredible turnover of metabolites and transformations within the intracellular samples which can make their monitoring a challenge.

1.2.4 Metabolomic Footprinting (The Exo-Metabolome)

Subsequent to the utilization of metabolite fingerprinting techniques, another novel approach, metabolite footprinting [28], was devised in an attempt to overcome the difficulties associated with the rapid transformations within the sample matrix. This approach is based on the measurement of metabolites through their secretion products into their growth medium (extracellular supernatant or exometabolome) rather than by the intracellular matrix [29-32]. This approach also allows for an investigation into the functional analysis and characterization of cells by utilizing their metabolome. It allows monitoring of the intracellular metabolites by 'overflow' metabolism in the medium of choice, thus giving the capability to probe, inhibit and stress the organism as desired [27].

The excretion of the metabolites can be probed in different ways, such as by altering the available carbon source. This can assist in monitoring active metabolic pathways and the resultant response to induced stress factors such as phosphate starvation, or other additive increases or decreases in the growth medium [33]. Active sites within metabolic pathways can be monitored by introducing inhibitors into the medium while the mode of action and metabolite profiles can be determined for gene knockout strains by the use of growth inhibitors [34]. There is a direct link between the operational metabolic pathways and the changes which occur in the secretions in the extracellular matrix. For the majority of metabolic footprints of organisms, having a single gene knockout results in a marked difference in the profile of metabolites exhibited in the extracellular medium. The function of genes with unknown functions can therefore be inferred based upon calibrations of knockout genes of known, determined function [35-37].

Metabolite footprinting therefore allows for physiological level characterization of micro organisms which could be amenable to higher organisms. It provides a tool that can be used to obtain reproducible, simple, high throughput analyses of different aspects of the genome [38]. The methods which are usually used for monitoring the profiles and changes in the exometabolome include CE-MS, LC-MS and GC-MS.

The main advantage which metabolite footprinting presents over metabolic fingerprinting is the ability to examine the intracellular composition/metabolites without having to quench the metabolism or separate the metabolites from the intracellular space.

The technical problems of having rapid changes in the sample medium in the range of milliseconds are also significantly minimised [36].

1.3 The Significance of Amino Acid Metabolites

Amino acids are divided into two classes depending on whether they can be synthesised in the human body or whether they must be supplied in the diet. The former group are referred to as non-essential and the latter group as essential [39].

Table 1-1: Table showing the essential and non essential amino acids in humans.

Non Essential	Essential
Alanine	Arginine
Aspartic Acid	Histidine
Aspartate	Isoleucine
Cysteine	Leucine
Glycine	Lysine
Glutamic Acid	Methionine
Glutamine	Phenylalanine
Proline	Threonine
Serine	Tryptophan
Tyrosine	Valine

Most amino acids are chiral and the determination of the ratios of their enantiomers have tremendously important roles in various areas such as metabolomic studies (metabolomic fingerprinting, footprinting etc.), determination of gene functions, pharmacology, protein/peptide analysis, geological dating, food chemistry and many other areas [40].

All amino acids found in proteins occur in the L-configuration about the chiral carbon atom. An example of the stereochemistry of an amino acid is given, along with the structures of the 20 proteinogenic amino acids [41]:

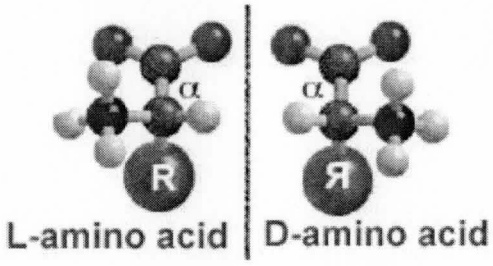

Figure 1-2: General L and D assignment of enantiomers of amino acids [80].

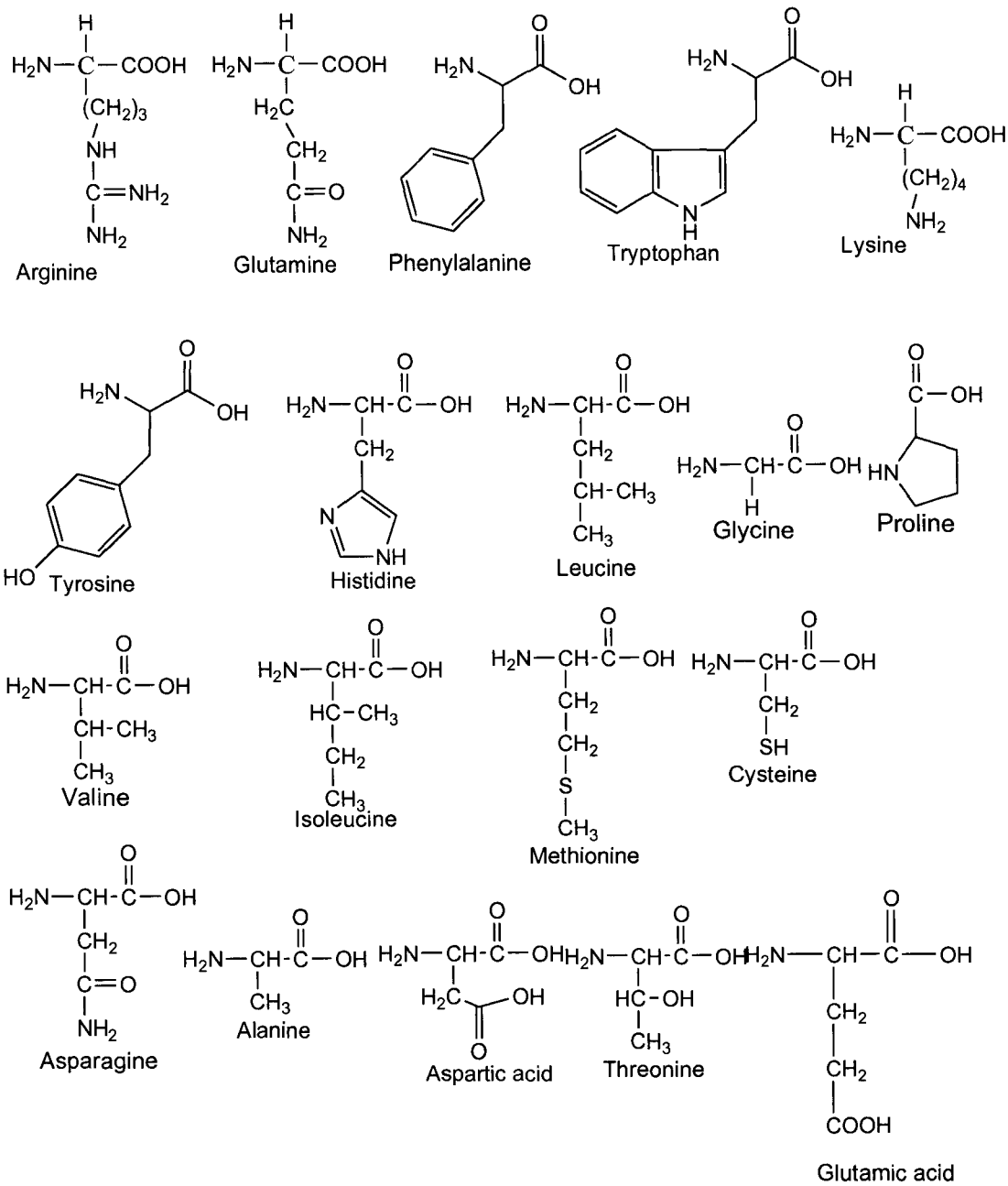

Figure 1-3: Structure of 20 proteinogenic amino acids.

Table 1-2: Table showing the short term, letter code and polarity of each amino acid.

Amino Acids	Short Term	Letter Code	Polarity
Alanine	Ala	A	Neutral
Arginine	Arg	R	Basic
Asparagine	Asn	N	Neutral
Aspartic Acid	Asp	D	Acidic
Cysteine	Cys	C	Neutral
Glutamic Acid	Glu	E	Acidic
Glutamine	Gln	Q	Neutral
Glycine	Gly	G	Neutral
Histidine	His	H	Basic
Isoleucine	Iso	I	Neural
Leucine	Leu	L	Neutral
Lysine	Lys	K	Neutral
Methionine	Met	M	Neutral
Phenylalanine	Phe	F	Neutral
Proline	Pro	P	Neutral
Serine	Ser	S	Neutral
Threonine	Thr	T	Neutral
Tryptophan	Trp	W	Neutral
Tyrosine	Tyr	Y	Neutral
Valine	Val	V	Neutral

Amino acids form the basis for the structure of proteins. By the process of translation, mRNA templates are formed, which are important for protein biosynthesis. Non proteinogenic amino acids, which are formed by post translational modifications in protein synthesis, are important for the efficient functioning of the proteins in processes such as carboxylation of glutamate, the hydroxylation of proline etc [42].

With regards to the twenty proteinogenic amino acids, which encode the standard genetic code, the L-enantiomer is the more abundant, naturally occurring species. The D-amino acids are less common, with its existence being more dominant in exotic sea

dwelling organisms and the peptidoglycan cell walls of bacterial. D-amino acids have been considered as unnatural amino acids and it has been the common belief that D-amino acids are not present in eukaryotes [43-45]. However, improvements and developments of analytic methods over the past decades have clearly demonstrated that the D enantiomer of amino acids are present in a considerable amount of eukaryotes and even in humans (teeth cavities, brain tissue and gum tissue) [46]. Some of these D-amino acids have even been shown to play essential roles in several physiological functions [47].

1.3.1 The Importance of Amino Acids

The utility and importance of a few amino acids is briefly discussed in order to point towards the importance of having methods which would allow for accurate and efficient identification and quantification of their enantiomers [46, 48].

Aspartic acid an endogenous amino acid present in vertebrates and invertebrates plays an important role in the neuroendocrine system, as well as in the development of the nervous system. During the embryonic stage of birds and the early postnatal life of mammals, a transient high concentration of D-asp takes place in the brain and in the retina. D-asp also acts as a neurotransmitter/neuromodulator. This amino acid has been also detected in synaptosomes and in synaptic vesicles, where it is released after chemical (K^+ ion, ionomycin) or electric stimuli. In the endocrine system, D-asp is involved in the regulation of hormone synthesis and release. For example, in the rat hypothalamus, it enhances gonadotropin-releasing hormone (GnRH) release and induces oxytocin and vasopressin mRNA synthesis. In the pituitary gland, it stimulates the secretion of the

following hormones: prolactin (PRL), luteinizing hormone (LH), and growth hormone (GH) In the testes, it is present in Leydig cells and is involved in testosterone and progesterone release. Thus, a hypothalamus–pituitary–gonads pathway, in which D-Asp is involved, has been formulated [49].

Tyrosine is a precursor of the neurotransmitters Norepinephrine and Dopamine, both of which regulate mood, cognition and behavior. This amino acid has been proposed as a natural and safe treatment for various conditions in which mental function is impaired or slowed down, such as chronic fatigue or depression [50].

L-tyrosine is known as the 'antidepressant' amino acid because it appears to have a mild stimulatory effect on the central nervous system. It has a mild antioxidant effect, binding up free radicals that can cause damage to the cells and tissues, and is useful in smokers, or those exposed to chemicals and radiation. L-tryptophan aids in the functions of the adrenal, thyroid and pituitary glands. This specific amino acid is easily converted into thyroid hormone, or thyroxin, which plays an important role in controlling metabolic rate, skin health, mental health, and growth rate. Tryptophan is specifically used to treat depression because it is a precursor for those neurotransmitters that are responsible for transmitting nerve impulses and essential for preventing depression [49].

The optimum amino acid balance in the body/mind is an essential and often critical component of our mental health state. Neurotransmitters are 'manufactured' in the brain from amino acids. A deficiency of any single nutrient can alter brain function and lead to depression, anxiety, and other mental disorders.

In the case of cancer, these cells perform two simultaneous tasks in order to defend themselves while trying to establish a tumor. The cells take in the amino acid which makes immune system cells unable to attack, and they also release a toxin which kills immune system cells which come too close [51].

Over the past decade, there has been an increased level of applications utilising tandem mass spectrometry in studying inborn errors of metabolism, including the study of individual groups of these metabolites such as amino acids, organic acids, puridines, pyrimidines and fatty acid (oxidation). With the screening of amino acids in their native state, their chiral resolution could potentially allow for the identification of neonatal disorders of inherited amino acid disruption. This direct screening approach has been utilised and successfully applied to the diagnosis of phenylketonuria, maple syrup urine disease, homocystinuria and a range of other diseases using metabolite markers such as amino acid butyl esters [52].

1.4 Challenges of Metabolomic Studies

There are many challenges which exist in metabolomic studies which are far outweighed by the potential benefits and usefulness of such research. One of the main issues and difficulties is the nature of the sample itself. The stability and variability of the sample plays a huge role in the analysis. The rapid turnover and susceptibility of the metabolites within the sample to environmental factors, influences the way in which analyses can be done and also the reproducibility associated [37, 53]. Additionally, the

level of complexity of biological samples is tremendously vast in the range of tens of thousands [34, 54].

There is no current knowledge regarding the exact number of metabolites present in any organism since there are amino acids, organic acids, lipids, fatty acids along with a variety of other metabolites present at any given time in varying concentrations. However, compared to the number of genes, mRNA species or proteins, these endogenous molecules are of a significantly smaller number [55]. The fact that the metabolome is one of the fastest systems to respond to changes or stimuli, could potentially be a problem in terms of sample stability and reproducibility, but it can also be seen from a positive point of view in that the most recent picture of the organism's activity can be obtained in a snap shot. Since the metabolome is the fastest system to react to stimuli or to change it enables the most current view to be possible for the organism [27, 56].

Sample clean up for metabolic studies also poses its own challenge since the stability of the sample is low. All cleanup procedures need to be done either before storage, or after storage, prior to analysis. This affords the sample sufficient exposure to the environment to effect changes within the composition. High throughput measurements and methods are therefore necessary for metabolic studies such as GC-MS, LC-MS, CE-MS and NMR studies. Each analytical platform presents its own unique advantages and challenges. Methods employing the use of GC-MS offer both high throughput capability and automated analysis with quite good to moderate sensitivity [57], but is limited to volatile samples. NMR offers non destructive analysis and the

ability to look at intact tissue, while offering high throughput analyses. However, this method suffers from poor sensitivity. HPLC offers high sensitivity and precision but may be low throughput [58].

Capillary electrophoresis (CE) encompasses a family of related separation techniques that use narrow-bore fused-silica capillaries to separate a complex array of large and small molecules. High electric field strengths are used to separate molecules based on differences in charge, size and hydrophobicity. Depending on the types of capillary and electrolytes used, the technology of CE can be segmented into several separation techniques.

In general, CE should be considered first when dealing with highly polar, charged analytes. CE excels in the analysis of ions when rapid results are desired, and has become the predominant technique for the analysis of both basic and chiral pharmaceuticals. The advantages of using this technique include that the equipment needed is quite inexpensive, while having the capacity to perform analyses on small samples in a rapid automated way. It also provides high separation efficiency. However, it suffers from the disadvantage of being unable to identify or analyse neutral compounds, have no shape discrimination and also suffer from Joule Heating. The limits of detection tend to be quite high compared to LC and GC methods [59].

HPLC is a universal separation technique that is capable of separating both volatiles and non-volatiles without the need for derivatization [60].

Liquid chromatography (LC)-MS is the preferred technique for the separation and detection of the large and often unique group of semi polar secondary metabolites in

plants. Specifically, high resolution accurate mass MS enables the detection of large numbers of parent ions present in a single extract and can provide valuable information on the chemical composition and thus the putative identity of large numbers of metabolites [61].

When analyzing samples which are polar and/or non volatile, the technique of choice is usually LC-MS. Gas chromatography mass spectrometry (GC-MS) would remain the choice method for the detection and quantification of pharmaceuticals and samples of a volatile nature, and thus non volatiles naturally fit better with LC-MS analysis. CE-MS may also be strongly considered for analyses of non volatile compounds, as this technique is suited towards the analysis of highly polar, ionic compounds. However, the poor sensitivity and lack of robustness in complex mixtures in CE-MS allows LC-MS to be the method of choice for complex biological samples, such as bacterial supernatant, and is not necessarily a valid substitute for LC-MS for comparable or better results. Additionally, if this is coupled to tandem mass spectrometry (MS/MS), there are the inherent advantages of increased sensitivity and selectivity along with the advantages of being able to better identify and confirm the identity of analytes in a sample [59].

1.4.1 Analytical Techniques used for the Identification and Resolution of Enantiomers of Amino Acids.

In order to understand the diverse, vital nature of enantiomers of amino acids in living organisms, it is necessary to separate them in order to make quantifications

possible. The method by which we resolve these amino acids can be done either directly or indirectly [62].

Direct methods involve using a chiral stationary phase (such as teichoplanin) or a chiral mobile phase additive which would resolve the chiral moieties directly. Indirect methods however involve derivatizing the mixture with a chiral agent to form the diastereomers, then separating these diastereomers which would then be detected [63].

There are a variety of analytical techniques available for amino acid analysis and their corresponding enantiomers in different matricies. These analyses require methods which provide a high degree of sensitivity, selectivity and reproducibility coupled with the capability of being robust and rapid.

1.5 Derivitization of Amino Acids

While the separation of amino acids can be achieved in a variety of ways, the separation of their enantiomers is usually achieved by derivitization with any number of available chiral derivitization agents to form diastereomers which are then subsequently separated and detected. The derivitizations can be performed either on columnor pre column and offer a high degree of selectivity and sensitivity. These derivitizations follow either clean up techniques or are performed directly on native samples. The choice of the derivitization agents is of crucial importance since it needs to fulfil a variety of requirements. The agent needs to be stable, give rapid reaction in high yield at low temperatures and be able to produce derivatives which are sufficiently stable [64].

There are a tremendous number of such derivitization agents, each with its own specifications and preferred method of detection.

A list of some of these reactions is provided in Figure 4 along with a schematic of the formation of diastereomers using derivatizing agents in Figure 3 [64, 65].

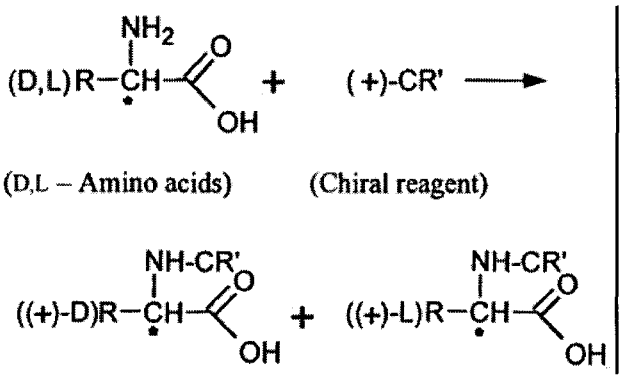

Figure 1-4: Reaction of amino acids to produce a pair of diastereomers.

Methods based on derivitization can often be confounded by reagent interferences, derivative instability and are time consuming in terms of preparation and analysis [65, 66].

1.5.1 Direct Separation of Enantiomers

Direct enantiomeric separation techniques such as the use of chiral selectors can also be employed. In this application, the chiral selector (such as crown ethers, cyclodextrins and their derivatives, chiral polymers etc) is added to the background electrolyte (as in the

case of CE) for interaction to occur between the chiral selector and the enantiomer. The enantiomer and the complex then forms diastereomeric pairs which may have differing stability constants and thus different effective mobilities for the two enantiomers.

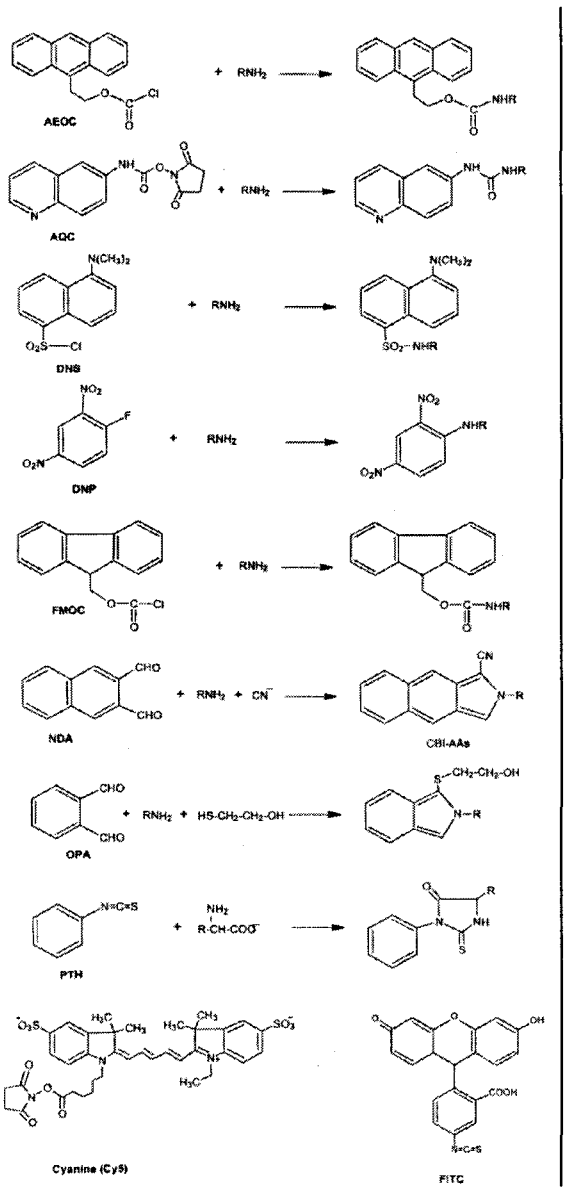

Figure 1-5: Examples of derivatizing agents and their derivatized products.

The choice of chiral selector therefore is of great importance for the subsequent separation of the diastereomers formed. For this application in HPLC, the chiral selector may be used in either the mobile phase or as the stationary phase and conditions such as pH may be altered for the effective separation of the resultant diastereomers. A number of other separation techniques which could be employed include gas chromatography and capillary electrophoresis. These can be coupled with a multitude of detection techniques such as fluorescence, UV absorbance and mass spectrometry [64-66].

Direct methods are preferred to indirect methods not only because it is much more rapid and less time consuming, but they also have advantages when there are enantiomeric impurities, for kinetic discrimination, and for the minimization of racemization issues. The errors associated with derivative instability, side reactions and reagent interference are minimised [67].

The fastest and most efficient method available for the separation of amino acid enantiomers is the use of chiral stationary phases via chiral columns. Since enantio-recognition occurs directly between the enantiomers of the amino acids and the chiral stationary phase, the step of forming diastereomers is eliminated and there is no need for using derivatizing agents or chiral selectors [68].

1.6 Chiral LC-Stationary Phase

The use of chiral HPLC columns eliminates the need for derivitization of enantiomers in order to produce the diastereomers which are then separated. Specific columns are available tailored to the enantiomer resolution of different classes of

compounds. The Chirobiotic T (Teichoplanin) column, developed by Astec, is designed specifically for the separation of the enantiomers of amino acids. Teichoplanin is a macrocyclic glycopeptide (antibiotic) which is naturally produced by the *Actinoplanes teicomycetus* mildew with molecular weights ranging between 1500 and 1900. This oligophenolic glycopeptide has been used to resolve a variety of neutral and negatively charged compounds but specifically those of underivatized α, β, γ or cyclic amino acids [76]. Separations normally obtained on chiral crown ethers or ligand exchange phases are also possible on the Chirobiotic T stationary phase.

There are several unique characteristics of the teichoplanin molecule that are involved in the amino acid interactions. The first main feature of teichoplanin is the aglycone 'basket' within the structure which has apolar character. The aglycone has the form of a semi rigid basket with four fused macrocyclic rings. It has seven aromatic rings, two of which have chlorosubstituents and four of which have phenolic moeties. The aromatic rings are linked by six amido groups and three ether groups. Within the aglycone basket, there is a single carboxylic acid group with cationic tendancies and a single primary amine with anionic tendancies. This characteristic controls the teichoplanin zwittweionic charge at pH values between 3 and 8. The central basket has three carbohydrate moieties consisting of two D-glucose amines and one D-mannose [77].

These strong charge-charge interactions are responsible for the net behaviour of the amino acids. Several factors can affect their resolution such as mobile phase pH. Also, each R group of the amino acids affects the selectivity and the retention of each amino acid.

The chiral recognition of the amino acids on the teichoplanin stationary phase is based on dipole-dipole interactions, hydrophobic interactions, π- π interactions, hydrogen bonding, stearic repulsions and ionic or charge-charge interactions, though the exact mechanisms of chiral recognition and resolution are yet to be formalised [78].

The structure of the teichoplanin is shown below with the active sites being pointed at.

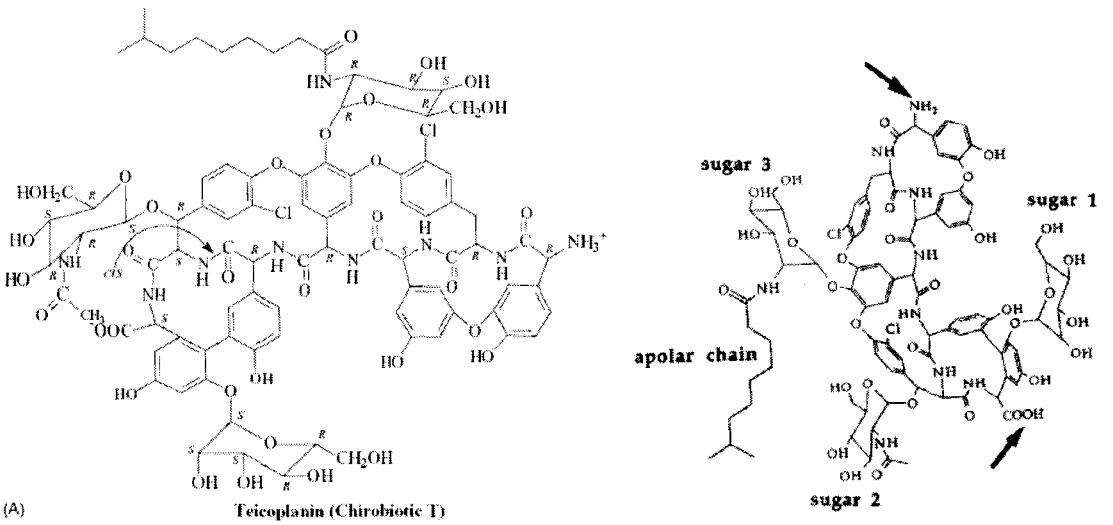

Figure 1-6: Structure of the Teichoplanin chiral stationary phase.

1.7 Mass Spectrometric Methods

The analytical technique of mass spectrometry utilises the mass to charge ratio of charged particles of a compound or sample as the basis of its ability to identify the chemical composition of that sample. After the sample is fragmented into charged particles, they are separated via movement through an electric and magnetic field, allowing for the measurement of the mass and charge of the charged particles. The basic design of a mass spectrometer employs an ion source; in which the sample is converted

into ionized fragments, a mass analyzer; in which electric and magnetic fields allow for the separation based on mass and charge, and finally, the detector which detects the resultant ions, and provides data for other processing [72].

1.7.1 Mass Spectrometers

After the sample is ionized, there are a range of mass spectrometers which could be employed. These include sector instruments, quadrupole instruments, time of flight instruments, quadrupole time of flight instruments; ion trap instruments and fourier transform ion cyclotron resonance mass spectrometers. Sector instruments such as the double focusing sector instrument offer the advantage of having high resolution (~60,000) and a high degree of accuracy while providing a large dynamic range of about 10,000. However, the sector instruments offer quite poor resolution unless interfaced with multiple analysers which are very expensive. The greatest drawback of this instrument for our purposes in particular, is the difficulty in interfacing with the electrospray ionisation ion technique. On the other hand, the quadrupole ion trap can be easily interfaced with ESI and is quite inexpensive [72-74].

The disadvantages associated with this instrument include low accuracy, low resolution, low mass range, and mass shifts which may be caused by space charging. For the time of flight instruments, the linear TOF suffers from similar disadvantages of having low accuracy and resolution while providing a superior, high mass range with fast scan times. One of the greatest drawbacks of this method for our purposes however is the inability to perform MS/MS analyses. With the use of a reflectron, low resolution MS/MS

can be performed with significant improvement on the resolution and accuracy. FT-ICR instruments offer the ability to perform slow MS/MS analyses in one analyser. It offers extremely high resolution and accuracy, but is very expensive and necessitates the use of superconducting magnets [72].

With a quadrupole instrument, while easily interfaced with ESI and is relatively inexpensive, has a low resolution, low accuracy, low mass range and scans slowly. Interfacing a quadrupole with a time of flight as in a quadrupole time of flight instrument allows for these disadvantages to be corrected to a large degree on account of the advantages associated with the reflectron time of flight instrument. This instrument allows for the analysis of polar compounds such as amino acids, since it's easily interfaced with electrospray ionisation. Performing LC-MS/MS analyses can be easily done while offering high resolution, up to about 7000 and a high accuracy while still being affordable [73-75].

1.7.2 Ion Source

Within the ion source the sample is ionized, before being sent to the mass analyzer. There are many different techniques which are used for ionising the samples and the particular ionisation source being chosen for any experiment will be determined by the nature of the sample being analysed. For samples which are volatile, gaseous or are vapours, the ionisation source of choice is usually either chemical ionisation or electron ionisation [72, 73]. Samples which are polar, such as amino acids in biological fluids, employ eletrospray ionisation. Another choice for such samples would be MALDI; matrix

assisted laser desorption/ionisation. Other methods of ionisation also include atmospheric pressure chemical ionisation, inductively coupled plasma, field desorption, fast atom bombardment, thermospray, glow discharge and several others [73].

1.8 Literature Results based on Studies Done for Amino Acid Analysis by LC-MS/MS.

Tabulated in Table 3 are the reported concentrations of amino acids which were detected and quantified using LC-MS/MS analysis. The first two result columns represent the reported concentrations in *E. coli* bacterial samples. The Der sample refers to the derivatized bacterial sample whilst the Und. refers to the underivatized samples. The last (4^{th}) column shows the determined concentrations of the detected amino acids in human blood plasma. The blood plasma samples were not derivatized but analysed directly by LC-MS/MS.

The analysis of chiral amino acids in bacteria is not novel and has been done for decades. However, within these studies, the primary focus is on the endo-metabolome of bacteria, thus metabolomic fingerprinting studies. Metabolomic footprinting is however significantly less common, with relatively few studies being published over the past decade. The exo metabolome is hardly ever studies mainly because it contains the exuded material of cellular metabolism and cellular processed. In our literature searches, we were able to uncover not more than five reports which examined the exo metabolome of bacterial cells [69, 70, 71, 77]. Of these reports, the first two dealt with *E.coli* in which they measured the concentration of amino acids present after derivitization. No chiral

analysis was done. In other cases, [75], *Aspergillus Niger* was examined both directly and indirectly by LC-MS/MS analysis. While chiral analyses has been done in different studies, with emphasis being placed on chiral resolution, to our knowledge, this research is the very first which examines the chiral resolution of amino acids in the bacterial exo-metabolome of *Sinorhizobium meliloti.*

Table 1-3: Conc. of amino acids found in bacterial and human samples by LC-MS/MS.

	Bacterial (Der)	**Bacterial (Und.)**	**Plasma (Und)**
Amino Acid	**Rel. Ab.[a] (ug/L)[69]**	**Rel. Ab[b] (ug/L)[70]**	**Rel. Ab.[c] (ug/L))[71]**
Alanine	33.70	13.14	13.5
Arginine	17.21	30.04	
Aspartic Acid	17.26	2.84	
Cysteine	-		
Glu.- Acid	-		
Histidine	23.51	23.66	
Isoleucine	-		7.6
Leucine	14.20	6.06	12.3
Lysine	13.97	12.48	
Methionine	19.05	2.26	
Proline	11.88	1.44	
Phenylalanine	23.4	22.42	8.7
Serine	13.26	2.16	
Tryptophan	13.57	2.84	
Threonine	15.16	5.03	
Tyrosine	102.5	88.14	
Valine	18.53	9.11	

a,b: Relative abundance from literature based on similar studies utilizing microbial fermentation broths of *E. coli*
c: Relative abundance from literature based on similar studies utilizing human blood plasma.

1.9 Goals

The aims of this research project were to develop an analytical method with the following targets:

1) To develop a rapid LC-MS/MS method (less than 20 minutes) for the chiral analysis of amino acid metabolites in a complex biological mixture.
2) To have resolve and quantify the D and L enantiomers of amino acids directly.
3) To compare amino acid profiles in the exo-metabolome of *Sinorhizobium meliloti* with that of its endo-metabolome.
4) To investigate the effect of different stimuli on the production of amino acids in bacteria (*S. meliloti*).
5) Identify pathways responsible for the production/suppression of the metabolites of interest.

2.0 Experimental

2.1 Chemicals

Almost all of the reagents and chemicals were purchased from Sigma-Aldrich (Milwaukee, WI, USA).The L and D forms of each of the amino acids listed were purchased as a 'kit: aspartic acid, arganine, alanine, asparagine, cysteine, glycine, glutamine, glutamic acid, histidine, isoleucine, leucine, lysine, methionine, phenylalanine, proline, serine, tryptophan, tyrosine, threonine, valine. L-aspartic acid-2,3,3-d_3, was purchased from Cambridge Isotopes, Woburn, MA, USA.

2.2 Gases and Solvents

High purity nitrogen carrier (>99.999%) was purchased from VitalAire (Hamilton, ON, Canada); HPLC grade solvents were purchased from Caledon Laboratories Ltd. (Georgetown, ON, Canada). A Milli-Q water purification system (Millipore Corporation, Bedford, MA, USA) was used for the purification of deionised water.

2.3 Samples for Analysis

All bacterial samples were obtained from Dr. Rahat Zaheer (Department of Biology, McMaster University). The samples used for analysis was the extracellular supernatant (supernatant) of the wild type of *Sinorhizobium meliloti.*

The bacterium was cultured on three different media and allowed to reach their stationary phase. The purpose of growing the bacteria on three separate cultures was to investigate the effect of each of the three different growth media on the production of

enantiomeric amino acids. For the first growth medium, in addition to a standard chemical composition listed in Table 2-1, this medium contained 40 mM of phosphate. Based on this, it is referred to by the term P40 medium, the P representing phosphate (KH_2PO_4) while the number 40 represents the concentration in mM of phosphate in the sample. Similarly, the second growth medium, referred to as P2, there is 2 mM of phosphate present in the growth medium. This media is also referred to as minimal growth media, since it contains the minimum amount of nutrients needed for bacterial growth. The third growth media contains no phosphate (referred to by the term P0 medium) or is referred to as phosphate starved media. This causes the bacteria to be stressed in order to survive and perform metabolic processes without phosphate. The samples were thus identical in every respect except for their concentration of phosphate in the form of KH_2PO_4.

The standard chemical composition of the growth medium is shown in Table 2-1.

Table 2-1: Composition of the growth media

MOPS Growth Medium	**Concentration in media (mM)**
MOPS	40
Succinic Acid	15
$MgSO_4$	2
$CaCl_2$	1.2
NH_4Cl	20
NaCl	100
KH_2PO_4	0, 2 or 40

After inoculation and incubation of *Sinorhizobium meliloti* onto the respective growth media for a 48 hour period, the bacteria was then harvested and centrifuged. In order to separate the bacterial cells from the supernatant, the cells were aliquoted into centrifuge tubes and then spun for separation. The supernatant which remained above these cells was then decanted. Aliquots of 10 mL of the decanted supernatant was then transferred to 10 mL eppendorf vials, lyophilized overnight for approximately 12 hours to remove any traces of moisture and then stored at -80°C until they were to be analysed.

The three growth media described in Table 2-1; (0 mM (P0), 2 mM (P2) and 40 mM (P40) phosphate) were prepared in excess in order to collect 10 mL aliquots of the growth media, which were then lyophilized in the same manner as the bacterial supernatant for comparison purposes. These were also stored at -80°C, until analysis, at which time they were run alongside the bacterial samples. Each 10 mL aliquot of lyophilized bacterial supernatant corresponded to approximately 18.5 mg dry weight of sample, while a 10 mL aliquot of lyophilised growth medium was approximately 15.5 mg dry weight.

2.3.1 Preparation of Sample for Analysis

Lyophilized samples of growth media and bacterial extracellular material, stored in 10 mL vials at -80°C were removed from the freezer and placed in dry ice. The samples were then transferred to individual glass vials prior to analysis, weighed and reconstituted with a 70:30 mixture of methanol/water. The volume of solution which was used for reconstituting the lyophilised samples depended on which of the three the growth

media (P0, P2 or P40) which was used for the bacterial culture. An example of actual dissolution volumes is given in Tables 2-2 and 2-3.

After lyophilisation and subsequent reconstitution, the sample was effectively concentrated. Hence, the total composition of the growth medium was concentrated by the same factor. Tables 2-2 and 2-3 demonstrate an example of the factor by which the samples were concentrated since they were reconstituted with a minimum volume of mobile phase. This allows for all of the constituents presenting this supernatant sample to be concentrated by a certain amount. This 'certain amount' by which the original samples were concentrated could be calculated accurately in order to assign a concentration factor.

By calculating the concentration factor relative to the original supernatant solution prior to lyophilization, we could back calculate the actual concentration of amino acids present in the original supernatant samples. This value would be a true representation of the enantiomeric amino acids present in the extracellular supernatant of *S. meliloti*.

Table 2-2: Dry Weight, Reconstitution Volume and Concentration Factor of Growth Media.

Sample: Growth Medium	**Dry Weight (mg)**	**Volume of Methanol/Water (μL)**	**Concentration Factor**
P40	17.85	250	40
P2	17.85	100	100
P0	18.10	82.5	121

Table 2-3: Dry Weight of 10ml growth medium, Volume of MeOH/H_2O and volume of internal standard added prior to LC-MS/MS analysis

Sample: Bacterial Supernatant	Dry Weight (mg)	Volume of MeOH/Water (μL)	Volume I.S. solution added (μL)	Concentration of I.S. added (pg/μL)
P40	15.57	900	270	20
P2	15.14	250	75	20
P0	15.73	200	60	20

Upon reconstitution, each sample was then kept at -10°C between infusions/injections in a mini-refrigerator and on dry ice between individual runs. The reconstitution volumes for the samples containing growth media versus the samples containing bacterial cells and growth medium were different on account of the increased level of compounds present in the bacterial sample possibly due to the production of metabolic products, substrates and intermediates.

2.4 Enantiomer Resolution: Infusions Vs Injections.

Infusion of sample refers to the direct introduction of the sample into the electrospray ion source of the mass spectrometer by way of an external Harvard syringe pump. No chromatography is performed on the sample before entering the ionisation source (ESI) of the MS for detection. A 500 μL syringe was used to infuse the sample directly into the ion source at a flow rate of 5 μL/min. The mass spectra were collected for a one minute period and these spectra (~100 spectra) were averaged. An injection refers to the direct introduction of the sample onto the LC column (Chirobiotic T) for chromatographic separation by way of a manual 1μL Rheodyne injection system directly coupled to the ESI-MS/MS.

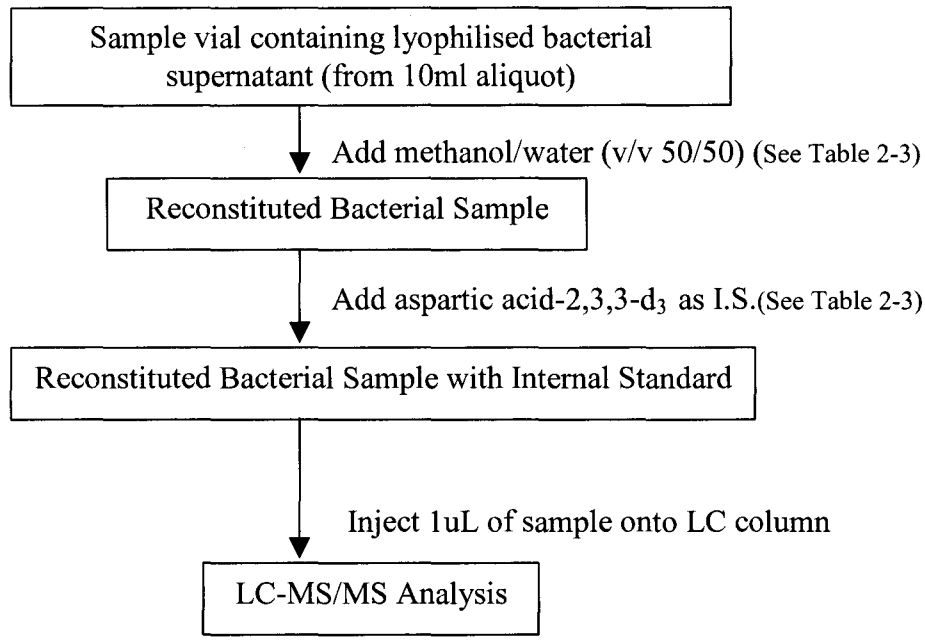

Scheme 1-1: The protocol followed for sample preparation prior to analysis by LC-MS/MS.

2.5 Internal Standards

A single deuterated amino acid, L-aspartic acid-2,3,3-d_3, was used as an internal standard. The internal standard was added to samples in a 10:1 ratio of sample/internal standard. The internal standard was prepared by dissolving a weighted amount of L-aspartic acid-2,3,3-d_3 in deionised, distilled water to make a stock solution of 120 pg/μL. Dilutions of the stock solutions were then made with a solution of 50:50 (v/v) of methanol/water. After removing the lyophilized bacteria samples from storage at -80°C they were reconstituted with a solution of methanol /water (Scheme 1). The diluted solution of concentration 20 pg/μL of the internal standard was then injected into the

reconstituted bacterial sample as shown in Scheme 1. These samples were then subject to either injection or infusion. Scheme 1 illustrates the preparation of the sample, and introduction of the internal standard into the sample.

2.6 Calibration Data

Calibration curves were obtained for the enantiomers of the 20 amino acids. Along with the calibration of the enantiomeric amino acids, calibrations were also performed of the internal standard L-aspartic acid-2,3,3-d_3. This data gave the linear range of the enantiomeric amino acids, the detection limits and response factors. The calibrations were performed over the range of 50-00 μg/μL in order to determine the linear range of the amino acids. (Figures 3-3, 3-4)

2.6.1 Detection Limits

The detection limit was defined in this research as that amount which gives a signal to noise ratio (S/N) of 3.

There were two main factors that needed to be determined with respect to detection limits. The first was the actual detection limit of each enantiomer of each amino acid of interest. The second was the minimum ratio of one enantiomer that can be resolved and quantified relative to the presence of the other enantiomer.

Amino acid standard solutions of concentrations between 50 pg/μL to 100 μg/μL were prepared in order to test not only the single amino acid detection limits but also their detection limits when being targeted as a group by Full scan and also Multiple Reaction

Monitoring programs. Amino acid standards were prepared singly and then combined into several different groups for comparison purposes.

The first group (Group 1) started with a minimum of 2 amino acids and increased in multiples of 2 up to a maximum of 20 amino acids; a total of 10 sub-groups of Group 1. Group 2 started with a minimum of 3 amino acids and increased in multiples of 3; a total of 7 sub groups. Group 3 contained the six amino acids of primary interest for bacterial analysis; threonine, arginine, valine, serine, proline and alanine (Table 3-6, 3-7).

2.6.2 Response Factors

Solutions consisting 6 amino acids were prepared. From each stock solution of 6 amino acids, aliquots were combined to give a total of 20 amino acids. The samples were diluted with a solution of 50:50 methanol/water. Analysis of the samples was done by LC/MS/MS utilizing the MRM program mode (2.6.3). The total response was the peak area of each amino acid. The peak of each amino acid standard was plotted against the mass of the internal standard injected (ng); L-aspartic acid-2,3,3-d_3. Using Excel, a linear least square line of best fit was drawn through the data points, hence determining the value of R^2 for each amino acid.

The response factor was determined by the ratio of the best fit line of the slope of the internal standard to the slope of the amino acid standards. The following formula gives the relative response factors reported in this study.

$$\textbf{Response Factor (RF)} = (A_{\text{cal std}}/M_{\text{cal std}})/(A_{IS}/M_{IS});$$

where $A_{cal\ std}$ is the area of the calibration standard, $M_{cal\ std}$ is the mass (ng) of the calibration standard injected, A_{IS} is the area of the internal standard injected and M_{IS} is the mass of the internal standard injected.

2.6.3 Quantitation

In order to quantify the amino acids identified in the samples, the peak areas of the enantiomers were compared against the area of the internal standard peak (L-aspartic acid-2,3,3-d_3) of known concentration. The internal standard, L-aspartic acid-2,3,3-d_3 was injected into the sample in a 10:1 ratio. The internal standard was therefore approximately 10 times less in concentration than the sample. For the purpose of quantification, the mass of the analytes were calculated by the following formula:

$$\mathbf{M_{analyte} = (A_{analyte} \times M_{IS}) / (RF \times A_{IS})}$$

where $M_{analyte}$ is the mass (ng) of the analyte, the peak area of the enantiomers of the amino acid analyte is $A_{analyte}$. M_{IS} represents the mass (ng) of the internal standard while A_{IS} is the peak area of the L-aspartic acid-2,3,3-d_3.

2.7 LC-MS/MS Analysis: Instrumentation

In order to detect and quantify the amino acids present in the extracellular bacterial supernatant of *S. melilot*, a Waters/Micromass liquid chromatography tandem mass spectrometry system consisting of a Waters 2795 LC directly coupled to a

Micromass Quattro Ultima triple quadrupole mass spectrometer was used. LC separations were carried out on an Advanced Separation Technologies chiral Chirobiotic T column at room temperature. For the protection of the chiral Chirobiotic T column, a chiral Chirobiotic T guard column was used in conjunction with the LC column. The attachment of the guard column facilitated no mobile phase accumulation between the column and the guard column as a result of the specifications of the joints which were designed to accommodate this.

The parameters of the ESI-MS-MS system were obtained from literature. The method was tested and a few of the parameters were altered in order to be optimal for our purpose. The LC-MS/MS analysis was carried out in positive ion mode, under multiple reactions monitoring mode (MRM) (section 2.4). The column specifications along with the guard column specifications are given in Table 2-4.

Table 2-4: Chiral column properties used for chiral separation of enantiomeric amino acids in the supernatant of *S. meliloti*.

Column Properties	
Column Type	Astec (Chiral) Chirobiotic T
Stationary Phase	Teicoplanin glycopeptide bonded to5um spherical silica gel
Column Length (cm)	150 x 2.1mm
Guard Column Length (cm)	2cm x 2.0mm
Column I.D. (cm)	2.0mm
Curtain Gas	Nitrogen
Elution Mode	Isocratic: 50% MeOH.H_2O
Flow Rate	200µL/min

2.7.1 Analysis Programs

For analysis by the LC-MS/MS method described, two modes of analysis were utilised. Full scan analysis, monitoring all of the ions present within a selected range along with the multiple reaction monitoring mode (MRM).

2.7.2 Full Scan Method

Since the molecular masses of all of the compounds of interest (primary amino acids) were below 200, the full scan mode was programmed to scan between 80 and 300 amu. The composition of the growth media also constituted masses less than 200amu, and hence there was no need for monitoring any ions above this range.

Within this range, using the full scan mode allowed for the identification of all of the amino acids of interest at the detection limits specified (Table 3-5, 3-6). This mode is of critical importance for the identification of unknown compounds or for those metabolites which do not have any established or determinable unique transitions by which they can be identified from the other components of the sample matrix.

2.7.3 MRM Programs

When a compound is injected or infused into the electrospray of a mass spectrometer, it will fragment to produce ions. The protonated molecular ion, of the notation $[M+H]^+$, referred to as the parent ion, will fragment based on the collision energy chosen to produce a serried of ions of lower m/z ratios, referred to as the daughter ions.

For analysis of amino acids, it was found in literature reports [36-42] that each amino acid affords a unique 'transition', which is a parent-daughter ion pair, which is used to uniquely identify each amino acid.

These literature results were experimentally verified through parent-daughter/precursor ion scans confirming that each amino acid does indeed undergo fragmentation to afford ions which are unique in the positive ion mode of electrospray ionisation. An exception to this is leucine and isoleucine which would have the same MRM transition for identification. Using these verified transitions shown in Table 2-5, the unique MRM transitions formed the basis for subsequent MRM transition programs created.

Table 2-5: Mass Spectral Transitions for 20 amino acids.

Amino Acid	Transition
Alanine	90-44
Arginine	175-116
Asparagine	133-87
Aspartic Acid	134-88
Cysteine	122-76
Glycine	76-30
Glutamine	146-102
Glutamic Acid	148-102
Histidine	156-110
Isoleucine	132-86
Leucine	132-86
Lysine	134-60
Methionine	150-104
Proline	116-70
Phenylalanine	166-120
Serine	106-60
Tryptophan	205-146
Threonine	120-74
Tyrosine	182-136
Valine	118-72

In deciding on the type of MRM programs to be used for this research, an evaluation of the sensitivity of each program was tested before deciding on the 'best' method by which analyses could be performed. Different combinations of amino acid transitions were grouped into single MRM programs in order to compare the sensitivity difference for each amino acid. For example, an MRM program seeking to identify only one amino acid would have the advantage of performing more scans per second for that amino acid compared to an MRM program seeking to identify 6 amino acids.

2.7.4 Deconvolution of Co-eluting peaks

The co-elution of peaks is usually a considerable issue for identification and quantification of analytes in any sample. In this research, the analytes being identified and quantified were all known amino acid enantiomeric pairs, whose retention times were determined by our initial experiments. By using standard solutions, the retention times of each amino acid enantiomer had been determined under optimal experimental LC conditions.

2.7.5 Monitoring Column Performance

The chiral HPLC column used for all analyses was a Chirobiotic T column (15 x 2.1 cm, Astec, Teichoplanin, bonded glycopeptide.). The manufacturer recommended that a test standard be run to establish the performance of the column. The test standard, 2,4-dimethylphenylhydantoin was injected in 50:50 methanol:water and retention times and peak shapes of the two enantiomers indicated that the column was in excellent condition and performing according to the manufacturer's specifications. Column performance changed over time depending on the level of usage, the conditions under which the column was being used and also the nature of the sample being introduced onto the column. By using a guard column, the lifetime of the column can be lengthened and damage to the column can also be prevented and/or minimised. Thus, a guard column (2cm x 4.0mm) was used in all analyses. Column performance changed with usage and therefore needed to be monitored routinely. This is discussed in detail in section 4.2.2.

2.7.6 Ion Suppression Factors

For the determination of detection limits and ion suppression factors for the amino acids, twenty amino acid enantiomer pair standards were prepared. This gave a total of 40 sets of calibrations; 20 D-amino acid enantiomers and 20 L-amino acid enantiomers. These calibrations are shown in Appendix 1.

2.7.7 Ion Suppression

The extracellular supernatant of *Sinorhizobium meliloti* is very 'dirty' and consists of the excreted waste products, the growth medium and a combination of cellular metabolites that travelled across the cell wall of the bacteria. In this research, we chose not to use any clean up procedure prior to analysis in order to develop an unbiased analytical method that could be used directly for extracellular supernatants.

In the present work, *Sinorhizobium meliloti*, were grown on minimal growth media consisting of 100 mM of sodium and either 0 mM, 2 mM or 40 mM of phosphate (Refer to Table 2-1). After sampling, the medium was freeze dried, transferred to 10 mL eppendorf vials and reconstituted in a small volume prior to analysis by MRM. The concentration factor was between 40 to 150 fold. (Refer to Tables 2-3, 2-4). The evaluation of ion suppression was done by comparing the instrument response of the calibration standards in methanol/water solutions to that of the same calibration standards prepared in reconstituted growth media which were previously freeze dried and hence, concentrated, as per the analytical method. Since the growth media were concentrated, they will be referred to as $P0_{(40)}$, $P2_{(100)}$ and $P40_{(121)}$, with the subscripts representing the

concentration factor. The amino acid standard was added as a 'spike' to the reconstituted media. This allowed for the evaluation of the effect of the sample matrix on the MS response thereby providing an insight into the magnitude of the ion suppression. Since there was no extraction or derivitization protocol followed, ion suppression in this case was solely based on the actual sample matrix. Three sets of 20 amino acid enantiomer pairs' standards were prepared individually as P40, P2 and P0 amino acid standards stock solutions. The total number of standards produced was 120; 3 sets of 20 amino acids, each of which contained the D and L enantiomer of each amino acid. A separate set of the same combination of amino acid standards were prepared using methanol/water (50:50(v/v)) as the solution instead of the growth medium solutions.

Two different groups of calibration evaluations were then performed using LC-MS/MS. The first group of calibration standards to be run comprised of the 20 amino acids (D/L enantiomer pairs) which were prepared using methanol/water as the solvent. The second group of calibrations was done in three separate phases. The first involved running the calibration standards of the 20 amino acids (D/L enantiomer pairs of each amino acid) which were prepared by using the $P40_{(121)}$, growth medium as the solvent. The second and third phases involved running calibrations of the 20 amino acids (D/L enantiomer pairs of each of the 20 amino acids) which were prepared using the $P2_{(100)}$ growth medium and the $P0_{(40)}$ growth medium as the solvent respectively. The elution time of phosphate and sodium using our method was also checked to verify whether there would be co-elution of these salts and the amino acids of interest.

2.8 Optimised Methodology

After experimenting with the LC and MS/MS experimental conditions and parameters, the optimal methodology for the LC-MS/MS was decided upon. This is described in this section.

LC Parameters on chiral Chirobiotic T column. (Injections)

Flow Rate: 200 μL/min

Injection Volume: 1μL (manual Rheodyne Injection system)

Mobile Phase Composition: 50:50 Methanol/Water acidified with 0.25% Acetic Acid.

Infusions

Flow Rate: 5 μL/min

Injection System: Harvard syringe pump equipped with a 250 μL syringe

MRM Program

MRM Program C (2.4.2)

Mass Spectrometric Parameters

Ion Mode: Positive ion

Ionisation: (ESI^+)

Collision Energy: 12V

Interscan Delay: 0.02/sec

Interchannel Delay: 0.03/sec

Dwell Time: 2.4 sec

Capillary: 3.5V

Cone: 20V

Hex: 1

Aperture: 1V

Hex 2: 0V, Multiplier 650

Source Temperature: 100°C

Desolvation Temperature: 350C

Desolvation Gas: 500L/h

Cone Gas: 40L/h

Low Mass Resolution (Q1): 12.0

High Mass Resolution (Q2): 12.0

Ion Energy: 0.2

Entrance: -5V

Low Mass Resolution (Q2): 15.0

High Mass Resolution (Q2): 15.0

Ion Energy (Q2): 0.5

3.0 Analytical Method Development

The aim of this project was to develop a method which would be capable of chiral separation of amino acids in the exo-metabolome of *S.meliloti* by way of a direct method which by-passed sample clean up protocol. In this chapter, we discuss

1) The verification of multiple reaction monitoring transitions obtained from literature.
2) The development of MRM programs which increase the sensitivity and selectivity of analyses
3) The determination of the retention characteristics and the reproducibility associated with these characteristics.
4) Determination of the elution mode and composition to be used for analyses.
5) The determination of calibration curves, response factors and detection limits for the enantiomers of each amino acid.
6) Fragmentation mechanisms of amino acids by electrospray ionisation.

3.1 Infusion of Samples

Infusions are performed by introducing the sample directly into the mass spectrometer without having any chromatographic separation of a column and monitoring the ions under full scan. The infusion of a bacterial sample is illustrated below. The infusion was done by introducing a concentrated sample of *S.meliloti*, reconstituted with a 50:50 solution of methanol:water, directly into the mass spectrometer and run under full scan mode within the range of 1 and 1000.

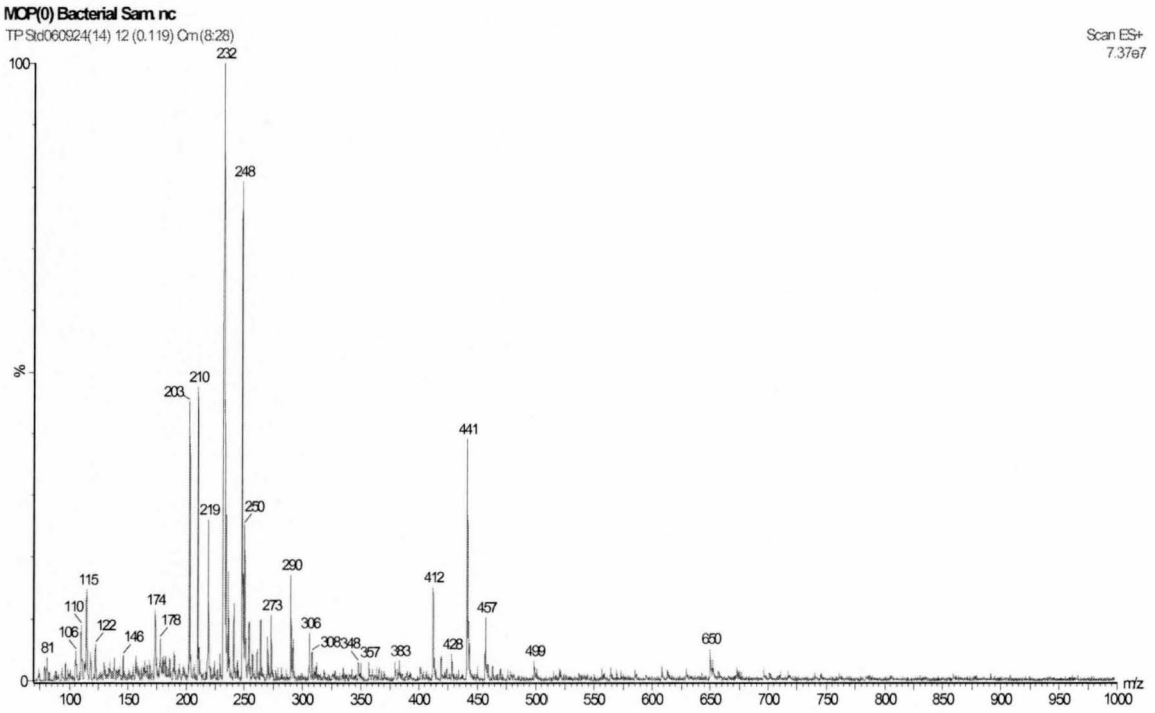

Fig 3-1: Full Scan infusion of *S.meliloti* grown in P0 medium.

By infusing the sample under a full scan method, all of the ions within this range are monitored. However, the amino acid ions of interest are under 200 amu. On taking a

closer look at the infusions of sample within this region, we try to identify the amino acids directly, without any chromatography.

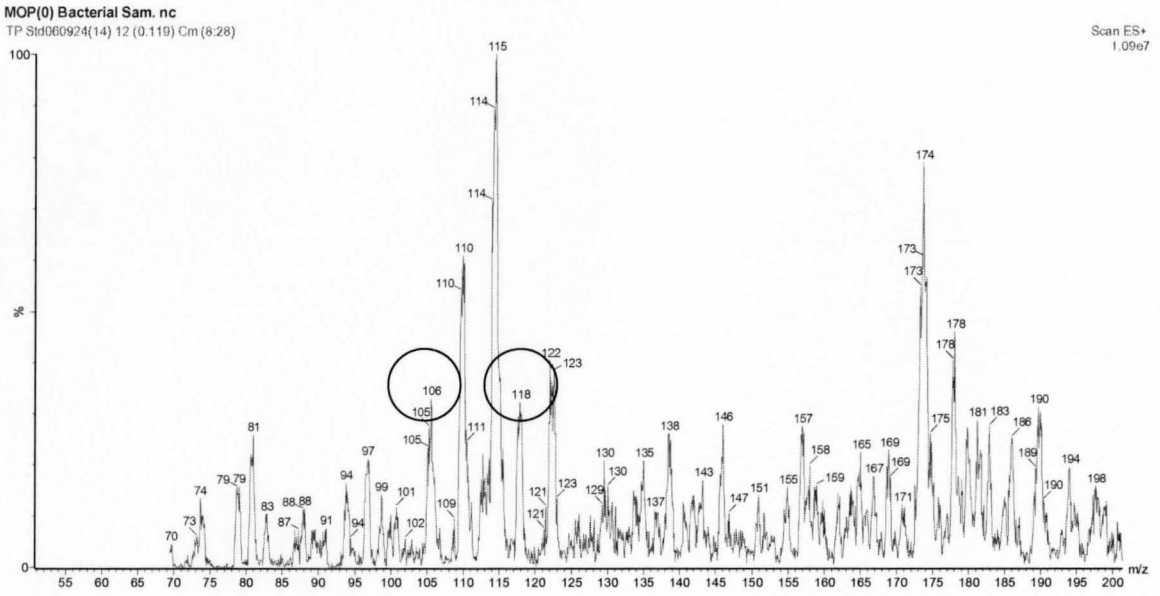

Fig 3-2: Full Scan mass spectrum of infusion of P0 media over the mass range of 50-200 Da.

Utilising infusion experiments, we were only able to identify serine (106) and valine (118) .in the bacterial samples (identified in Fig 3-2). We weren't able to identify any other amino acids in the bacterial sample by this methodology. For this reason, all subsequent experiments were performed by LC-MS/MS. Infusion experiments were therefore not performed beyond this point. Further to this point, all experiments were done to optimize the LC method which would be used for subsequent analyses.

3.2 LC-MS/MS Analytical Conditions

Parent-Daughter Ion Scan: Determination of Optimum Collision Energy

A fixed precursor ion scan was conducted for all of the amino acids by first selecting the protonated molecular ion of each amino acid and bombarding it with different collision energies, until the optimum value for the collision energy was determined. The amino acid standards were introduced into the mass spectrometer by infusion using a Harvard syringe pump at a flow rate of 5 μL/min. Mass spectra were acquired over the mass range of 30-250 by accumulating 100 scans using 2.4 sec scans. The scan time was decided upon based on the peak widths of the enantiomeric amino acids. Since the peak width was no less than approximately one and a half minutes wide, this scan rate allowed for a minimum of 60 scans per peak. The effect of averaging 60 scans versus a much smaller number allows for significant improvement of the S/N ratio and also a reduction in the number of artefacts produced. Each amino acid scan was performed with different collision energies varying from 5 to 32 eV, with a step size of 2 eV. The value of 32 eV was obtained from literature reports, and was thus the first collision energy investigated. It was desirable to reduce the protonated molecular ion to 10% of its original height. Bombarding the protonated molecular ion of each amino acid with 32 eV resulted in 100% reduction of the molecular ion peak in almost all cases. Most amino acids responded similarly, and were reduced to about 10% of their original peak height using 12 eV. For each amino acid, an optimal collision energy was determined, in which the sensitivity was highest for our instrument. However, it would not be feasible to have an MRM program which detects six or more amino acids, each having different collision

energies, since this can cause a reduction in the performance of the instrument. Neither would it be feasible to have a single MRM program for each amino acid, as this would lead to significant losses in sample and time, while gaining little in terms of sensitivity. The transitions (pairs of precursor and product ion generated by amino acid molecules, listed in (Table 3-2) verified were then used to create MRM (Multiple Reaction Monitoring) programs (section 2.7.3) for detecting the enantiomers of each amino acid in the MRM mode. It was decided that 12 eV would be used in creating all MRM programs for the detection of the enantiomers of amino acids in this research.

Table 3-1 illustrates the results of using different collision energies for each amino acid. It is evident from these results that bombardment of the protonated molecular ion with12 eV allows for more than half of the amino acids to produce a peak of 10% abundance, while 18 eV produces a protonated molecular ion of 10% for only tyrosine, tryptophan, arginine and phenylalanine. Hence, the collision energy of 12 eV was used throughout this research.

Table 3-1: Effect of different collision energies on the peak height of the protonated molecular ions of 18 amino acids.

Amino Acid	**$[M+H]^+$**	**Approx. % $[M+H]^+$ after collision**		
		12 eV	**18 eV**	**26 eV**
Glycine	76	9%	0%	0%
Alanine	90	9%	0%	0%
Serine	106	9%	2%	0%
Proline	116	10%	2%	0%
Valine	118	10%	2%	0%
Threonine	120	10%	2%	0%
Cysteine	122	10%	2%	0%
Leucine	132	10%	2%	0%
Isoleucine	132	10%	2%	0%
Aspartic Acid	134	10%	2%	0%
Lysine	134	11%	6%	0%
Glutamine	146	11%	6%	0%
Methionine	150	12%	6%	1%
Histidine	156	12%	8%	1%
Phenylalanine	166	12%	9%	1%
Arginine	175	12%	9%	3%
Tyrosine	183	13%	10%	3%
Tryptophan	205	13%	10%	3%

3.2.1 Parent-Daughter Ion Scan: Verification of MRM Transitions

A fixed precursor ion scan was conducted for all of the amino acids by first selecting the protonated molecular ion of each amino acid and bombarding it with 12-15 eV collision energy in order to observe the fragment ions section 3-2. The dominant, reproducible ions in each mass spectrum of each amino acid was noted. They were then compared to the values obtained from the literature.

Figure 3-1 demonstrates a precursor ion scan with fragments being produced on bombardment of the protonated molecular ion of tyrosine with collision energy of 12 eV.

The dominant and most abundant ion is the unique fragment ion of mass 136. Other minor, secondary ions are present which are common for other amino acids, or are simply not reproducible enough to be used for identification purposes.

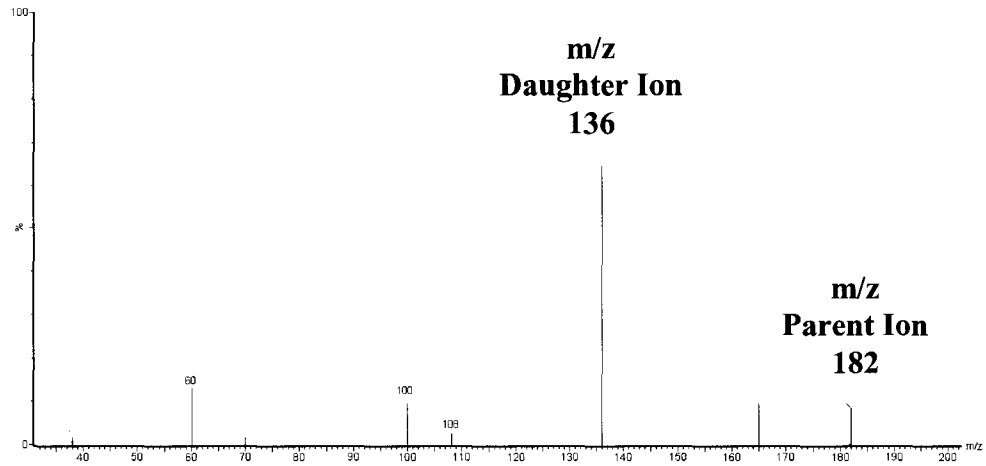

Figure 3-3: Daughter ion scan of Tyrosine, showing the dominant peak of 136 of the MRM transition 182-136.

Each amino acid was subjected to a precursor ion scan in a similar manner in order to verify each of the transitions which were in literature reports. Each of the transitions were verified and were thus used in creating specific MRM programs.

Table 3-2: MRMs determined based on literature reports. [35]

Amino Acid	Transition	Letter Code
Alanine	90-44	A
Arginine	175-116	R
Asparagine	133-87	N
Aspartic Acid	134-88	D
Cysteine	122-76	C
Glutamine	146-102	E
Glutamic Acid	148-102	Q
Glycine	76-30	G
Histidine	156-110	H
Isoleucine	132-86	I
Leucine	132-86	L
Lysine	134-60	K
Methionine	150-104	M
Proline	116-70	F
Phenylalanine	166-120	P
Serine	106-60	S
Tryptophan	205-146	T
Threonine	120-74	W
Tyrosine	182-136	Y
Valine	118-72	V

3.3 Analysis of Amino Acids Standards as Groups for Sensitive and Selective Analyses.

In deciding on the type of MRM programs to be used for this research, an evaluation of the sensitivity of each program needed to be tested before deciding on the 'best' method by which analyses could be performed. Different combinations of amino

acid transitions were grouped into single MRM programs in order to compare the sensitivity.

There are 6 major groups, A-F. Within each group are sub groups (A: 1-10, B: 1-7, C: 1-4, D1-3, E: 1, F: 1). For example, in Group A, there are 10 individual MRM programs in which each program will detect the enantiomers of only two amino acids. Group A-1 for example will detect the enantiomers of amino acids D and G (aspartic acid and glycine), while A-7 detects amino acids C and F. Similarly, Group D detects 10 amino acids and thereefore D-1 will only detect amino acids A,P,T,I,N,D,Q,M,R and W. Table 3-3 lists the groups A-F horizontally, while the subgroups of each group are listed vertically below each major group.

Table 3-3: MRM transition programs separated into groups and sub groups for sensitivity comparison.

Groups of Standards					
Group A	**Group B**	**Group C**	**Group D**	**Group E**	**Group F**
(1) G,D	(1) G,I,E	(1) G,V,L,K,F W	(1) A,P,T,I,N,D ,Q,M,R,W	(1) G,A,S,P,V,T,C,D, R, N,W,F,M,Q,K	(1) 20 Amino Acids
(2) A,D	(2) A,L,Y	(2) A,T,N,D, Q,R	(2) G,S,V,C,L, D,K,E,F,Y		
(3) S,K	(3) S,N,F	(3) G,S,I,D,E, Y			
(4) P,Q	(4) P,D,W	(4) W,M,N,C, P,A			
(5) V,E	(5) V,D,V				
(6) T,M	(6) T,K,R				
(7) C,F	(7) C,Q,M				
(8) I,R					
(9) L,Y					
(10) N,W					

The LC conditions and MS/MS parameters under which the MRM programs listed in Table 3-2 were performed are detailed in Section 2.6.6 and subsequent discussion. Since each group was subjected to the same method, including the same dwell times and scan times, the groups with fewer amino acids had better sensitivity compared to the groups containing more amino acids. This was on account of the dwell times and scan

times. A program with just one amino acid had the advantage of spending all of the scan time on that single MRM transition compared to a program which scans for all twenty amino acids, with some time also being devoted to switching between MRM transitions. Consequently, the sensitivity for the individual groups is as follows:

Group A=Group B>Group C>Group D>Group E>Group F. Within each group, the amino acids with transitions in which both parent and daughter ion were above 100, generally performed better compared to the lower MRM transition amino acids such as alanine. Groups A, B and C demonstrated 2 orders of magnitude greater sensitivity than Groups D and E. For the remainder of the research, Group C was used as the primary method for the identification of the enantiomeric amino acids.

The limit of detection for the enantiomers of amino acids using MRM methods of group C is reported in Table 3-5 and 3-6.

One factor which impacted the sensitivity of the measurements made in this research which was beyond our control was based on the calibration of the mass spectrometer. The mass spectrometer (Waters Quattro Ultima) was intended to make measurements above 100 amu. Therefore, for amino acids such as alanine, serine, valine and proline which have one or both components of their MRM transition close to or below 100, suffer from decreased sensitivity.

3.4 Dead Volume and Dead Time

Before determining the retention times of the amino acid enantiomers, it was necessary to determine the dead volume of the LC-MS system. Dead volumes in LC systems are of two types, thermodynamic and dynamic. The thermodynamic volume is defined as that volume of mobile phase which exists between the injection point and the detector sensor in which the solute is accessible. The areas such as unions and tubing are excluded from the constituent of dead volume. It does however include the volume of mobile phase which is in the pore packing of the stationary phase which is accessible to the solute. Unlike the thermodynamic volume however, the dynamic volume constitutes the mobile phase which is actually in motion through the system and therefore excludes the mobile phase which is in the pores of the packing or any static mobile phase within the system [79]. The thermodynamic dead volume is of importance when determining the retention time and retention data such as the capacity factor.

In our research, the dead volume was determined by injecting a neutral compound onto the column. The retention volume was taken as the volume from the injection to the peak maximum as detected by the mass spectrometer. A sample (1μL) was injected onto the teichoplanin LC column and the retention volume was determined at a flow rate of 200 μl/min. The dead time was found to be 1.3 minutes corresponding to a dead volume of 260 μL.

3.4.1 Retention Factors and Resolution.

The retention time, t_r, is defined as the time between injection and the peak maximum of that injected solute. The retention time of each amino acid enantiomer was determined by injection of 1µl of amino acid standard at a flow rate of 200 µl/min onto the LC column. Table 3-4 summarises the retention data of the enantiomers of 20 amino acid standards.

Table 3-4: k' and α values for the D and L enantiomers of the 20 amino acids under optimized method using 50:50 MeOH:Water; common extracellular bacterial amino acids are in bold font.

Amino Acid	R-Moiety[a]	k'_L[b]	K'_D[b]	α[c]
Aspartic Acid	$-CH_3$	0.7	1.1	1.5
Threonine	$-CHOH-CH_3$	0.7	1.1	1.6
Glutamic Acid	$-CH_2-CH_2-COOH$	0.8	1.3	1.4
Serine	$-CH_2OH$	1.1	2.00	1.8
Isoleucine	$-CH(CH_3)-CH_2-CH_3$	1.4	2.7	2.1
Glutamine	$-CH_2-CH_2-CO-NH_2$	1.4	2.4	1.7
Glycine	-H	1.5	Achiral	-
Tyrosine	$-CH_2-C_6H_{10}-OH$	1.6	2.7	1.6
Cysteine	$-CH_2-SH$	1.9	2.4	1.3
Valine	$-CH(CH_3)-CH_3$	2.1	2.9	1.4
Leucine	$-CH_2-CH(CH_3)-CH_3$	2.1	3.2	1.5
Methionine	$-CH_2-CH_2-S-CH_3$	2.2	3.5	1.6
Phenylalanine	$-CH_2-C_6H_{11}$	2.2	3.0	1.5
Alanine	$-CH_3$	2.2	3.3	1.5
Proline	$-CH_2-CH_2-CH_2-$	2.4	3.9	1.6
Asparagine	$-CH_2-CO-NH_2$	2.5	3.9	1.6
Tryptophan	$-CH_2-C_8H_{10}NH$	3.1	4.9	1.6
Lysine	$-(CH_2)_4-NH_3^+$	5.7	7.4	1.3
Arginine	$-(CH_2)_3-NH-C(NH_2)_2^+$	5.9	7.3	1.2
Histidine	$-CH_2-NH^+-CH-NH-CH$	6.1	6.8	1.1

a: Amino acids have the general structure $NH_3-CHR-COO^-$
b: k'_L and k'_D represent the capacity factors
c: α the selectivity factor

Based on the retention times, retention factors, k' were calculated. The selectivity factor, α, which describes the separation of two enantiomers on the column was also calculated for each of the amino acid enantiomers. These terms are defined.

$$k' = (t_r - t_0)/t_0$$

Where t_r is the retention time and t_0 is the time taken for the mobile phase to pass through the column from the time of injection.

$$\alpha = k'_B/k'_A$$

where k'_B refers to the retention factor of solute B and k'_A refers to the retention factor of solute A, where solute A elutes faster than solute B.

These values are easily obtained from the chromatograms obtained and are shown in Figure 9-11.

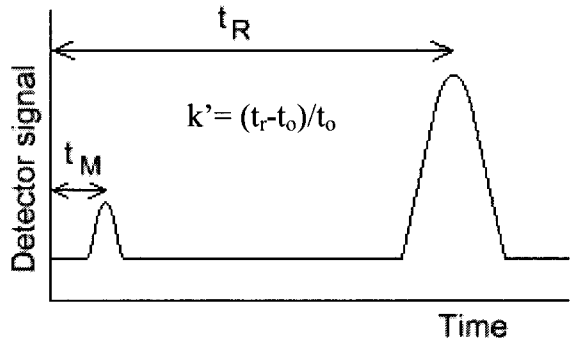

Figure 3-4: Illustration depicting the calculation of dead time and retention time of eluents [27].

3.5 Optimization of Isocratic Elution Mobile Phase Composition

Methanol/water was determined to be the best solvent combination for the elution of amino acids. There were 2 main challenges which needed to be dealt with in terms of the mobile phase composition, namely, the way in which each amino acid was resolved and secondly, the resolution of the amino acid enantiomers. Every amino acid required a different ratio of methanol and water to afford the best results. For example, a 60:40 ratio of methanol:water proved to be the best for the resolution of the enantiomers of glutamic acid, while a 70:30 ratio produced the best results for histidine. It was determined that a 50:50 ratio of methanol:water was the best compromise condition for the resolution of all of the enantiomeric amino acids. However, it was also found that after about 40 column volumes of mobile phase, amino acids such as arginine, histidine and lysine no longer eluted from the column. It is proposed that the anionic sites on the stationary phase can form interactions with cationic amino acids. Therefore basic amino acids such as arginine and lysine were too strongly attracted to the stationary phase while acidic amino acids such as glutamic acid and aspartic acid were repelled. To overcome this, the mobile phase was acidified by the addition of acetic acid.

The LC mobile phase was prepared from (A) methanol containing 0.25% acetic acid and (B) water containing 0.25% acetic acid. The isocratic solvent was 50:50 methanol:water containing 0.25% acetic acid. A flow rate was determined to be optimal at 200 µl/min for the 2.1 mm diameter column so as to keep the back pressure of the column below 132 bar while obtaining decent retention and elution of amino acids. Once the pressure of the column increased to about 180 bar or above, the LC pumping system

would automatically shut down or leaks would develop between the tubing connections of the system. To determine the optimal injection volume, injections of different volumes were made manually using an external Rheodyne injection system which was placed in line between the LC pump and the LC column. The LC injection volume was found to be 1μL.

3.6 Calibration Data: Detection Limits and Response Factors.

Calibration curves were obtained for both enantiomers of the 20 amino acids. These amino acids were divided into groups of 6, according to Table 10 C1-4, in order to have a spread of molecular masses within each group. These groups were then diluted with methanol:water (50:50) to cover a 100 fold range of concentrations. Each of the standard solutions contained internal standard, L-aspartic acid-2,3,3-d_3 . The individual groups of a range of diluted standards of amino acids was then analysed by LC-MS/MS. The total peak areas of the MRM total ion chromatogram of each amino acid standard was plotted against the mass of amino acid standard injected. A linear least squares line of best fit was drawn through each data set. The R^2 value (squares correlation coefficient value) and slope of each standard was obtained using excel. The response factor was calculated as the ratio of the slope of the line of best fit of a given amino acid to the slope of the L-aspartic acid-2,3,3-d_3 internal standard. Linear responses were obtained.

Within each group, each amino acid was represented by the D and L enantiomer in a 1:1 ratio. The choices for mixing amino acids in a particular group was based on molecular mass. The objective of each group was to have a spread of molecular masses.

The detection limits of the D and L enantiomers of the amino acids are presented in Table 3-4. The detection limits are defined as the concentration that produces a signal to noise ratio of 3:1. The detection limit of each enantiomeric amino acid was calculated from the observed signal to noise ratio at that particular concentration determined to be a 3:1 ratio.

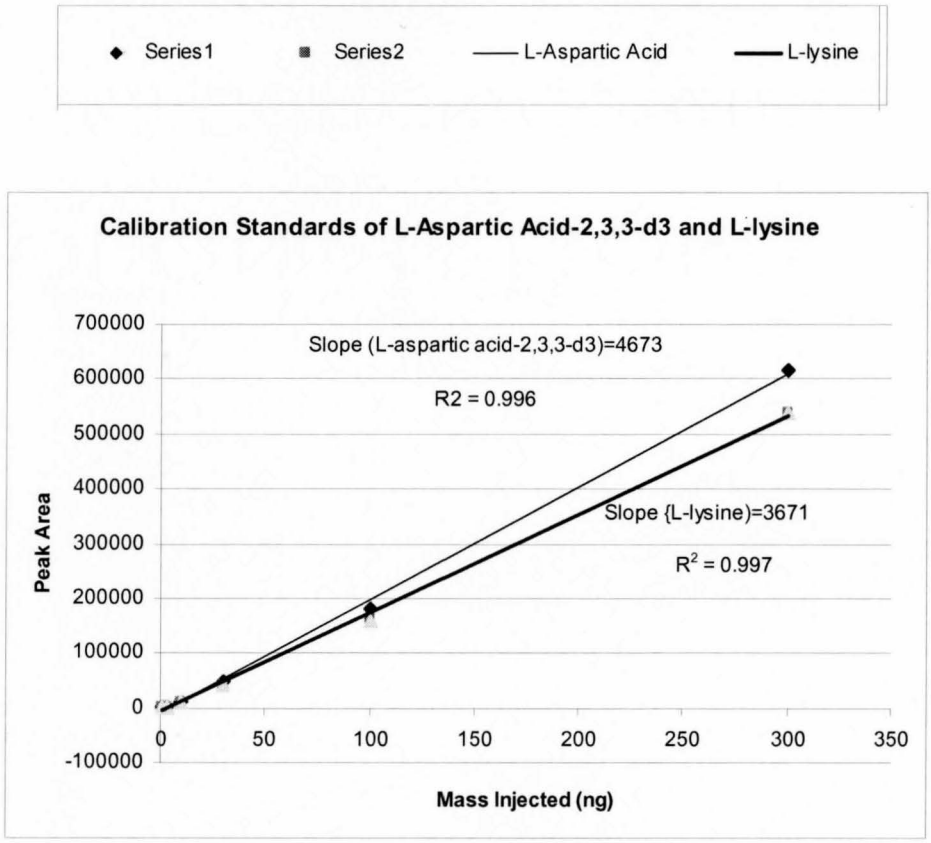

Figure3-5: Calibration standard of L-lysine and internal standard, L-aspartic acid-2,3,3-d_3

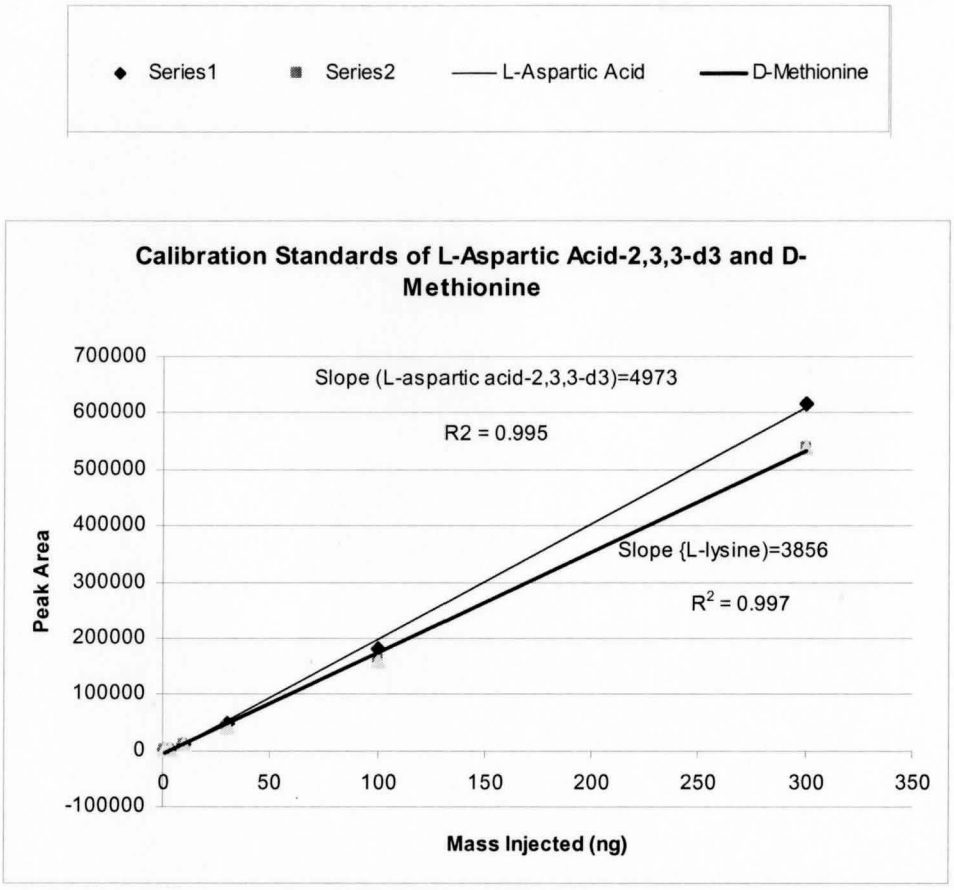

Figure 3-6: Calibration standard of D-methionine and internal standard, L-aspartic acid-2,3,3-d_3

Table 3-5: Detection Limits of 20 enantiomeric amino acids in methanol: water and P0 growth media.

L-Amino Acid Standard	R^2	Response Factor Relative to L-aspartic acid-2,3,3-d_3	Detection Limit µg/L	Linear Conc Range[c] µg/L	R^2 P0	Response Factor (P0) Relative to L-aspartic acid-2,3,3-d_3	Detection Limit (P0) µg/L	Linear Conc Range (P0) µg/L
Alanine	0.995	0.7	1.8	2.7-475	0.997	1.27	2.1	3.5-450
Arginine	0.994	1.9	2.9	4.2-475	0.995	3.16	5.2	7.1-800
Asparagine	0.996	0.8	4.1	5.5-550	0.999	1.12	3.0	5.5-800
Aspartic Acid	0.998	1.0	1.3	4.5-475	0.993	1.57	5.72	7.5-750
Cysteine	0.995	0.5	2.7	7.2-720	0.997	1.44	3.2	6.5-750
Glycine	0.996	0.7	3.6	6.3-530	0.994	1.40	2.0	5.4-610
Glutamine	0.997	1.5	2.8	4.5-475	0.990	1.16	4.2	6.3-750
Glu-Acid	0.997	0.4	4.1	6.2-620	0.991	0.91	3.9	5.2-750
Histidine	0.998	0.8	0.8	2.7-310	0.998	0.96	2.3	4.1-750
Isoleucine	0.998	1.7	3.1	4.7-475	0.996	2.06	5.0	7.2-750
Leucine	0.996	0.6	3.6	7.6-760	0.996	1.13	5.0	7.7-750
Lysine	0.997	1.3	4.2	8.3-910	0.995	1.62	4.0	6.5-750
Methionine	0.996	1.2	2.5	6.4-630	0.996	0.97	4.5	7.2-820
Proline	0.998	1.6	3.8	5.3-630	0.998	1.37	4.1	6.1-800
Phenylalanine	0.999	2.1	2.0	6.2-620	0.994	2.51	5.5	9.5-1250
Serine	0.998	0.83	2.5	4.7-475	0.997	1.39	3.6	5.5-750
Tryptophan	0.996	1.8	3.0	4.1-475	0.996	3.1	4.7	6.0-750
Threonine	0.997	1.4	3.7	9.1-910	0.993	2.4	4.1	6.5-800
Tyrosine	0.992	0.57	2.1	4.3-430	0.991	0.96	3.2	5.1-800
Valine	0.999	0.84	2.9	5.7-610	0.990	0.87	3.0	5.5-725

Table 3-6: Detection Limits of 20 enantiomeric amino acids in P2 and P40 growth media.

L-Amino Acid Standard	R^2 P2	Response Factor (P2) Relative to L-aspartic acid-2,3,3-d_3	Detection Limit (P2) µg/L	Linear Conc Range[c] µg/L	R^2 P40	Response Factor (P40) Relative to L-aspartic acid-2,3,3-d_3	Detection Limit (P40) µg/L	Linear Conc Range (P40) µg/L
Alanine	0.997	0.9	2.6	3.6-465	0.996	4.2	14.6	17-1750
Arginine	0.997	2.1	4.7	5.7-465	0.995	5.6	24.5	25-3000
Asparagine	0.994	0.8	3.6	5.0-465	0.998	3.2	13.9	19-1750
Aspartic Acid	0.995	1.6	4.8	6.2-475	0.994	4.7	29.3	34-3200
Cysteine	0.992	0.7	3.0	7.2-710	0.996	5.4	37.1	41-3200
Glycine	0.996	1.7	2.7	5.5-530	0.994	4.4	18.8	21-3000
Glutamine	0.997	2.3	5.1	7.3-465	0.990	3.7	11.3	14-1600
Glu-Acid	0.996	1.3	3.7	5.2-620	0.992	4.1	19.3	22-3200
Histidine	0.995	1.3	2.8	3.6-310	0.993	3.6	17.3	23-3000
Isoleucine	0.998	1.7	5.4	5.7-475	0.996	4.6	31.5	36-4210
Leucine	0.995	0.7	4.0	6.8-750	0.995	5.3	25.0	30-2500
Lysine	0.994	1.5	3.7	4.8-710	0.997	4.6	19.5	24-3000
Methionine	0.998	1.4	3.2	5.4-630	0.992	4.9	14.7	18-1750
Proline	0.997	2.6	3.8	5.3-630	0.993	5.4	21.7	26-1950
Phenylalanine	0.998	2.3	4.7	6.2-620	0.997	4.1	22.3	25-3000
Serine	0.998	1.7	4.6	6.4-455	0.997	3.9	21.4	27-3000
Tryptophan	0.996	2.8	4.3	7.0 -465	0.996	5.3	13.7	17-1750
Threonine	0.996	1.4	3.8	8.4-710	0.998	4.5	14.6	17-1750
Tyrosine	0.992	1.7	2.7	4.8-430	0.992	3.6	24.5	29-3100
Valine	0.997	2.2	3.6	5.2-625	0.996	4.7	13.9	16-1750

3.6.1 Fragmentation Patterns of Amino Acids

Electrospray ionisation was used for converting the sample to the gaseous phase for detection by quadrupole mass spectrometry. There are three main decomposition pathways documented in the literature for the fragmentation of underivatised amino acids by ESI . These are:

1) The formation of an immonium ion by the loss of CO and H_2O
2) The loss of NH_3 from the N-terminus
3) The loss of the heteroatom-containing small molecule from the side chain

The ionic complex formed as a result of the ionisation of the amino acids in a methanol/water solution is of the general form $[M+H]^+$ or $[AAH^+]$, which upon collisional dissociation produces fragment ions. With the exceptions of lysine, arginine and tryptophan, the protonated molecular ions of the amino acids follow a general pattern of fragmentation which is the sequential loss of CO and H_2O, forming the immonium ion.

For the amino acids such as leucine, which have a functional group on their side chain, there is a competition for the formation of the immonium ion either by the loss of a small molecule from the side chain or the loss of ammonium from the amino terminus. However, at higher collisional energies (Higher than 12eV), it is possible for protonation to occur to less basic sites X (X=SH, SCH_3, OH, NH_2....).

The experiments done with precursor ion scans allowed us to look at the fragmentation patterns of each amino acid in order to verify whether they fragmented according to the literature reports. From our observations, the enantiomeric amino acids fragmented as shown in Table 3-5, as reported in the literature.

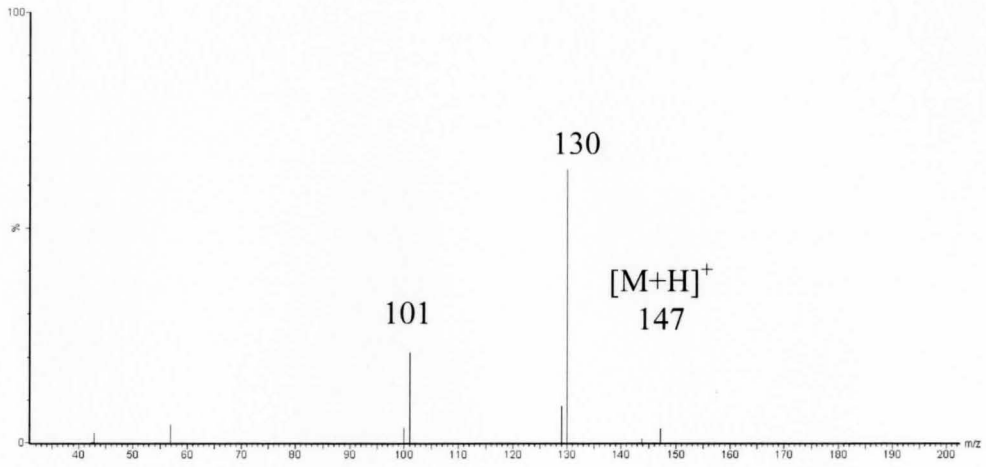

Figure 3-7: Mass Spectrum of lysine showing the fragments produced on collision with 12 eV of collision energy. The dominant fragment ion of 130 shows the dominant loss of NH_3.

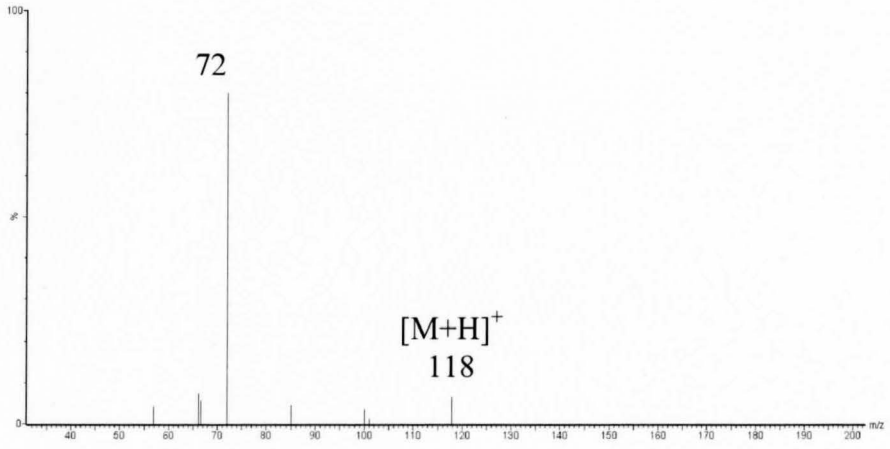

Figure 3-8: Mass Spectrum of valine showing the fragments produced on collision with 12 eV of collision energy. The dominant ion of 72 shows the dominant loss of CO_2 and H_2O.

Lysine produces fragments of masses 130, 129 and 101, however the dominant fragmentation pattern occurs as a consequence of the loss of NH_3 corresponding to the transition of 147-130. Valine on the other hand shows a dominant loss of 46, corresponding to the loss of $CO + H_2O$. Table 3-5 shows the major fragmentation of the amino acids of interest in this research, under positive ion electrospray ionisation.

Table 3-7: The fragment ion masses of amino acids corresponding to various losses [17].

	$[M+H]^+$	Loss of NH_3	Loss of H_2O	Loss of $CO + H_2O$	Loss of mass 63	Loss of mass 64
Glycine	76			**30**		
Alanine				**44**		
Serine	106		88	**60**		42
Proline	116			**70**		
Valine	118			**72**		
Threonine	120		102	**74**		
Cysteine	122	105		**76**		
Leucine	132			**86**		
Isoleucine	132			**86**	69	
Asparagine	133	116		**87**		
Aspartic Acid	134		116	**88**		
Lysine	147	**130**	129	101		
Glutamine	148		130	**102**		
Methionine	150	133		**104**		
Histidine	156			**110**		
Phenylalanine	166			**120**	103	
Arginine	175	**158**		**116**		
Tyrosine	182	165		**136**		
Tryptophan	205	**188**		146		

Bold = most intense, dominant fragment ions

These results were verified under neutral or slightly acidic conditions. The mass fragments in bold are indicative of the dominant fragments ions which were therefore used as the MRM transition for all of the amino acids. For most amino acids, this

corresponds to the loss of CO + H_2O to form the immonium ion. The loss of mass 63 refers to loss of NH_3 from the immonium ion while loss of mass 64 refers to loss of H_2O from the immonium ion.

4.0 Results and Discussion

The chiral resolution and analysis of amino acids in different bacterial strains and media has been reported in several different literature reports. The majority of analyses allow for derivitization of the amino acids in order to separate, identify and quantify the enantiomers of the detected amino acids. There has also been some work done on the direct analysis of fermentation broths by LC-MS/MS by- passing the clean-up protocols. We were able to verify the MRM transitions identified in these reports and use them in our analyses for the chiral resolution of 20 amino acids. These methods were found to be reproducible and with few changes, were well tailored for our analyses of the supernatant of *Sinorhizobium meliloti*. The novel aspect of this work is also reported in this section. This chapter will highlight the results of the following:

1) The issue of deconvolution of peaks
2) The enantiomeric ratios, namely, the minimum ratio of one enantiomer which could be detected in the presence of the other.
3) Effect of the sample on the LC column performance
4) The ion suppression caused by the sample matrix and the significance of the ion suppression factor.
5) The difference between the two growth media, P0 and P2 in these analyses.
6) The analysis of enantiomeric amino acids in the supernatant of *Sinorhizobium meliloti* by MRM programs.

7) The enantiomeric amino acids detected in different growth media, namely P0 and P2 growth media.

4.1 Separation of Enantiomers of Amino Acids

In this research, the D and L enantiomers of all 19 of the amino acids investigated as standard mixtures were well separated from each other. They generally fell into one of three categories with respect to their resolution. They were either perfectly separated from each other (baseline resolution), with large α values greater than 1.8, (Figure 4-1), slightly overlapping each other with α values between 1.3 and 1.6 (Figure 4-2), or very poorly separated with α values below 1.3 (Figure 4-3), possibly on account of a decrease in column performance due to the sample matrix.

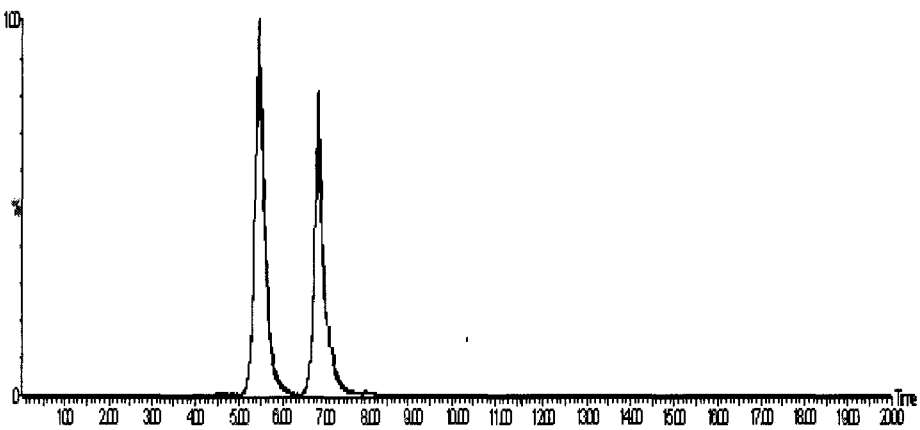

Figure 4-1: Chromatogram of L and D-serine standard separated with an α value of 1.8.

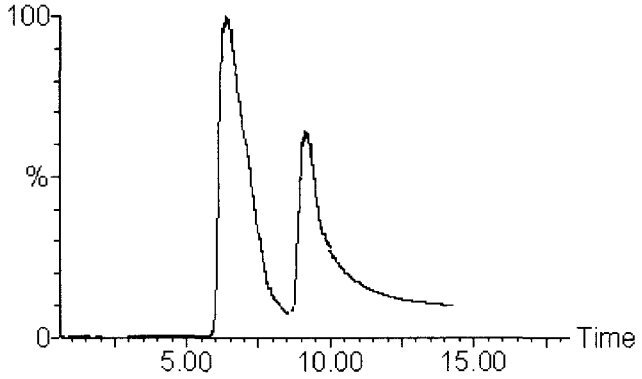

Figure 4-2: Chromatogram showing L and D methionine standard with moderate enantioresolution.

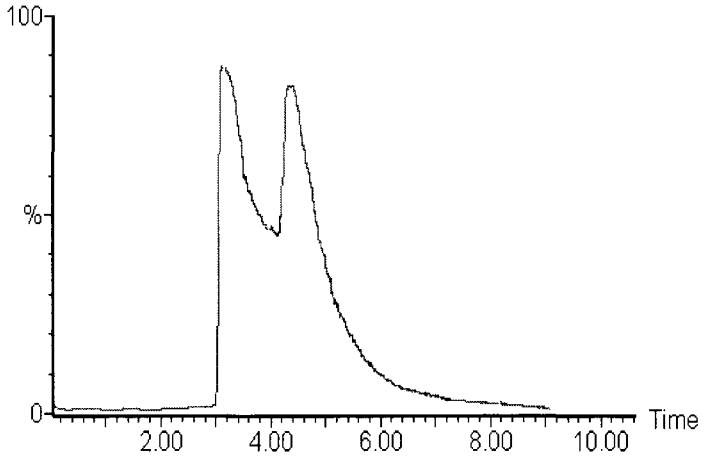

Figure 4-3: Chromatogram showing L and D cysteine standard showing very poor resolution.

The majority of amino acids investigated, including all six amino acids of interest in this bacterial research, fell between the first two categories of perfect to moderate separation of the enantiomers. Cysteine, lysine, tryptophan and especially histidine, exhibited the lowest α values, which become closer to 1 with decreasing column efficiency. To a large extent, the problem created by the column performance is easily rectified by a washing protocol described under monitoring column performance (4.2.2).

In terms of separating these significantly overlapping enantiomer peaks, changing the mobile phase composition to the optimum composition for that particular amino acid improved the situation slightly. However, having different mobile phase compositions for each amino acid within a particular MRM program was not feasible due to interface problems with the instrument and pumping system. Table 4-1 demonstrates the effect of changes in the mobile phase composition for enantiomeric amino acids with the lowest α values. The ratio (50:50, 70:30 etc) represents the mobile phase composition of methanol:water.

Table 4-1: The effect of changing mobile phase composition of methanol:water on the α values.

Amino Acid	**α 50:50**	**α 70:30**	**α 90:10**
Arginine	1.3	1.37	1.41
Cysteine	1.12	1.16	1.19
Histidine	1.23	1.3	1.37
Lysine	1.32	1.4	1.37

From Table 4-1, it can be seen that increasing the alcohol content of the mobile phase had little effect on the selectivity factor and therefore by using the compromise ratio of 50:50 methanol:water did not require much sacrifice in terms of separation of the enantiomers. The calculations for the k' and α were computed as described (section 2.2). From the α values obtained, it is clear that the D and L enantiomers of each of the amino acids are well separated from each other. Histidine and arginine have the worst separation while isoleucine and glutamine have the best separations. All of the other amino acids have a

fair degree of separation which would allow for separation and quantitation of both enantiomers of the amino acids. Hence, chiral resolution by this method is possible.

4.2 Identification of Co-eluting Peaks

In this study, deconvolution of coeluting peaks did not present a significant problem since each amino acid being detected has a unique MRM transition (parent-daughter ion pair) by which it is identified rather than being identified by retention times. This avoids convolution problems which occur when the compounds of interest have similar retention times.

By using the Mass Lynx 4.0 software, it was possible to obtain a chromatogram of each amino acid in a separate window. The MRM program therefore provides individual chromatograms for each MRM transition within that particular MRM program. An example of this is shown in Fig 4-4.

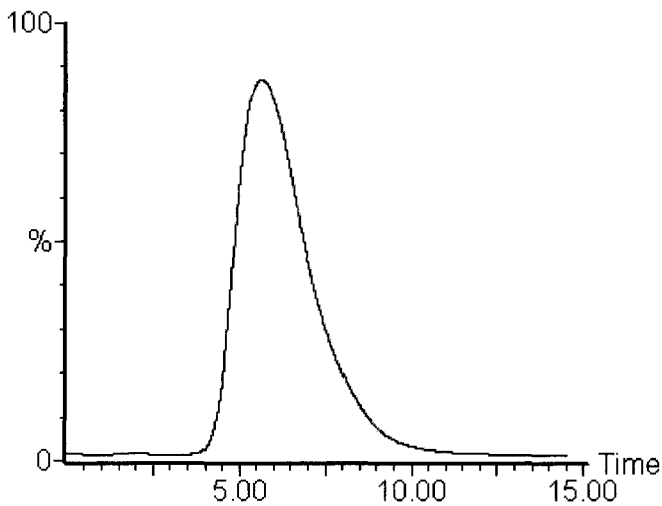

Figure 4-4: Total ion chromatogram produced for an LC MS/MS run with an MRM program to identify 6 amino acids.

Figures 4-4 shows the total ion chromatogram in order to identify and quantify each amino acid present. The ions produced by this LC run are detected by the MS/MS system which has been programmed to detect 6 amino acids, and hence 6 MRM transitions, corresponding uniquely to each amino acid.

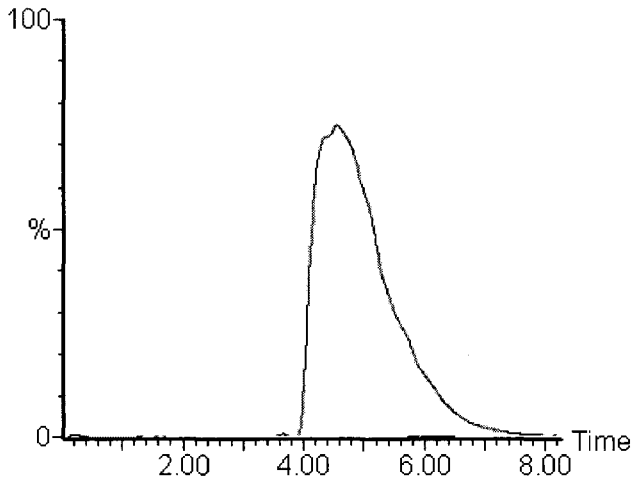

Figure 4-5: Chromatogram of the 175>116 MRM transition of which corresponds to phenylalanine.

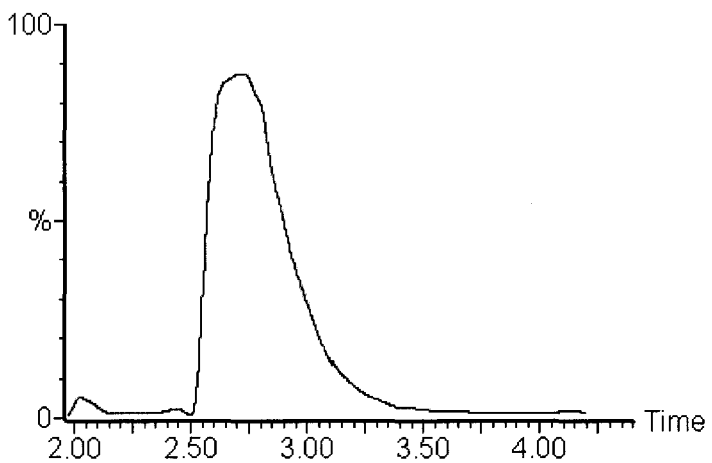

Figure 4-6: Chromatogram of the 166>120 MRM transition of which corresponds to arginine in a sample of standards.

The separation of the enantiomers of an amino acid is however a different issue and is required since the MRM transition for two enantiomers of a given amino acid are identical. The resolution of D and L enantiomers is determined with the relative retention times and peak widths.

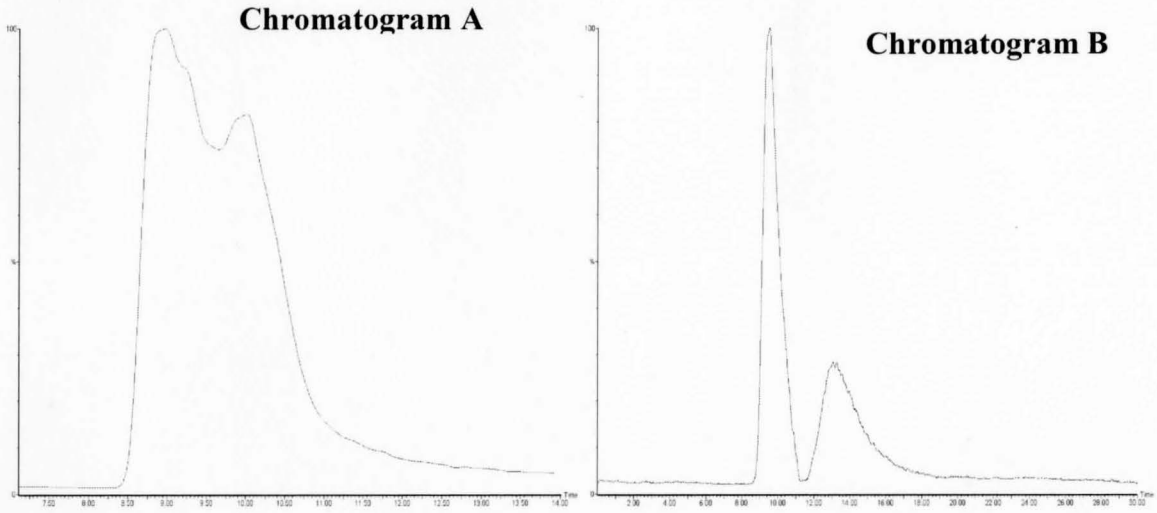

Figure 4-7: Chromatogram A showing poorly separated standards of D and L enantiomers of threonine compared to Chromatogram B, in which the D and L enantiomers are clearly separated.

Figure 4-7 shows the separation of the D and L enantiomers of threonine under different conditions. In chromatogram A, the D and L enantiomers are overlapped after injecting the sample onto the column, having previously run 12 bacterial supernatant samples. Chromatogram B illustrates the separation which can be achieved after washing the column with water, and then injecting a sample onto the column. Other examples are documented in section 4.2.1.

4.2.1 Determination of Integration Parameters

The integrating parameter refers to the specifications and limits used by the software to calculate the area of a peak in a chromatogram.

The software package used for the integration of peaks was Waters Mass Lynx 4.0. There are 2 main ways of integrating chromatographic peaks. The first method is to manually integrate each peak to obtain each peak area separately. The second method is an automated integration method which can be done simultaneously for all the samples in the sample list (potentially a few hundred peaks) within the same retention time range. By using the automated integration method, hundreds of peak integrations can be performed in the time taken to complete one manual peak integration. However, with automated integration, if the peaks present in each of the different chromatograms do not have peak areas and noise the resulting peak area s greater or less than the manual integration value. Therefore, it is critical to check each peak within each chromatogram which has been integrated automatically in order to determine whether a proper integration has been done.

The sample matrix, supernatant bacterial supernatant, is a very complex matrix which under full scan methods produces very complex spectra. However, since the analyses in this research were performed using MRM methods unique to each amino acid, the issue of co-eluting amino acids and multiple peaks was avoided.

By grouping similar data in which the same MRM program was used (i.e. data in which the same amino acids are being detected, therefore producing chromatograms with

peaks having similar or identical retention times), automated integration is possible, which allows for minimal 'tuning' of the integration parameters.

In this research, all injections were made manually and therefore slight shifts in retention times were to be expected.

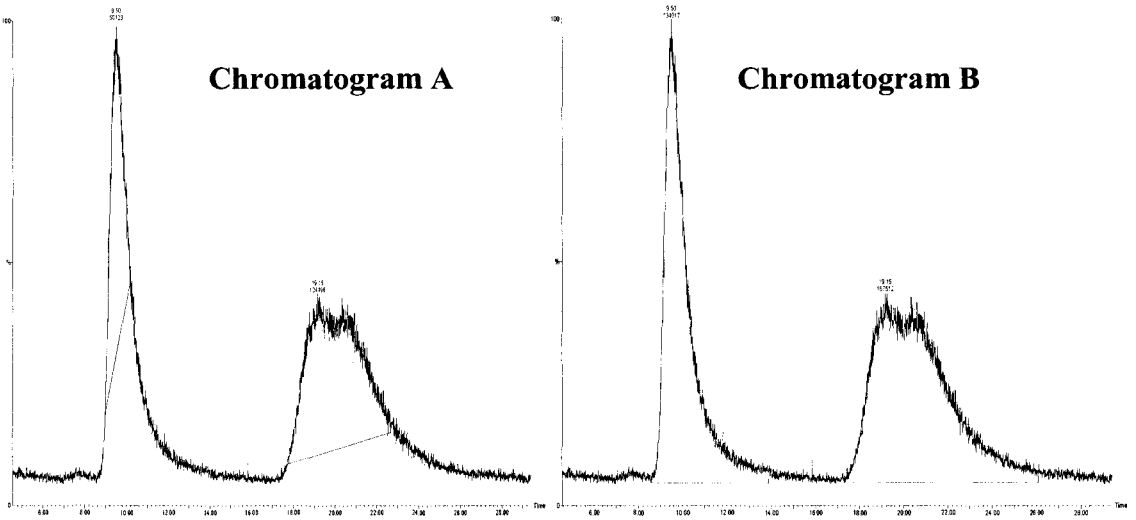

Figure 4-8: The difference between an automated integration (Chromatogram A) versus a manual integration (Chromatogram B).

Table 4-2: Difference in integration areas of peaks in Chromatograms A and B of Figure 4.8.

Chromatogram A (% Peak Integrated)		Chromatogram B (% Peak Integrated)	
Peak 1	45	Peak 1	100
Peak 2	80	Peak 2	100

Figure 4-8 demonstrates the difference in accuracy of automated versus manual integration and therefore the need to check whether a proper integration of the peaks has

been performed. In some cases, an automated integration produces chromatograms such as chromatogram B, where there is no need for tuning the integration parameters.

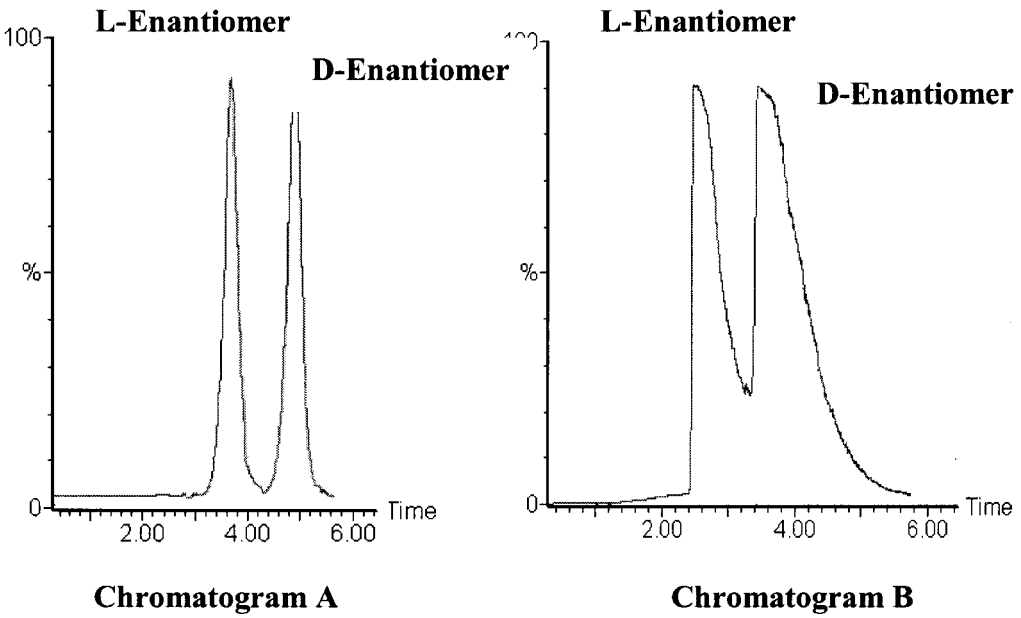

Figure 4-9: Chromatogram A shows a fully resolved separated pair of standards of D and L enantiomers of arginine under standard LC-MS/MS conditions compared to a partially resolved pair of enantiomers in Chromatogram B.

Figure 4-9 (A) illustrates the situation where the enantiomers of arginine are perfectly resolved such that no de-convolution is necessary and the area can be determined. The integration parameters are chosen such that integration for Figure 4-9, chromatogram A starts at the beginning of the point of curvature of the L-enantiomer (first eluting peak) and ends when the tail portion of the peak returns to the baseline. Chromatogram B of Figure 4.9 and Chromatogram A of Figure 4.10 demonstrate the situation of slightly unresolved peaks.

Their relative peak areas can be determined in one of two ways. In the first way a perpendicular line is dropped to the baseline at the minimum point on the valley between peaks (Figure 4-10 A).

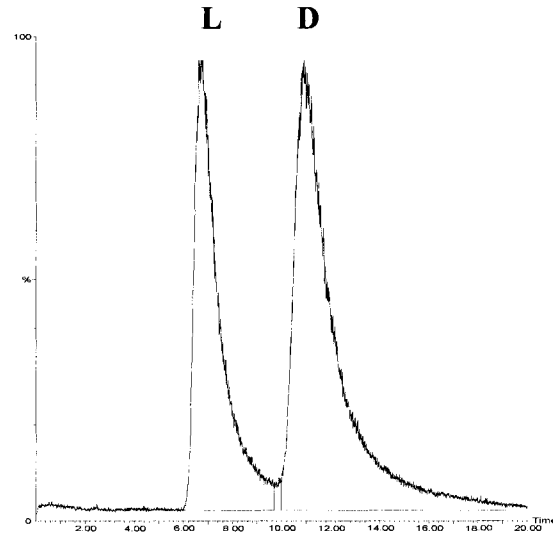

Figure 4-10: Deconvolution of overlapping peaks of the D and L enantiomers of valine.

4.2.2 Monitoring Column Performance

The column performance was monitored using 2,4-dimethylphenyl hydantoin, as recommended by the manufacturer (Astec).

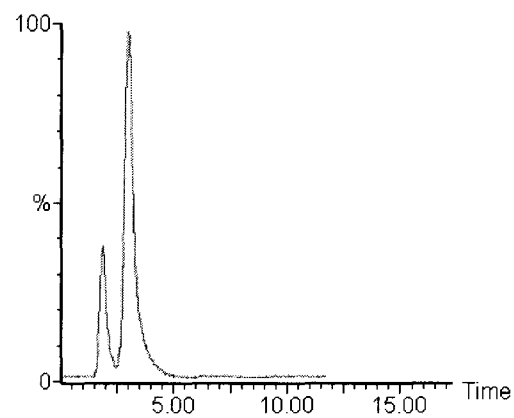

Figure 4-11: Chromatogram showing the resolution of the enantiomers of 2,4-dimethylphenyl hydantoin.

The chromatogram in Fig 4-11 indicates the performance of the column based on the shape and separation of the peaks. However, since this standard required a different mobile phase in order to evaluate the column performance, it was decided to use an amino acid standard to evaluate column performance routinely. A 20 pg/μL standard of L/D valine enantiomers was injected onto the column before any analyses were performed and after every 10 injections of samples. The peak shape (peak area and peak width) and the retention times of the enantiomers, was evaluated and compared to the initial injection of the valine standard. The column performance was deemed unacceptable when the retention time increased by approximately 0.5 minutes accompanied with increased peak broadening and peak tailing. Peak width increases greater than 35% were deemed unacceptable. An example of unacceptable column performance is shown in Figure 4-12. In this figure, there is tailing and peak broadening on the end of the chromatogram, compared to baseline resolution.

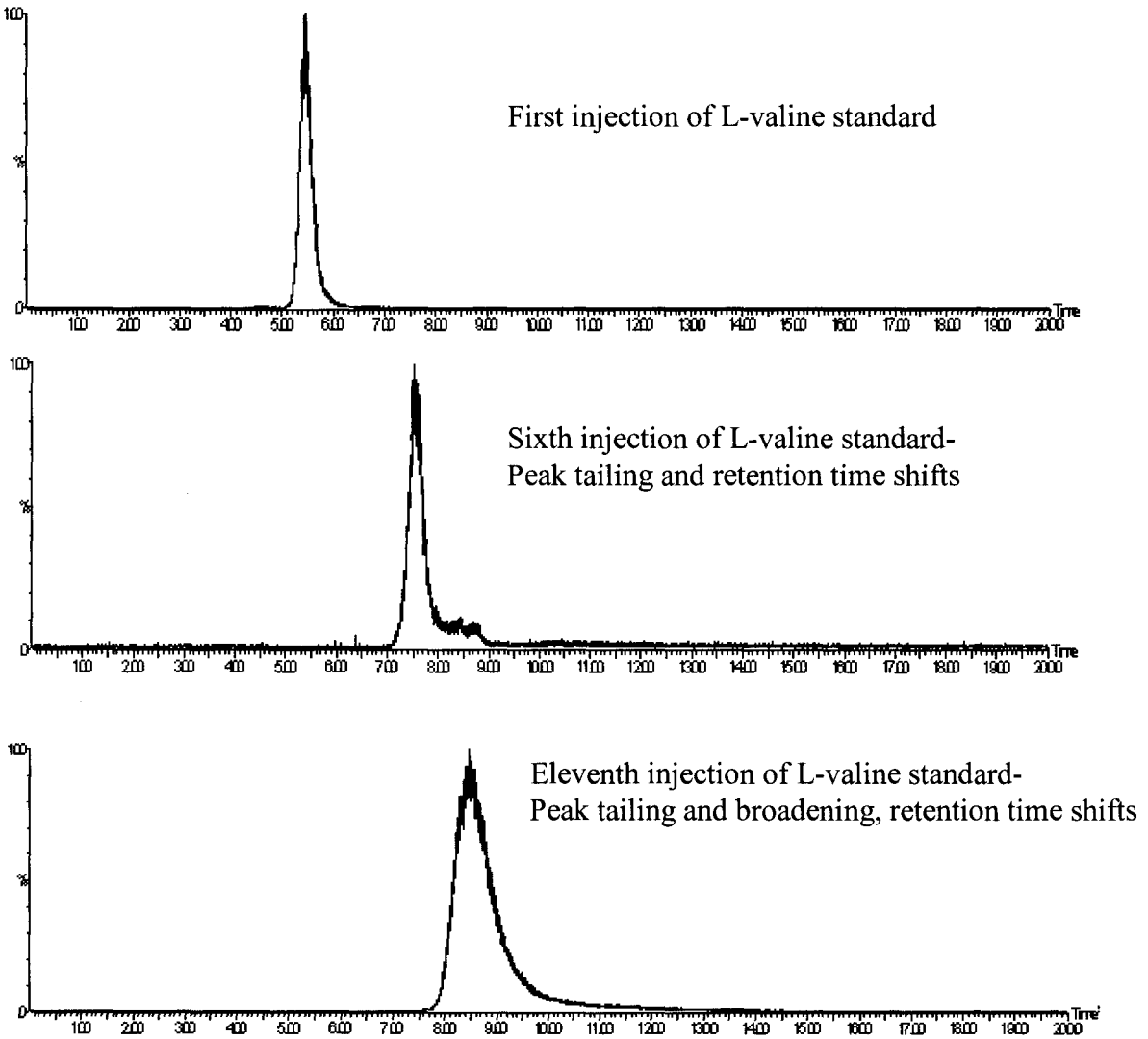

Figure 4-12: Changes in column performance demonstrated by an L-valine standard run under optimal LC-MS/MS conditions.

Figure 4-12 shows the change in column performance of an injection of L-valine. The first chromatogram illustrates good column performance with narrow peak widths and consistent retention times. The second chromatogram shows slight shifts in the

retention time accompanied by peak tailing. The third chromatogram shows significant peak broadening and shifts in retention time.

When the column performance has been determined to be unacceptable, as in the second and third chromatograms of Figure 4-12, the guard column is then detached from the column and each washed separately in reverse to the flow direction, with pure, distilled, de-ionized water at a flow rate of 1 mL/min for approximately 15 minutes or more depending on the subsequent column performance. Since one end of the column is open, there is no significant back pressure. The column and guard column are then flushed for a further 5 minutes with the mobile phase of 50:50 (v/v) methanol/water before being reattached and connected for analyses. The column performance is then rechecked with the same standard of valine and analyses restarted when the column performance returns to an acceptable level. The sample and standards are all highly soluble in water and therefore washing with water is sufficient and most rapid for restoring the column performance.

4.3 Determination of the Degree of Ion Suppression Factor

In the present work, *Sinorhizobium meliloti*, were grown on minimal growth media consisting of 100 mM of sodium and either 0 mM, 2 mM or 40 mM of phosphate (Refer to Table 4). After sampling, the medium was freeze dried, transferred to 10 mL eppendorf vials and freeze dried and stored at -80°C. Small volumes of methanol:water were added to reconstitute the samples resulting in concentrations which were higher than in the original media by factors ranging between 40 to 150-fold. (Refer to Table 6). The

potential for ion suppression in the ESI source exists so far as an evaluation of ion suppression was done by comparing the instrument response of the calibration standards in methanol/water solutions to that of the same calibration standards prepared in reconstituted growth media. Since the growth media were concentrated, they are referred to as $P0_{(40)}$, $P2_{(100)}$ and $P40_{(121)}$, with the subscripts representing the concentration factor. The amino acid standard was added as a 'spike' to the reconstituted media. This allowed for the evaluation of the effect of the sample matrix on the MS response thereby providing data on the degree of ion suppression. Three sets of 20 amino acid enantiomer pairs' standards were prepared individually as P40, P2 and P0 amino acid standards stock solutions. The total number of standards produced was 120; 3 sets of 20 amino acids, each of which contained the D and L enantiomer of each amino acid. A separate set of the same combination of amino acid standards were prepared using methanol/water (50:50(v/v)) as the solution instead of the growth medium solutions.

The calibration data for each amino acid was plotted using Excel and compared to the calibration plots for the amino acids which had been run in methanol/water (50:50 (v/v)).

The relative slopes of the calibration curves was the degree of ion suppression. Standards run in methanol/water were assigned a suppression factor of 1. The ion suppression factors are shown in Table 4-3.

The following calibration graphs illustrate the effect of ion suppression on amino acid standards caused in the three growth media compared to same standard run in methanol/water 1:1 ratio. The legend shown for the chart below is consistent for all

subsequent charts shown. The bold black trend line shown on certain charts indicates an overlapping of trend lines representing different conditions under which the standard was run, and thus having identical R^2 values.

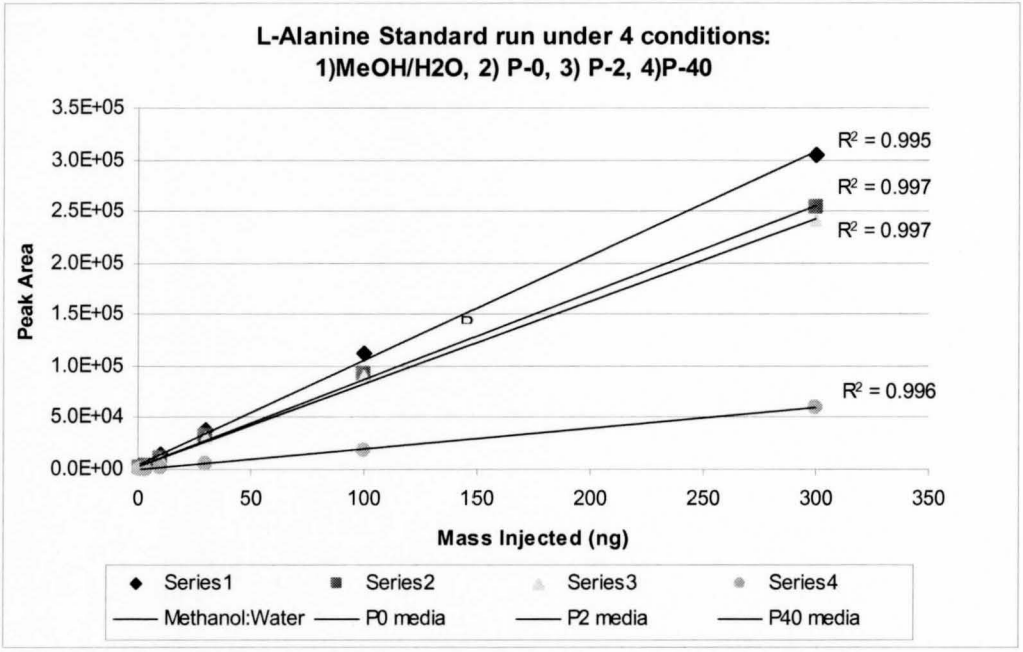

Figure 4-13: Calibration plot of an LC-MS/MS run of L-alanine, a neutral amino acid.

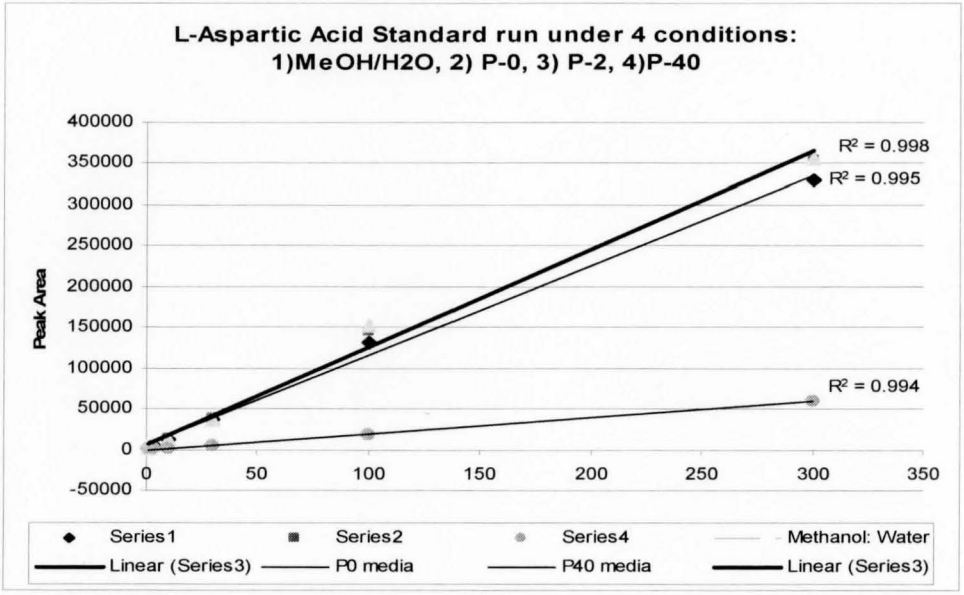

Figure 4-14: Calibration plot of an LC-MS/MS run of L-aspartic acid, an acidic amino acid.

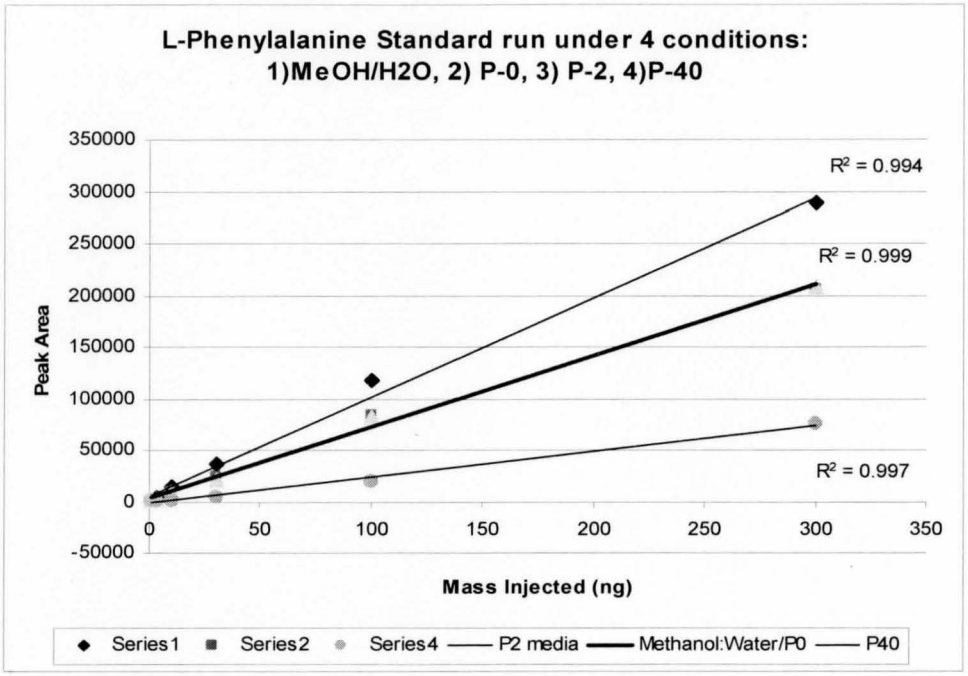

Figure 4-15: Calibration plot of an LC-MS/MS run of L-phenylalanine, a neutral amino acid.

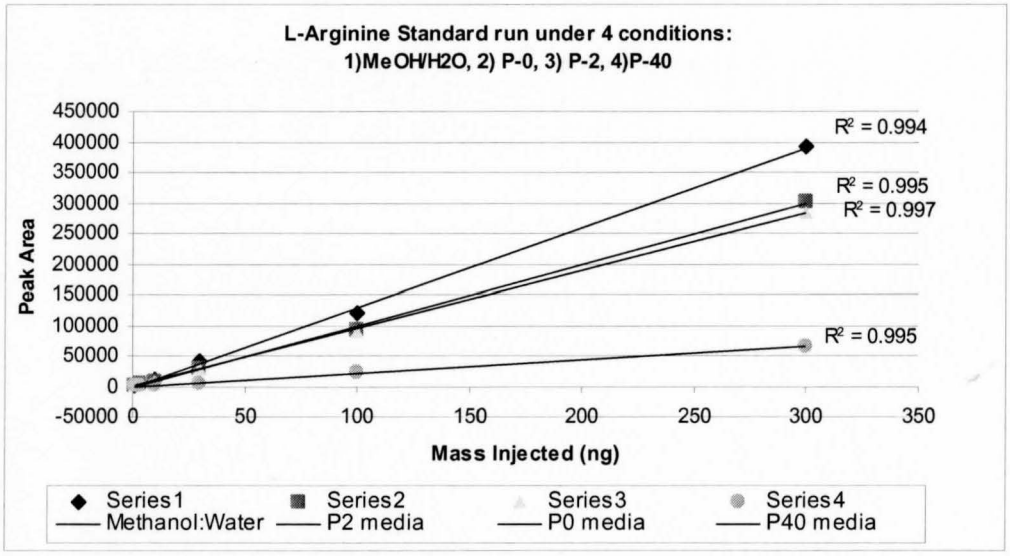

Figure 4-16: Calibration plot of an LC-MS/MS run of L-arginine, a basic amino acid.

Table 4-3: Ion Suppression Factors of amino acids in three concentrated growth media; $P0_{(40)}$, $P2_{(100)}$ and $P40_{(121)}$ compared to MeOH:H_2O.

	Ion Suppression Factors (n=5)		
Amino Acid	**$P0_{(40)}$**	**$P2_{(100)}$**	**$P40_{(121)}$**
Alanine	1.2 ± 0.06	1.2 ± 0.07	4.9 ± 1.3
Arginine	1.3 ± 0.08	1.3 ± 0.05	5.6 ±2.6
Aspartic Acid	0.9 ± 0.03	1.0 ± 0.05	7.1 ± 2.9
Cysteine	1.4 ± 0.08	1.6 ± 0.09	4.6 ± 3.2
Glutamic Acid	1.1 ± 0.04	1.1 ± 0.04	8.8 ± 3.1
Histidine	1.2 ± 0.05	1.2 ± 0.06	6.3 ± 2.4
Isoleucine	1.1 ± 0.04	1.2 ± 0.06	2.5 ± 1.7
Leucine	1.1 ± 0.06	1.1 ± 0.05	4.8 ± 2.6
Lysine	1.2 ± 0.08	1.2 ± 0.07	5.7 ± 2.5
Methionine	1.2 ± 0.05	1.2 ± 0.09	8.9 ± 3.8
Proline	1.3 ± 0.07	1.3 ± 0.10	7.2 ± 4.2
Phenylalanine	1.4 ± 0.10	1.2 ± 0.08	7.7 ± 4.2
Serine	1.2 ± 0.08	1.1 ± 0.04	7.5 ± 3.4
Tryptophan	0.8 ± 0.04	0.82 ± 0.04	6.0 ± 2.6
Threonine	0.8 ± 0.03	0.9 ± 0.05	4.4 ± 2.7
Tyrosine	0.7 ± 0.03	1.2 ± 0.07	6.8 ± 3.9
Valine	0.8 ± 0.05	1.3 ± 0.08	5.2 ± 2.8

Based on the four calibration plots shown in Figures 4-3 to 4-6, it is observed that the presence of the components of the growth media lowers the slope of the calibration standards. The greatest effects were experienced in the $P40_{(121)}$ medium, while the effect of the $P0_{(40)}$ and $P2_{(100)}$ media is significantly less. The ion suppression on account of the $P40_{(121)}$ medium was within the range of 3 to 8 times greater than the methanol/water solution while the suppression experienced on account of the $P0_{(40)}$ and $P2_{(100)}$ media was not greater than 0.6, which effectively means that no real ion suppression existed within

these media. The t-test which was done to compare the P values of the P0, P2 and methanol/water solutions showed that these three groups were effectively the same.
A sample of the t-test results are given in Table 4-4 showing the P values from t-tests comparing ion suppression values.

Table 4-4: Comparison of P values from t-test results of growth media P0, P2 and P40.

P0 vs Standard	**P2 vs Standard**	**P40 vs Standard**	**t-test for P0 vs P2**	**t-test for P2 vs P40**
Arginine				
0.86	0.82	0.16	0.76	0.24
0.82	0.76	0.39	0.89	0.14
0.97	0.98	0.24	0.97	0.35

The values obtained in the t-test clearly indicate that P2 and P0 are effectively the same sample since their t-values are above 0.5 compared to the values obtained for P40, which are significantly below 0.5.

Since the components of the growth media is exactly the same, with the exception of the phosphate concentration, then the effect observed by the $P40_{(121)}$ medium is due to the increase in ionic strength of this solution having 40mM of phosphate compared to $P0_{(40)}$, and $P2_{(100)}$ media respectively. Table 4-5 shows the difference in ionic strength of these three media.

Table 4-5: Ionic strength of three different growth media; P0, P2 and P40.

Growth Medium	$[PO_4^{3}]$ (mM)	Ionic Strength (M)
P0	0	0.168
P2	2	0.170
P40	40	0.311

As a consequence of this result, it was determined that all subsequent bacteria would be grown on $P0_{(40)}$, and $P2_{(100)}$ growth media. The $P40_{(121)}$ medium was therefore only used for determining the ion suppression caused by the 40mM of phosphate. No further work was done with P40 medium.

4.3.2 Ratio of Enantiomers

For the deconvolution of enantiomeric pairs, the L and D isomers can be resolved from each other and quantified accurately, provided that they are within a particular ratio. In all cases, the L enantiomer of any amino acid elutes before the D enantiomer. Our experiments were designed to determine what the chromatograms of the different enantiomeric ratios produced. With this data, it was determined what the minimum enantiomeric ratio needed to be for accurate deconvolution and quantification.

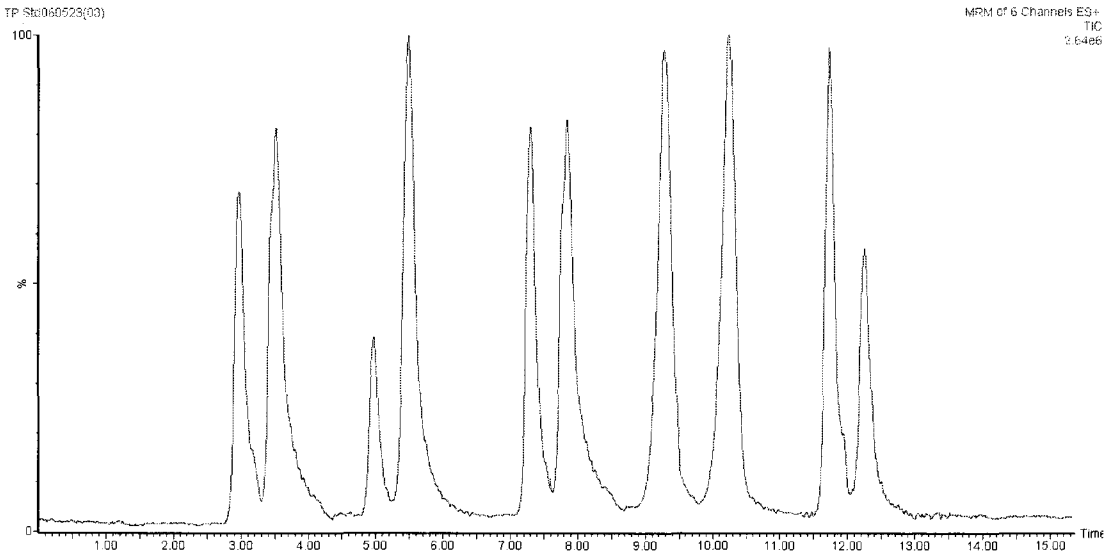

Fig 4-17: Ratio of five enantiomeric amino acid standards run in a single MRM program.

4.3.3 Determination of the Minimum Ratio for Enantiomeric Separation and Resolution of Amino Acids.

In order to determine the minimum ratio of one enantiomer that can be determined in the presence of the other, a series of different ratios of D to L enantiomers of amino acid was prepared. The following chromatograms illustrate the minimum percentage of the D enantiomer of valine which could be detected and resolved in the presence of the L enantiomer of valine. The first 2 chromatograms illustrate the chromatograms of D and L valine enantiomers, resolved independently as single solutions, while the subsequent chromatograms illustrate mixtures of D/L valine in varying percentages.

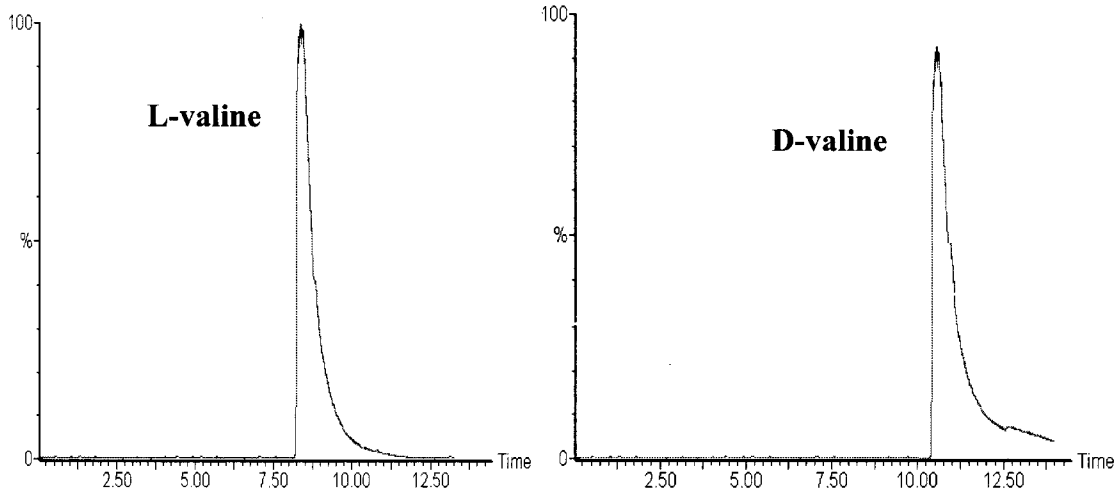

Figure 4-18: Chromatogram of D-valine and L-valine enantiomers run separately before being combined.

Figures 4-18 to 4-21 illustrate the minimum percentage of the D enantiomer of valine that could be resolved relative to a constant percentage of the L enantiomer of valine. The L enantiomer is always the first eluting peak.

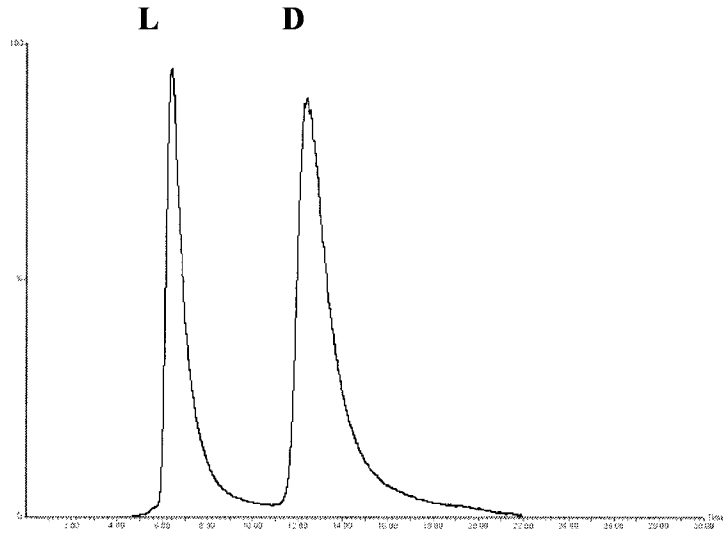

Figure 4-18': Chromatogram showing a 50:50 ratio of L:D enantiomers of valine

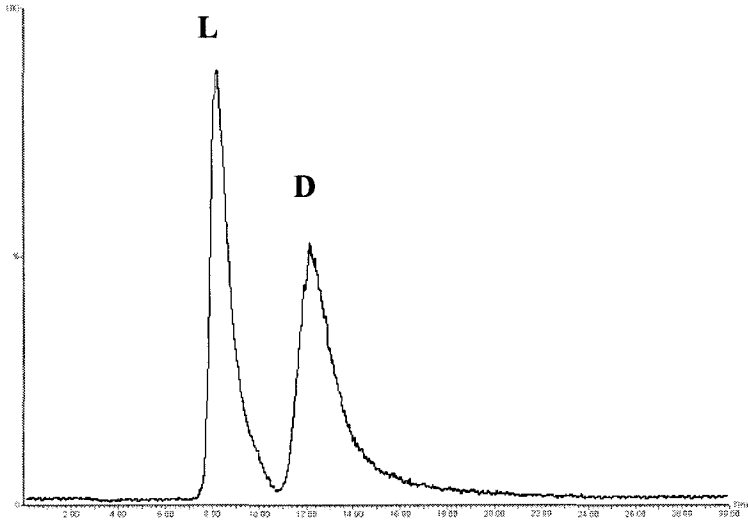

Figure 4-19: Chromatogram showing a 60:40 ratio of L:D enantiomers of valine

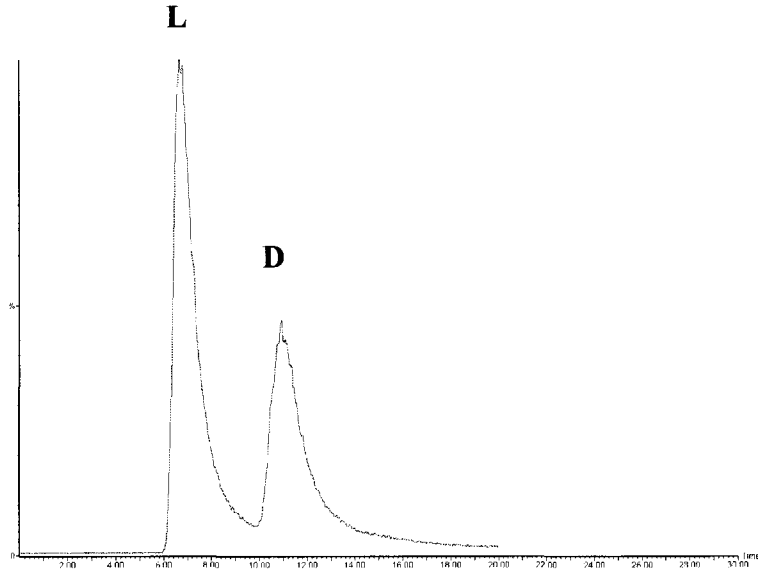

Figure 4-20: Chromatogram showing a 70:30 ratio of L:D enantiomers of valine.

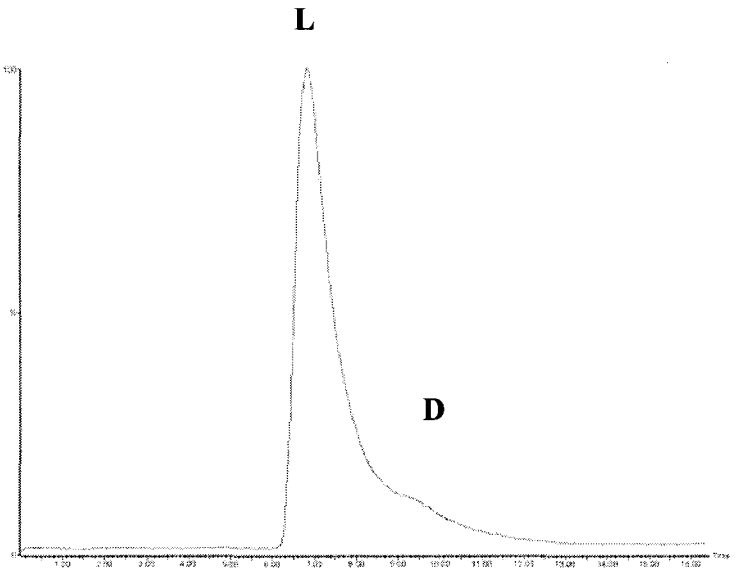

Figure 4-21: Chromatogram showing a 90:10 ratio of L:D enantiomers of valine.

Figures 4-22 to 4-26 illustrate the minimum percentage of the L enantiomer of valine which could be detected and resolved in the presence of the D enantiomer of valine.

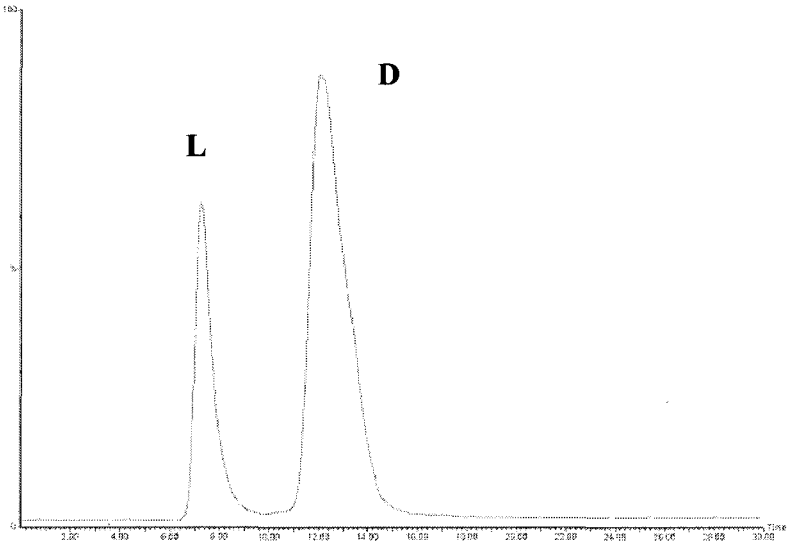

Figure 4-22: Chromatogram showing a 40:60 ratio of L:D enantiomers of valine

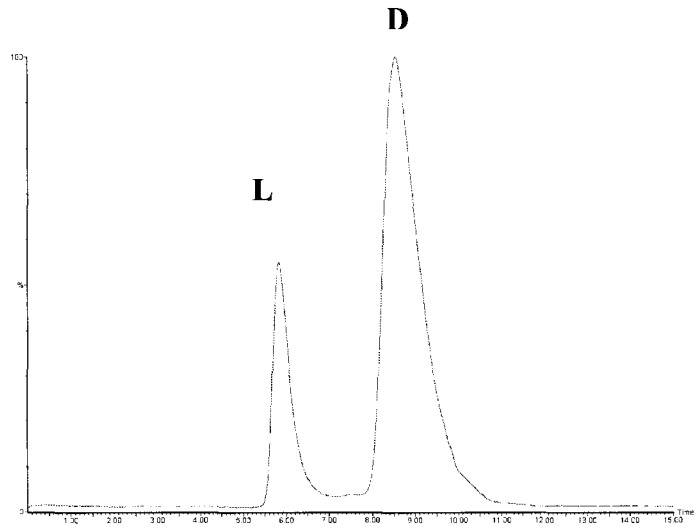

Figure 4-23: Chromatogram showing a 20:80 ratio of L:D enantiomers of valine.

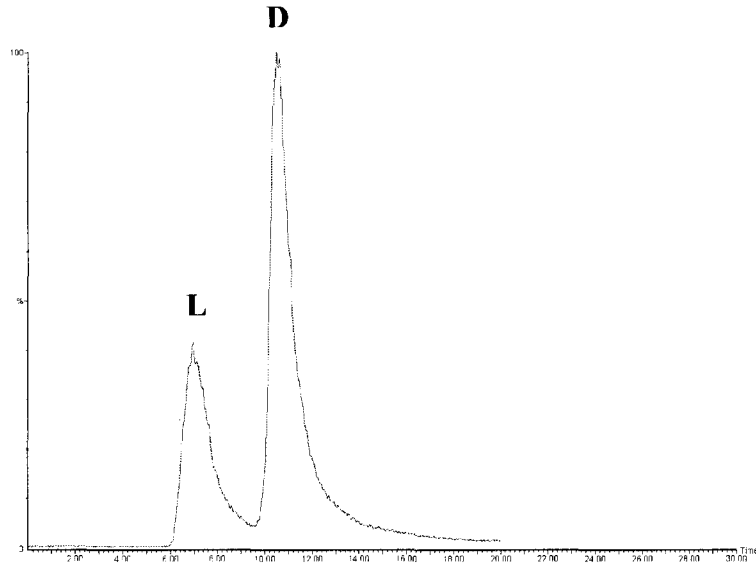

Figure 4-24: Chromatogram showing a 30:70 ratio of L:D enantiomers of valine

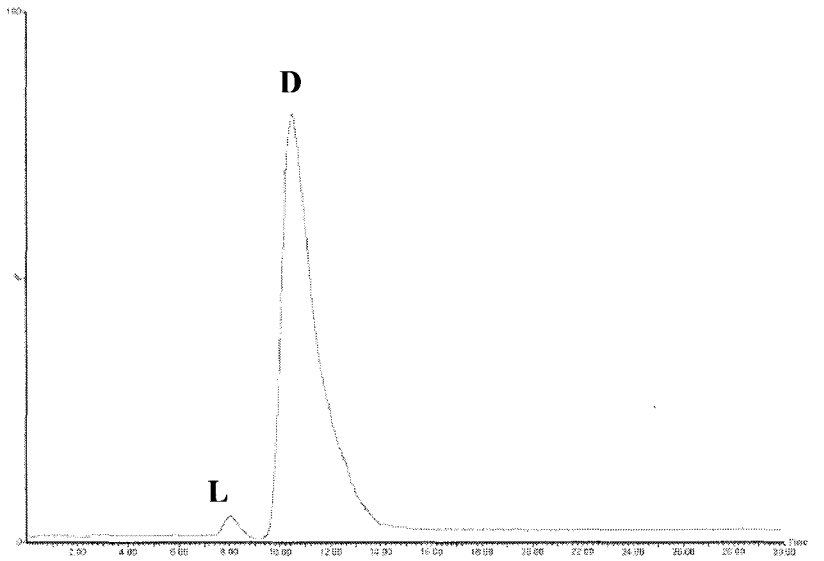

Figure 4-25: Chromatogram showing a 10:90 ratio of L:D enantiomers of valine

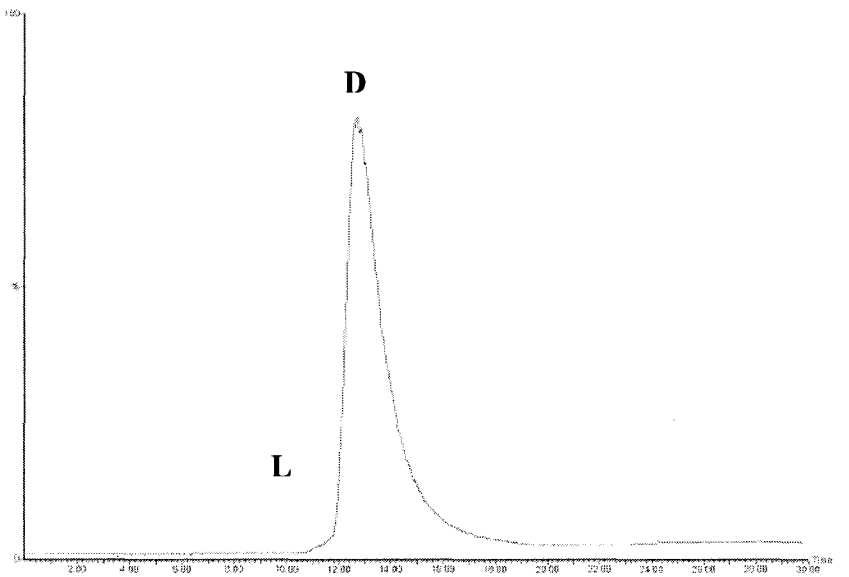

Figure 4-26: Chromatogram showing a 5:95 ratio of L:D enantiomers of valine

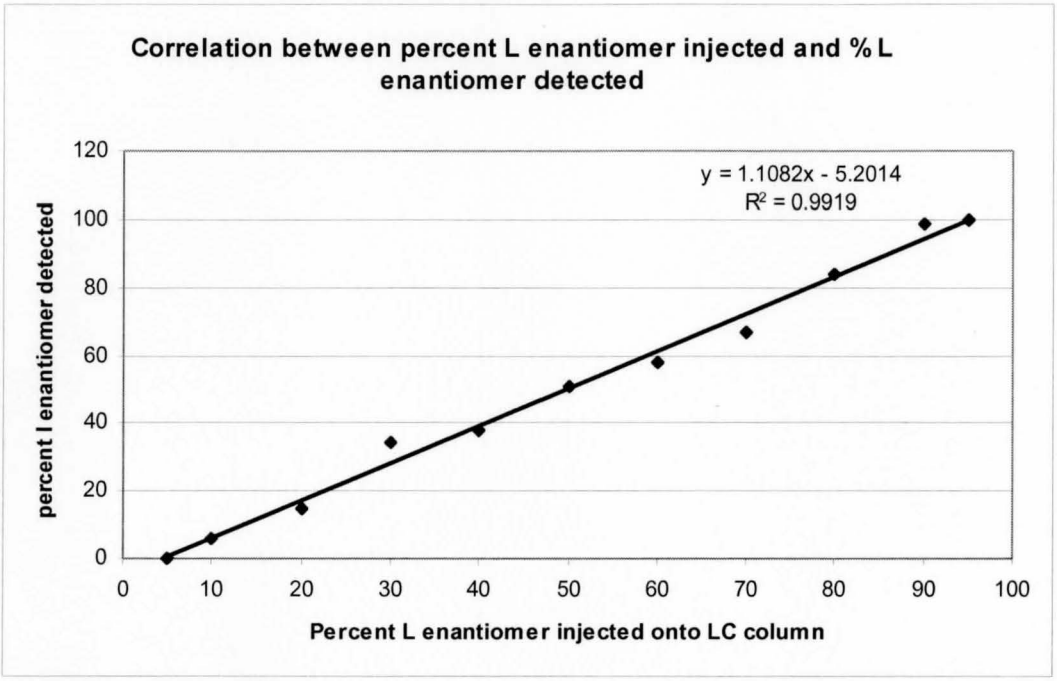

Figure 4-26': Correlation between percent L enantiomer injected and % L enantiomer detected.

The chart in Figure 4-26' illustrates the correlation between the percentage of the L enantiomer injected onto the LC column and the actual % of the L enantiomer detected. There is a strong correlation between the values of 20% to 80%. However, below 20% and above 80%, there are observable differences in the % of L enantiomer injected against that which is detected. Experimentally, the L and D enantiomer of each amino acid injected was distinguishable and quantifiable from each other, within the limit of a ratio of 90L:10D or 5L:95D. The minimum ratio for the observance of each amino acid

was tested for seventeen amino acids. They all conformed to the ratio of 90L:10D or 5L:95D.

4.4 Data from the Supernatant of *Sinorhizobium meliloti*

There were two groups of exo-metabolomic bacterial samples which were examined to determine the composition of detectable D and L amino acids present. The following chromatograms show the enantiomers in the exometabolome of *S. meliloti* bacteria which was grown on phosphate starved (P0) media, containing 0 mM phosphate.

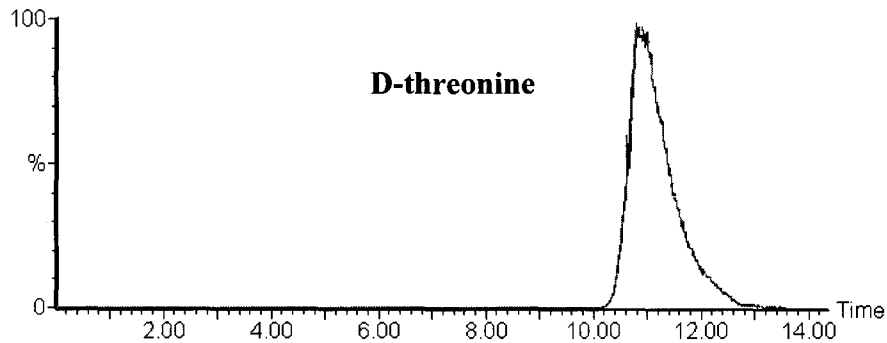

Figure 4-27: Chromatogram showing only D-threonine in a P0 supernatant sample of *Sinorhizobium meliloti*.

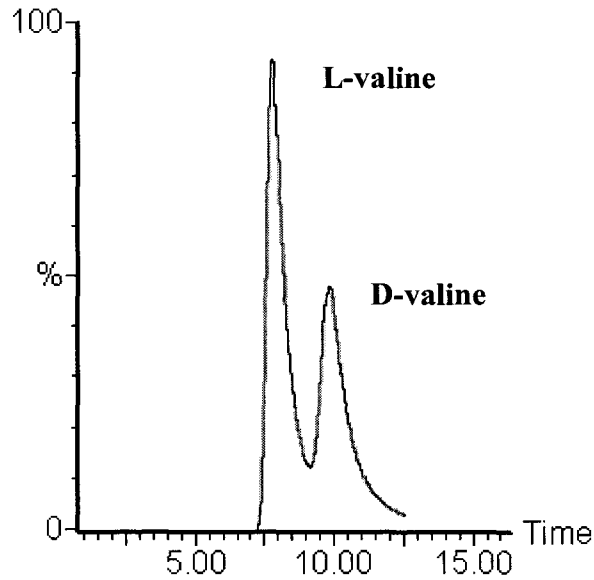

Figure 4-28: Chromatogram showing D/L-valine in a P0 supernatant sample of *Sinorhizobium meliloti.*

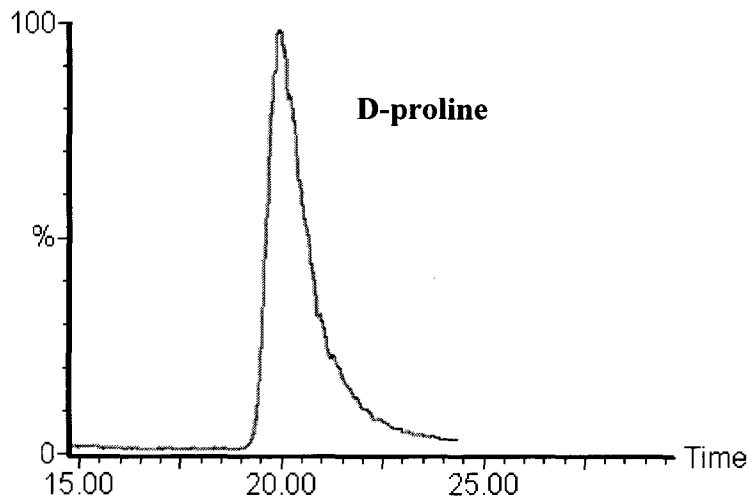

Figure 4-29: Chromatogram showing only D-proline resolved from a P0 supernatant sample of *Sinorhizobium meliloti.*

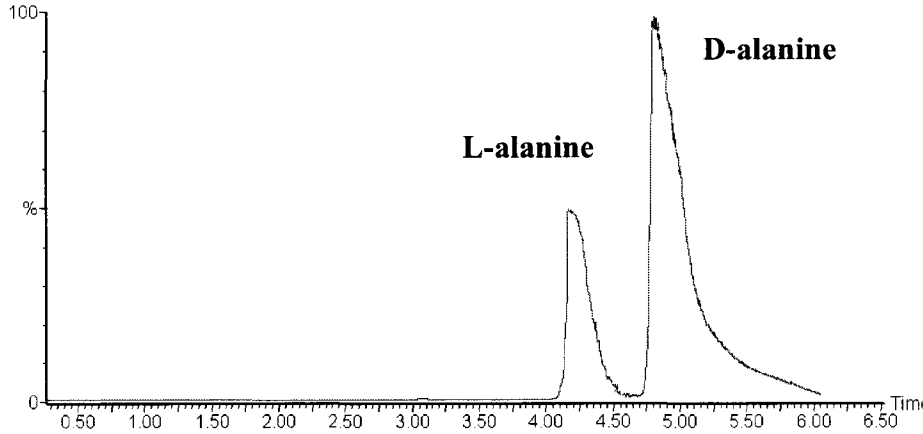

Figure 4-30: Chromatogram showing only D/L-alanine resolved from a P0 exo-metabolomic sample of *Sinorhizobium meliloti*.

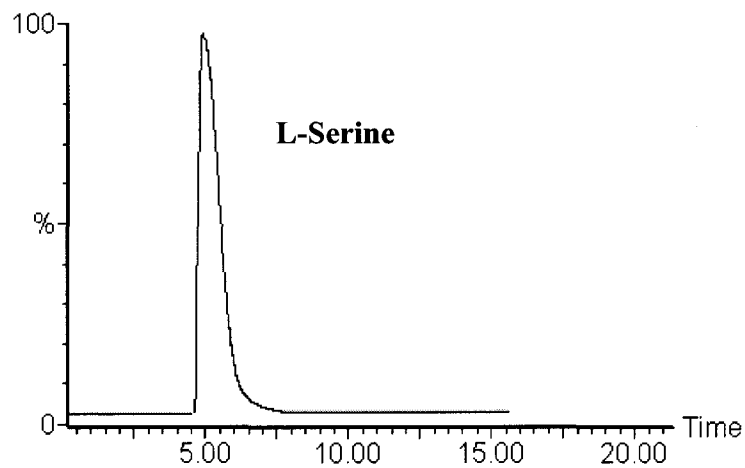

Figure 4-31: Chromatogram showing only L-serine resolved from a P0 exo-metabolomic sample of *Sinorhizobium meliloti*

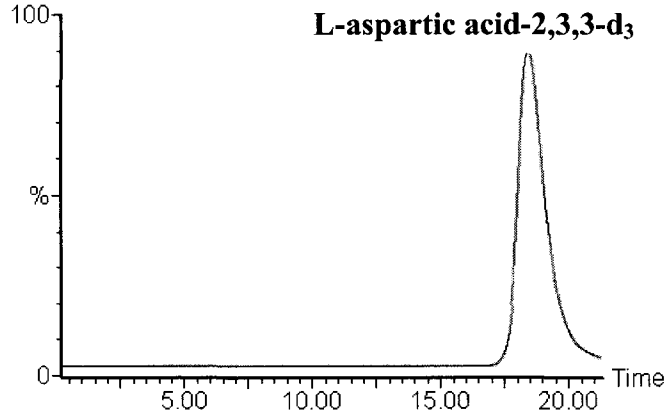

Figure 4-32: Chromatogram showing the L-aspartic acid-2,3,3-d_3 standard run in a solution of 50:50 methanol/water.

Figures 4-28 to 4-32 show the specific enantiomers of the detectable amino acids which were present in the supernatant of *Sinorhizobium meliloti* bacteria which was grown on minimal growth media (P2), containing 2 mM of phosphate.

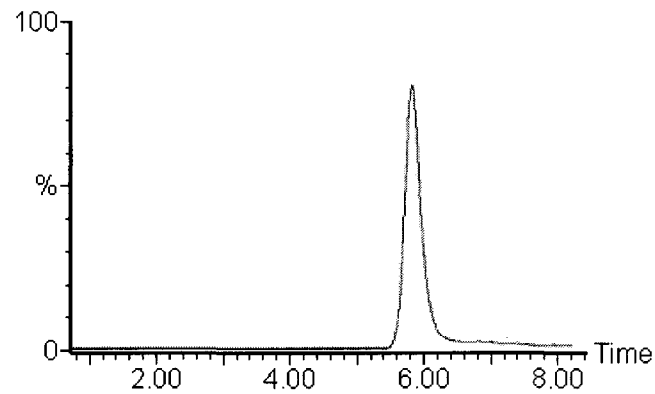

Figure 4-33: Chromatogram showing L-serine resolved from a P2 exo-metabolomic sample of *Sinorhizobium meliloti*

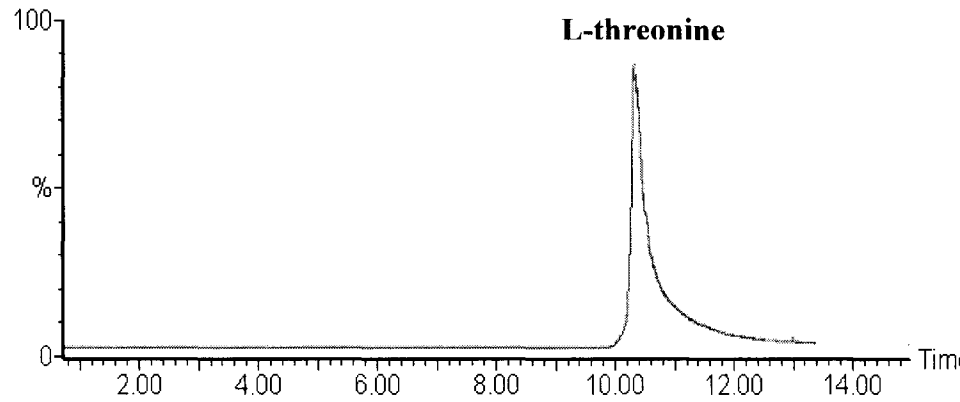

Figure 4-34: Chromatogram showing L-threonine resolved from a P2 exo-metabolomic sample of *Sinorhizobium meliloti*

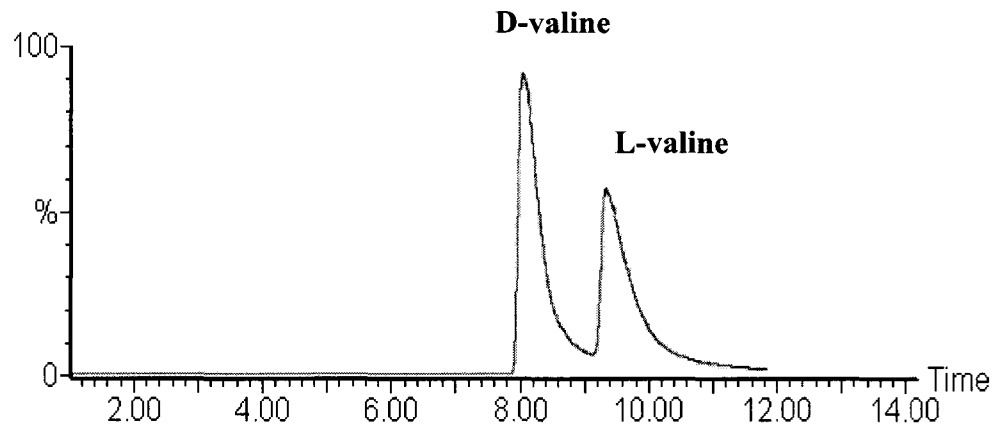

Figure 4-35: Chromatogram showing D/L-valine resolved from a P2 exo-metabolomic sample of *Sinorhizobium meliloti*

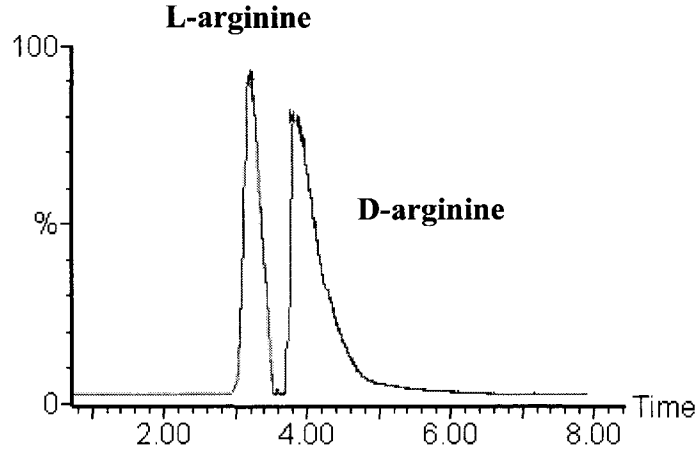

Figure 4-36: Chromatogram showing D/L-arginine resolved from a P2 exo-metabolomic sample of *Sinorhizobium meliloti*

For each of the two growth media investigated, several differences were observed, while there were also some similarities, as expected. For both media investigated, serine, threonine and valine were observed in comparable concentrations to each other. In neither case was aspartic acid detected. The striking differences in the amino acid composite was the absence of alanine and proline in the P2 growth medium while being present in the P0 medium and similarly, the absence of arginine in the P0 medium, when it is clearly present in the P2 medium. The absence of any amino acid from the given supernatant sample does not necessarily indicate a complete absence from the sample, but rather, an undetectable concentration of amino acid, which lies below the detection limit of the MS/MS. However, the 'absence' of these amino acids from either the P0 or P2 media does indicate that they are either being produced or restricted as a direct consequence of the differing concentrations of the necessary components for bacterial growth and metabolism.

A series of t-tests were performed on the data results obtained from samples which were grown on both P2 and P0. Based on the t-tests, these results showed no significant variation. Based on the calibration data, these two data sets were determined to have the same ion suppression factor, and hence, were considered to be the same data set.

Table 4-6: The mean concentrations of the D and L enantiomers of the amino acids detected in the sample of extracellular supernatant of *Sinorhizobium meliloti* grown in P2 growth medium.

Amino Acid / P2	**Retention Time (mins)**		**Concentration (μg/L)**		**L/D Ratio**
n = 15	**L**	**D**	**L**	**D**	
Serine	5.7		7.2 ± 1.16		
Threonine		11.3		11.2 ± 2.7	
Valine	7.4	10.8	15.5 ± 4.3	11.3 ± 3.7	1.38
Alanine					
Arginine	4.0	3.8	12.6 ± 3.1	10.1± 3.2	1.25
Proline					
Aspartic Acid					
Aspartic Acid-2,3-3d$_3$	4.7		120 ±10.2		

Table 4-7: The mean concentrations of the D and L enantiomers of the amino acids detected in the sample of extracellular supernatant of *Sinorhizobium meliloti* grown in P0 growth medium.

Amino Acid / P0	**Retention Time (mins)**		**Concentration (μg/L)**		**L/D Ratio**
n = 15	**L**	**D**	**L**	**D**	
Serine	5.9		7.6 ± 1.2		
Threonine		11.5		10.2 ± 3.2	
Valine	7.6	11.2	11.6 ± 2.3	10.1 ± 3.1	1.15
Alanine	4.1	5.1	7.7 ± 1.2	13.4 ± 2.5	0.57
Arginine					
Proline		21.3		8.6 ± 1.3	
Aspartic Acid					
Aspartic Acid-2,3,3d$_3$	4.8		120 ± 6.1		

Table 4.8: Detection limits of amino acids detected in *Sinorhizobium meliloti*

L-Amino Acid Standard	Detection Limit µg/L	Detection Limit (P0) µg/L	Detection Limit (P2) µg/L	Detection Limit (P40) µg/L
Alanine	1.8	2.1	2.6	14.6
Arginine	2.9	5.2	4.7	24.5
Aspartic Acid	1.3	5.72	4.8	29.3
Proline	3.8	4.1	3.8	21.3
Serine	2.5	3.6	4.6	21.4
Threonine	3.7	4.1	3.8	14.6
Valine	2.9	3.0	3.6	13.9

D-Amino Acid Standard	Detection Limit µg/L	Detection Limit (P0) µg/L	Detection Limit (P2) µg/L	Detection Limit (P40) µg/L
Alanine	1.6	2.4	3.1	15
Arginine	3.2	5.0	5.1	23.5
Aspartic Acid	1.7	5.6	4.6	31.2
Proline	3.5	3.5	3.2	24.7
Serine	2.7	3.6	4.1	23.6
Threonine	4.0	4.0	4.1	15.0
Valine	2.6	3.0	3.2	12.7

5.0 Conclusion and Future Work

The method which has been optimised and described within this research is a reproducible, effective methodology for separating, identifying and quantifying the D and L enantiomers of twenty amino acids in less than fifteen minutes. This methodology allows for the rapid analysis of metabolites without any pre treatments such as derivatization or clean up protocols.

By utilising an LC-MS/MS approach, the D and L enantiomers of the six bacterial amino acids were identified and quantified in the wild type strain of S*inorhizobium meliloti* bacteria. However, based on the studies done with multiple groups of amino acids, this method would be amenable to the simultaneous identification, quantification and chiral separation of twenty amino acids in less than fifteen minutes. The advantage of this method is that rapid analyses for the immediate detection of metabolic disorders from blood or urine samples may be a possible future application. Since the growth medium excluded all amino acids, it could be deduced that all of the detected amino acids were produced from the bacteria. The difference observed in detection of chiral amino acids in the P0 media against the P2 media can be attributed to the difference in phosphate levels resulting on an increase in the stress which the bacteria experienced in the P0 media since no phosphate is present for the formation of phosphor-compounds in bacterial metabolism. Therefore, through strained pathways, the bacteria may have produced proline in the P2 media versus the P0 media.

Studies which could be embarked upon in the future include probing through several different stress factors/stimulus on the production/suppression of the D and L amino acids present/metabolites, or on the amino acid/metabolite production in general.

The most severe limitation of this method arises as a result of not having a clean up protocol. Since the entire growth medium is present in the sample, it gives rise not only to ion suppression, but also causes the column to become clogged after running just ten 1ul samples. This problem however could be minimised or overcome very easily by utilising two columns. When one column becomes clogged, then the other column could be automatically switched over to for a continuation of analyses. Alternatively, two guard columns could be used and simply switched after ten samples have been run.

In this research it was not possible to make comparisons between the exo-metabolome and the endo-metabolome. As a consequence the pathways responsible for the differences seen in the two different growth media was not determined. The method optimized and tested within this research would allow for these further investigations to be done.

References:

1. Wan, H, Blomberg, L.G, *J. Chromatography A.*, 875 (2000) 43.
2. Piraud, M, Vianey-Saban, C, Petritis, K, Klfakir, C, Steghens, J. P, Moria, A,Bouchu, D, *Rapid Commun. Mass Spectrom.*, 17 (2003) 1297.
3. Petritis, K, Elfakir, C, Dreux, M, *J. Chromatography A.*, 961 (2002) 9.
4. Rogalewicz, F, Hoppilliard, Y, Ohanessian, G, *Int. J. Mass Spectrom.*, 195/196 (2000) 565.
5. Thorsen, G, Bergquist, J, *J. Chromatography B.*, 745 (2000) 389.
6. Barch, A, Patschkowski, T, Niehaus, K, *Funct Integr Genomics.*, 4 (2004) 219.
7. Zhao, Q, Sannier, F, Garreu, I, Lecoer, C, Piot, J. M, *J. Chromatography A.*, 723 (1996) 35.
8. Bordajandi, L.R, Ramos, L, Gonzales, M. J, *J. Chromotagraphy A.,*, 1078 (2005) 128.
9. Berthod, A, Liu, Y, Bagwill, C, Armstrong, D. W, *J. Chromatography A.*, 731 (1996) 123.
10. Lindley, N. D, Letisse, F, *Biotechnol. Letters* 22 (2000) 1673.
11. Hao, C, March, R. E, Croley, T, T, Smith, J, C, Rafferty, S, P, *J. Mass Spectrom.*, 36, (2001) 79.
12. Tesarova, E, Bosakova, Z, Pacakova, V, *J. Chromatography A.*, 838 (1999) 121.
13. Zhao, S, Song, Y, Liu, Y, M, *Talanta.*, 67 (2005) 212.
14. Berthod, A, Yu, T, Kullman, J. P, Armstrong, D. W, Gasparrini, F, Acquarica, I, D, Misiti, D, Carotti, A, *J. Chromatography A.*, 897 (2000) 113.

15. Berthod, A, Liu, Y, Bagwill, C, Armstrong, D. W, *J. Chromatography A.,* 731(1996) 123.

16. Kataoka, H, Matsumura, S, Makita, M, *J Pharmaceut Biomed Anal.,* 15(1997) 1271.

17. Hirose, K, Yongzhu, J, Nakamura, T, Nishioka, R, Ueshige, T, Tobe, Y, *Chirality.,*17(2005) 142.

18. Zoppa, M, Gallo, L, Zacchello, F, Giordano, G, *J. Chromatography B.,* 831(2006), 267.

19. Slyudkin, O. P, Tulupov, A. A, *Russ J Coord Chem.,* 31(2005), 83.

20. Ryu, J. W, Kim, D, W, Lee, K, P, Pyo, D, Park, J, H, *J. Chromatography A.,*814(1998) 247.

21. Ryu, J. W, Kim, D, W, Lee, K, P, Pyo, D, Park, J, H, *J. Chromatography A.,*814(1998) 247.

22. Elek, J, Mangelings, D, Ivanyi, T, Lazar, I, Heden, Y. V, *J Pharmaceut Biomed Anal.,* 38(2005) 601.

23. Xiao, T, L, Tesarova, E, Anderson, J, L, Egger, M, Armsgtrong, D, W, *J. Sep. Sci.,*29(2006) 429.

24. Chen, S, Ward, T, *Chirality.,* 16(2004) 318.

25. Dzygiel, P, Wieczorek, P, Kafarski, P, *J. Sep. Sci.* 26(2003) 1050.

26. Berthod, A, Chen, X, Kullman, J. P, Armstrong, D, W, *Anal. Chem.,* 72(2000) 1767.

27. Peter, A, Arki, A, Tourwe, D, Forro, E, Fulop, F, Armstrong, D, W, *J. Chromatography A.,* 1031(2004) 159.

28. Dalluge, J, Smith, S, Sanchez-Riera, F, McGuire, C, Hobson, R, *J. Chromatography A.,* 1043(2004) 3.

29. Lee, H. S, Hong, J, *J. Chromatography, A.,* 868(2000), 189.

30. Tang, W. H, Muderawan, W, Ong, T. T, Ng, S. C, *Anal Chim Acta.,* 546(2005) 119.

31. Stocchi, V, Piccoli, G, Magnani, M, Palma, F, Biagiareli, B, Cucchiarini, L, *Anal. Biochem.,* 178(1989) 107.

32. S.A. Cohen, D.P. Michaud, Anal. Biochem. 211 (1993) 279. [37] S.N. Brune, D.R. Bobbitt, *Talanta* 38 (1991) 419.

33. S.A. Cohen, K.M. De Antonis, *J. Chromatography, A* 661 (1994) [38] S.N. Brune, D.R. Bobbitt, Anal. Chem. 64 (1992) 166.

34 W.A. Jackson, D.R. Bobbitt, *Anal. Chim. Acta* 285 (1994)

35. H.A. Moye, A.J. Boning Jr., *Anal. Lett.* 12 (1979) 25. 309.

36. S.S. Simons Jr., D.F. Johnson, *J. Am. Chem. Soc.* 98 (1976)

37. P. Edman, in: S.B., X. Wang, D.R. Bobbitt, *Anal. Chim. Acta* 383 (1999) 213.

38. G. Ogde, P. Fo¨ldi, LC?GC 5 (1987) 28. [43] R. Schuster, *Anal. Chem.* 52 (1980) 617.

39. G. Sarwar, H.G. Botting, *J. Chromatogr.* 615 (1993) 1.

40. T. Iida, H. Matsunaga, T. Fushima, T. Santa, H. Homma, K. 41 Imai, *Anal. Chem.* 69 (1997) 4463. [45] K. Petritis, P. Chaimbault, C. Elfakir, M. Dreux, *J. Chromatography*

42. H. Godel, P. Seitz, M. Verhoef, LC–GC Int. 5 (1992) 44. *J.Chromatogr A* 833 (1999) 147.

43. V.A. Davankov, *Adv. Chromatogr.* 22 (1983) 71. togr. A 855 (1999) 191.

45 P. Chaimbault, K. Petritis, C. Elfakir, M. Dreux, Ellis Horwood, Chichester,*J. Chromatogr. A*, 1989, p. 446

46. S. Vidyasankav, M. Ru, R.H. Arnold, *J. Chromatogr. A* 775 togr. A 896 (2000) 253. (1997)

47. M. Remelli, P. Fornasari, F. Pulidori, *J. Chromatogr. A* 761 togr. A 896 (2000) 335. (1997) 79. [50] I.G. Casella, M. Gatta, T.R.I. Cataldi, *J. Chromatogr. A* 878

48. D.W. Armstrong, X. Yang, S.M. Han, R.A. Menges, Anal. (2000) 57.

49. M. Schlauch, A.W. Frahm, *J. Chromatogr. A* 868 (2000) 197.

50. F. Gimenez, M. Soursac, R. Farinotti, *Chirality* 9 (1997) [53] Chirobiotic Handbook, Advanced Separation Technologies 150. Inc., 3rd ed., 1999.

51. M.H. Hyun, J.S. Jin, W. Leu, *J. Chromatogr. A* 822 (1998)

52. D.R. Bobbitt, W.A. Jackson, H.P. Hendrickson, *Talanta* 467098. (1998) 565.

52. J. O. Castrillo and S. G. Oliver, J. Biochem. Mol. Biol., 2004, 37, 93–106.2 G.

53. S. G. Oliver, M. K. Winson, D. B. Kell and F. Baganz, *Trends Biotechnol.*, 1998, 16, 373-378.

54. G. G. H. a. R. Goodacre, Metabolic Profiling: Its Role in Biomarker Discovery and Gene Function Analysis, Kluwer Academic Publishers, London, 2003.

55. R. Goodacre, S. Vaidyanathan, W. B. Dunn, G. G. Harrigan and D. B. Kell, *Trends Biotechnol.*, 2004, 22, 245–252.

56. J. Forster, I. Famili, P. Fu, B. O. Palsson and J. Nielsen, *Genome Res.*, 2003, 13, 244–253.

57. O. Fiehn, Comp. Funct. Genomics, 2001, 2, 155–168.8 B. Lahner, J. M. Gong, M. Mahmoudian, E. L. Smith, K. B. Abid, E. E. Rogers, M. L. Guerinot, J. F. Harper, J. M. Ward, L. McIntyre, J. I. Schroeder and D. E. Salt, *Nat. Biotechnol.*, 2003, 21, 1215–1221.

58. J. K. Nicholson, J. C. Lindon and E. Holmes, Xenobiotica, 1999, 29, 1181–1189.

59. J. K. Nicholson, J. A. Timbrell and P. J. Sadler, *Mol. Pharmacol.*, 1985, 27, 644–651.

60. S. I. Goodman, *Am. J. Hum. Genet.*, 1980, 32, 781–792.

61. L. M. Raamsdonk, B. Teusink, D. Broadhurst, N. S. Zhang, A. Hayes, M. C. Walsh, J. A. Berden, K. M. Brindle, D. B. Kell, J. J. Rowland, H. V. Westerhoff, K. van Dam and S. G. Oliver, *Nat. Biotechnol.*, 2001, 19, 45–50.

62 J. H. Gross, *Mass Spectrometry*: A Textbook, Springer, Berlin, 2004.

63 J. C. Lindon, J. K. Nicholson and I. D. Wilson, *J. Chromatogr. B,* 2000, 748, 233–258.

64 R. Goodacre, S. Vaidyanathan, G. Bianchi and D. B. Kell, Analyst, 2002, 127, 1457–1462.

65 P. Frycak, R. Huskova, T. Adam and K. Lemr, *J. Mass Spectrom.*, 2002, 37, 1242–1248.

66. C. Wittmann, J. O. Kromer, P. Kiefer, T. Binz and E. Heinzle, *Anal. Biochem.*, 2004, 327, 135–139.

67. M. E. Hansen and J. Smedsgaard, J. Am. Soc. *Mass Spectrom.*, 2004, 15, 1173–1180.

135 R. M. Alonso-Salces, K. Ndjoko, E. F. Queiroz, J. R. Ioset, K. Hostettmann, L. A. Berrueta, B. Gallo and F. Vicente, *J. Chromatogr. A*, 2004, 1046, 89–100.

68. J. L. Wolfender, K. Ndjoko and K. Hostettmann, *J. Chromatogr.A*, 2003, 1000, 437–455.

69. J. J. Dalluge, S. Smith, F. Sanchez-Riera, C. McGuire and R. Hobson, *J. Chromatogr. A*, 2004, 1043, 3–7.

70. P. Schmitt-Kopplin and M. Frommberger, *Electrophoresis*, 2003, 24, 3837–3867.

71. T. Soga, Y. Kakazu, M. Robert, M. Tomita and T. Nishioka, *Electrophoresis*, 2004, 25, 1964–1972.

72. S. Zomer, C. Guillo, R. G. Brereton and M. Hanna-Brown, *Anal.Bioanal. Chem.*, 2004, 378, 2008–2020.

73. L. Jia, B. F. Liu, S. Terabe and T. Nishioka, *Anal. Chem.*, 2004, 76, 1419–1428.

196 R. M. Jarvis, A. Brooker and R. Goodacre, *Anal. Chem.*, 2004, 76, 5198–5202.

74. J. Schmitt, M. Beekes, A. Brauer, T. Udelhoven, P. Lasch and D. Naumann, Anal. Chem., 2002, 74, 3865–3868.

75. J. McElhinney, G. Downey and C. O'Donnell, *J. Food Sci.*, 1999, 64, 587–591.

76. M. Defernez and R. H. Wilson, *J. Sci. Food Agric.*, 1995, 67, 461–467.

77. F. J. Rambla, S. Garrigues, N. Ferrer and M. de la Guardia, *Analyst*, 1998, 123, 277–281.

78. B. S. Kristal, K. E. Vigneau-Callahan and W. R. Matson, *Anal.Biochem.*, 1998, 263, 18–25.

79. J. Forshed, I. Schuppe-Koistinen and S. P. Jacobsson, *Anal.Biochem,* 2003, 487, 189–199.

80 G. C. Lee and D. L. Woodruff, *Anal.Biochem*, 2004, 513, 413–416.

81 H. C. Keun, T. M. D. Ebbels, H. Antti, M. E. Bollard,O. Beckonert, E. Holmes, J. C. Lindon and J. K. Nicholson, *Anal.Biochem,* 2003, 490, 265–276.

Appendix 1

The following charts are the calibration curves of the L enantiomers of 20 amino acids which were each run in four different media. The media are specified as either methanol: water, P0 growth media, P2 growth media or P40 growth media. The legend is the same for all of the calibration plots.

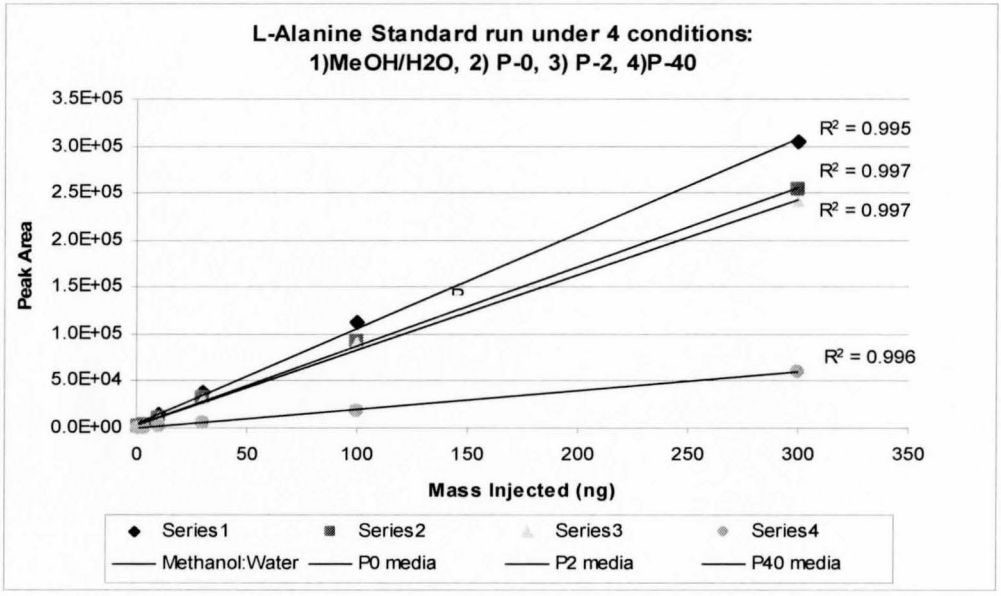

Figure 1: Calibration curve for a standard solution of L-alanine by LC-MS/MS.

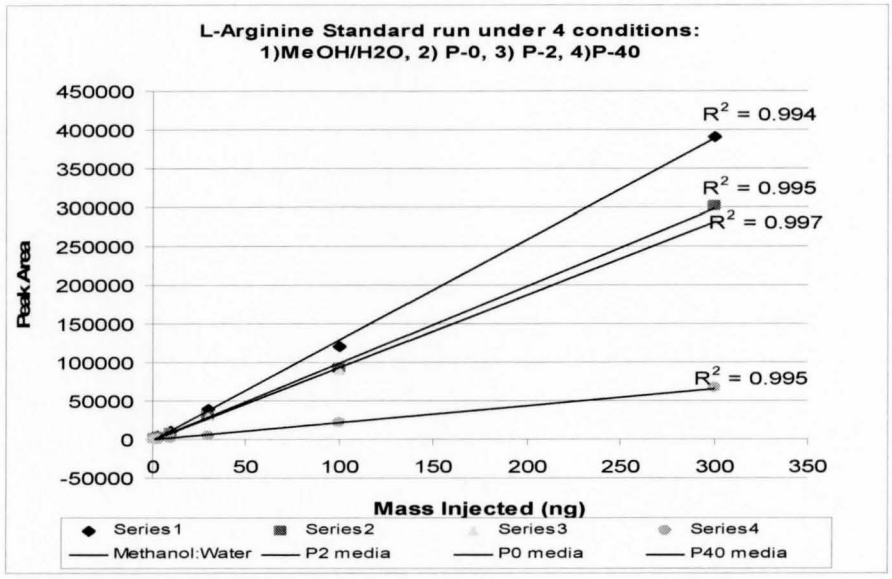

Figure 2: Calibration curve for a standard solution of L-arginine by LC-MS/MS.

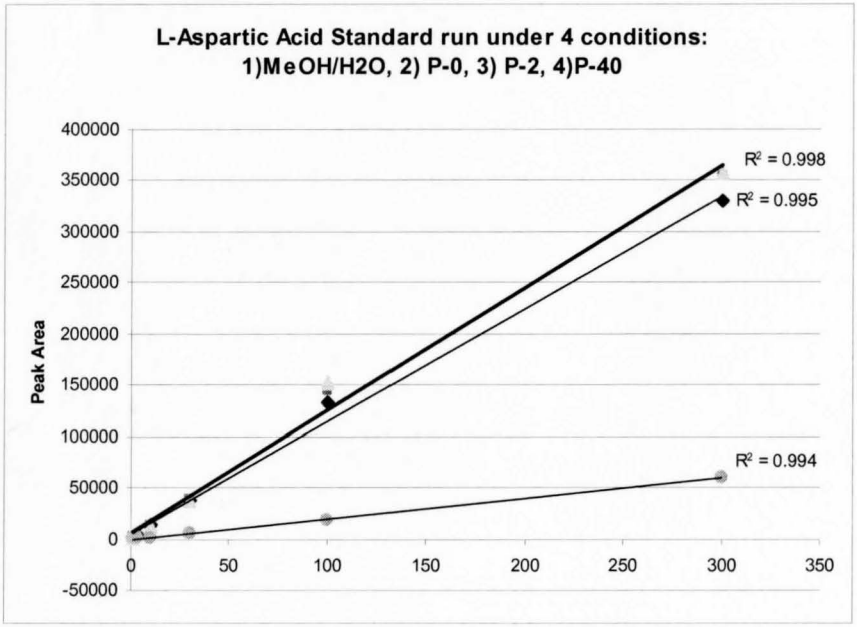

Figure 3: Calibration curve for a standard solution of L-aspartic acid by LC-MS/MS.

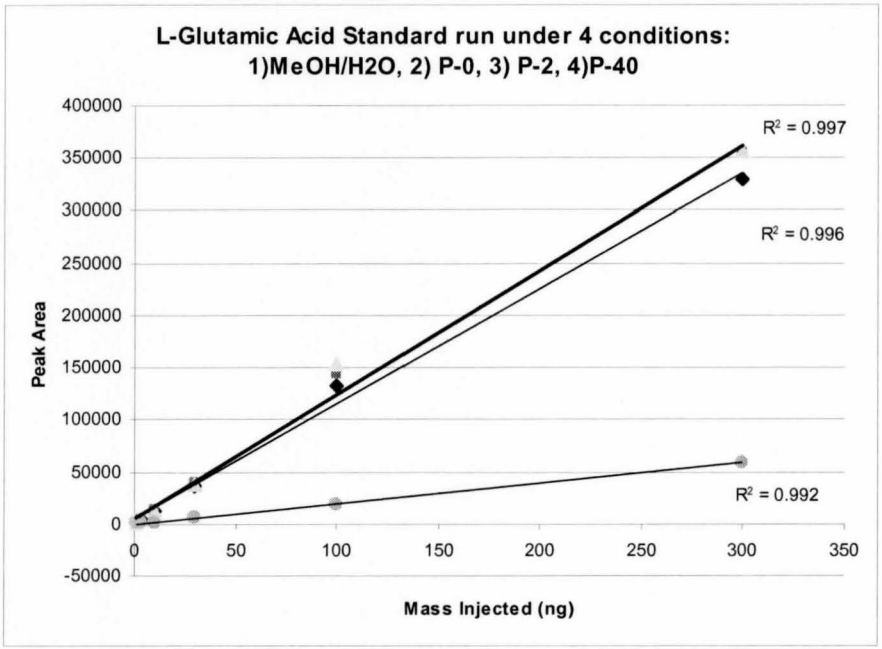

Figure 4: Calibration curve for a standard solution of L-glutamic acid by LC-MS/MS.

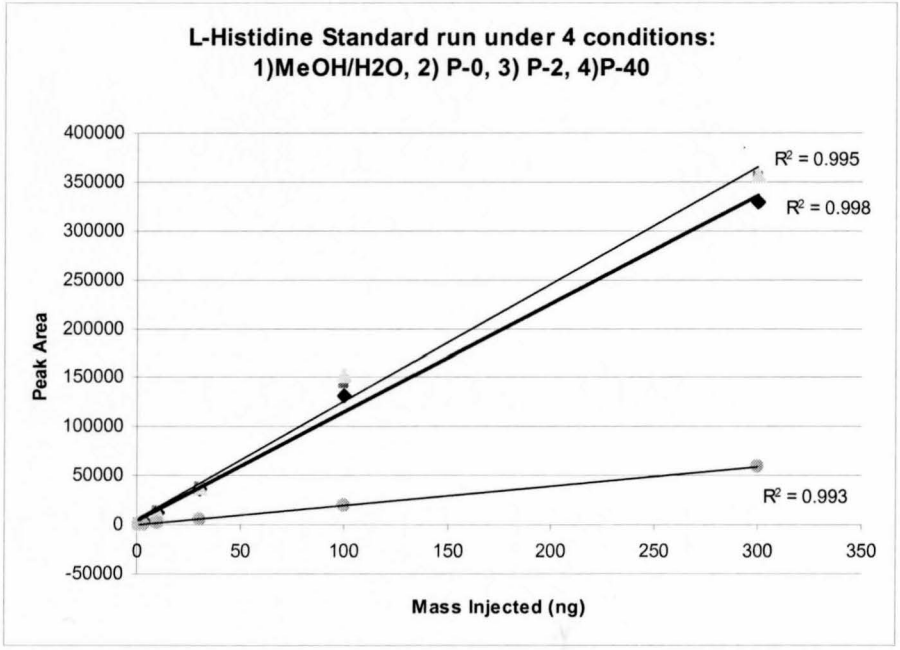

Figure 5: Calibration curve for a standard solution of L- histidine by LC-MS/MS.

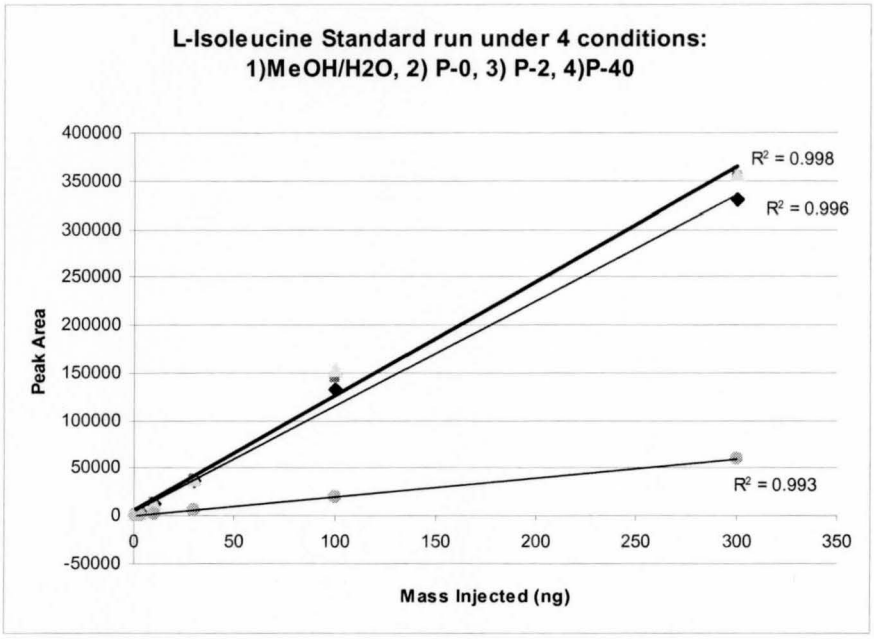

Figure 6: Calibration curve for a standard solution of L-isoleucine by LC-MS/MS.

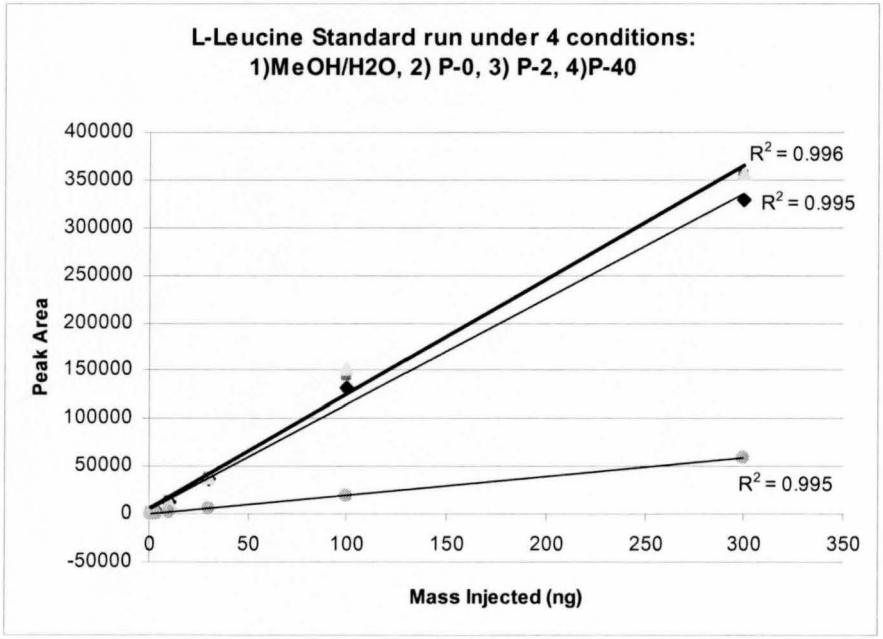

Figure 7: Calibration curve for a standard solution of L-leucine by LC-MS/MS.

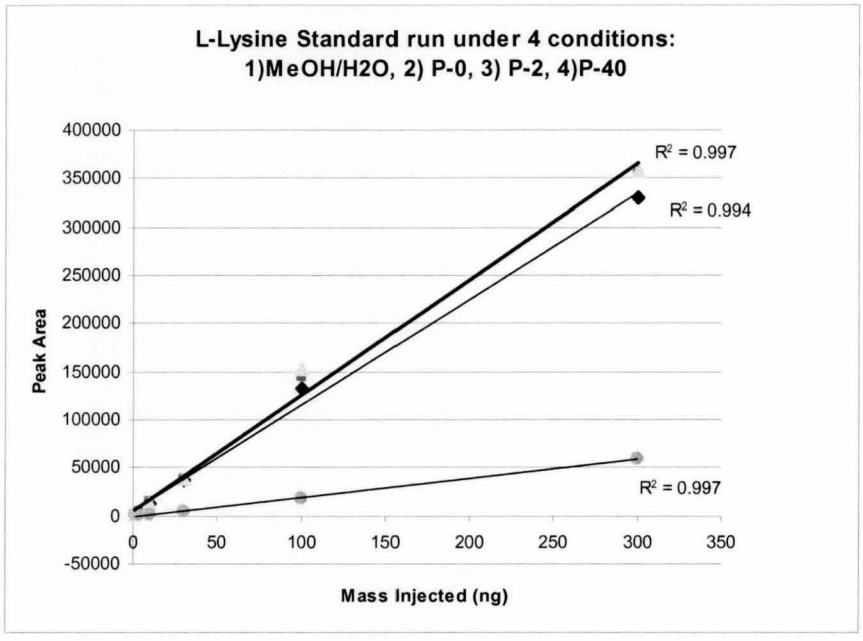

Figure 8: Calibration curve for a standard solution of L-lysine by LC-MS/MS.

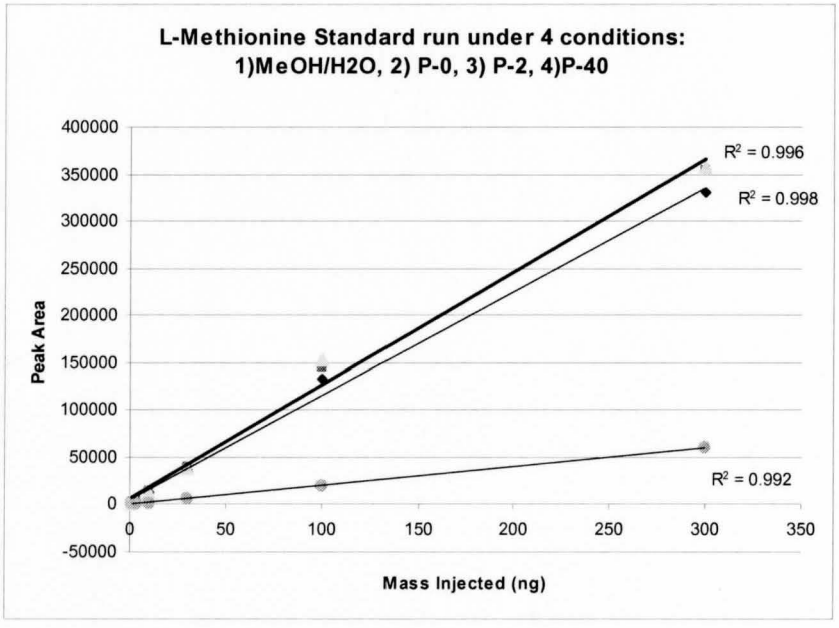

Figure 9: Calibration curve for a standard solution of L-methionine by LC-MS/MS.

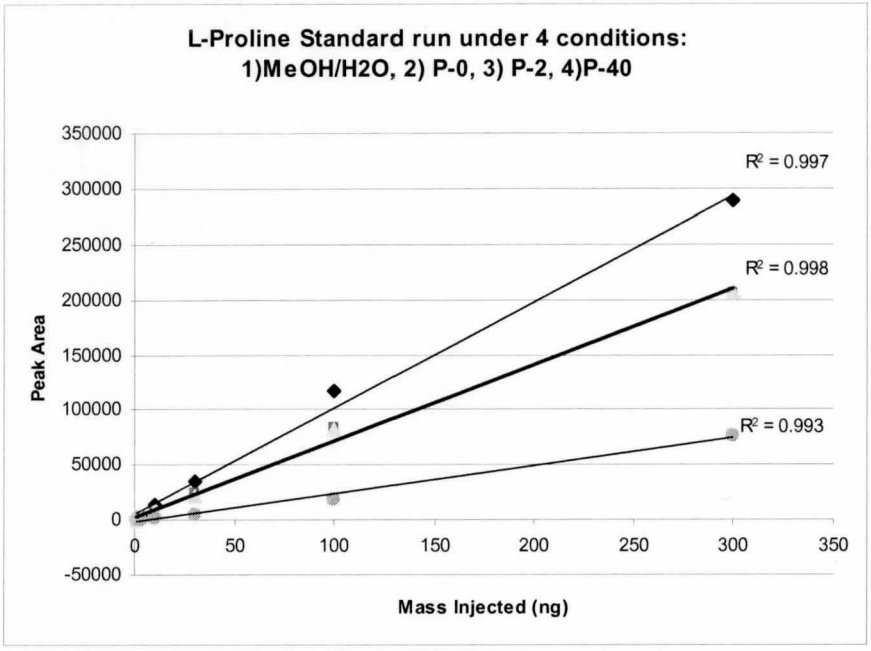

Figure 10: Calibration curve for a standard solution of L-proline by LC-MS/MS.

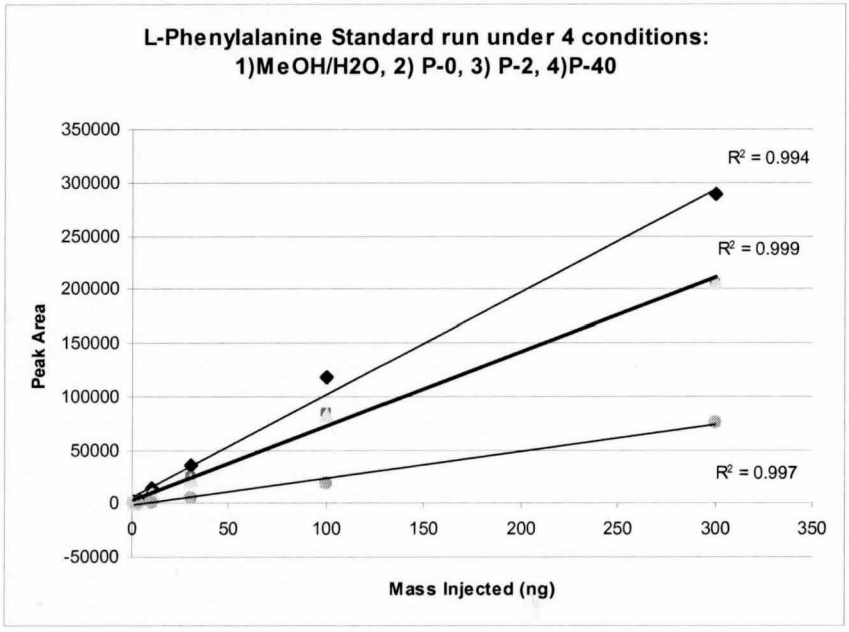

Figure 11: Calibration curve for a standard solution of L-phenylalanine by LC-MS/MS.

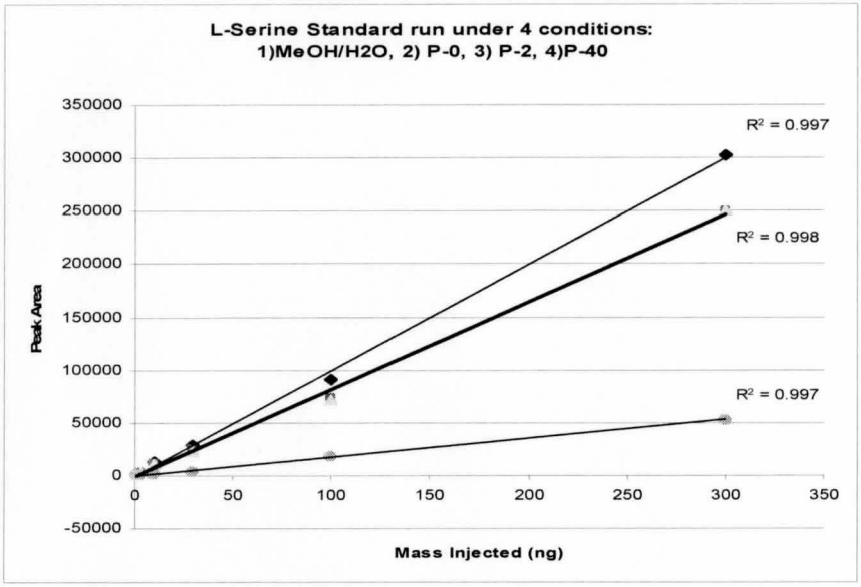

Figure 12: Calibration curve for a standard solution of L-serine by LC-MS/MS.

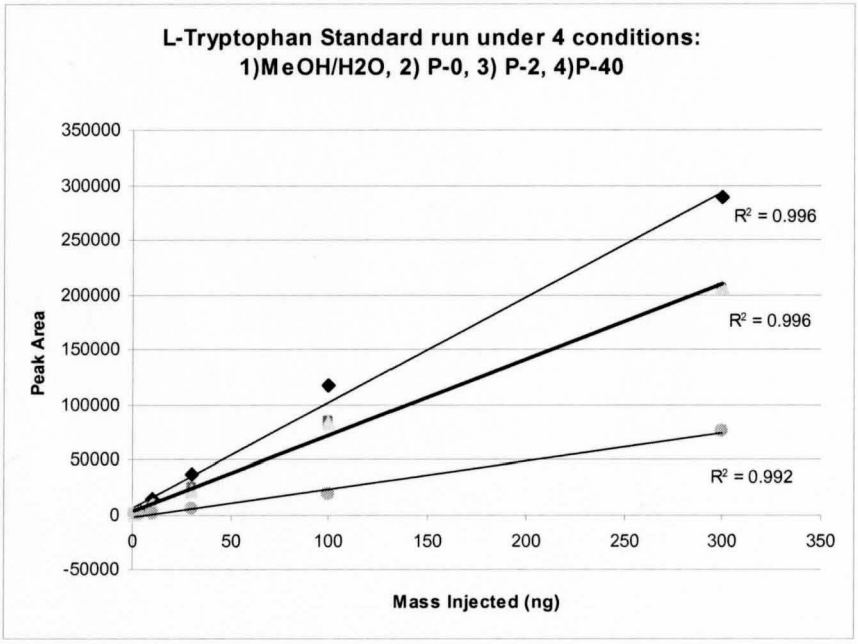

Figure 13: Calibration curve for a standard solution of L-tryptophan by LC-MS/MS.

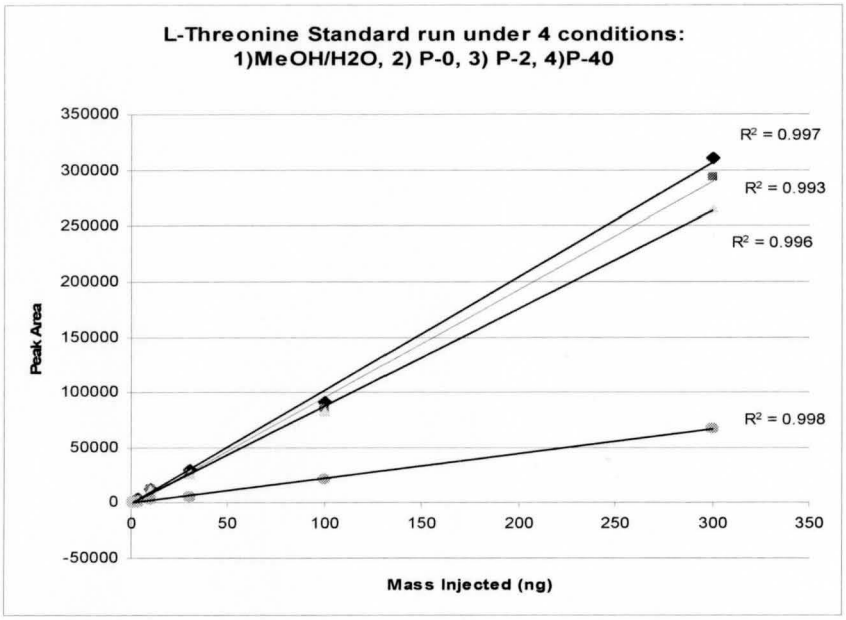

Figure 14: Calibration curve for a standard solution of L-threonine by LC-MS/MS.

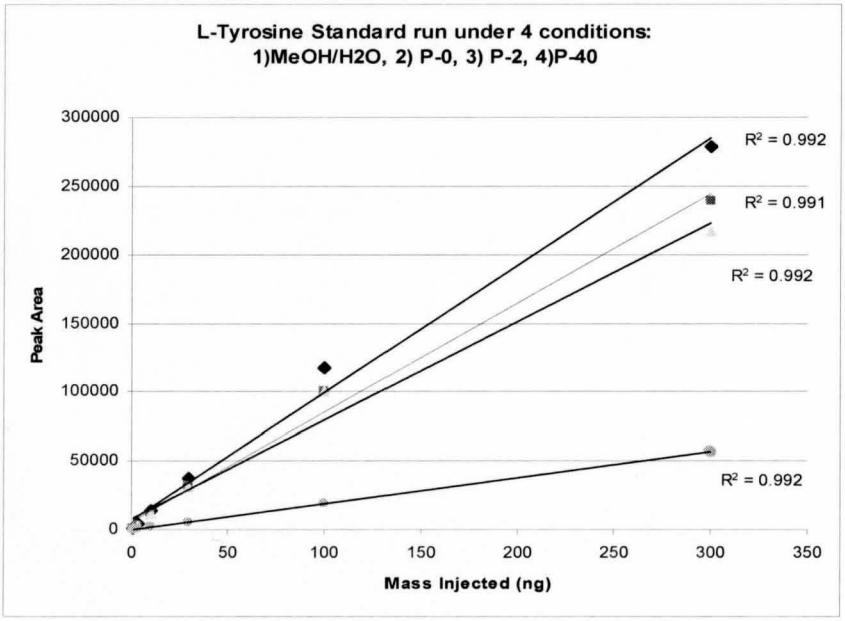

Figure 15: Calibration curve for a standard solution of L-tyrosine by LC-MS/MS.

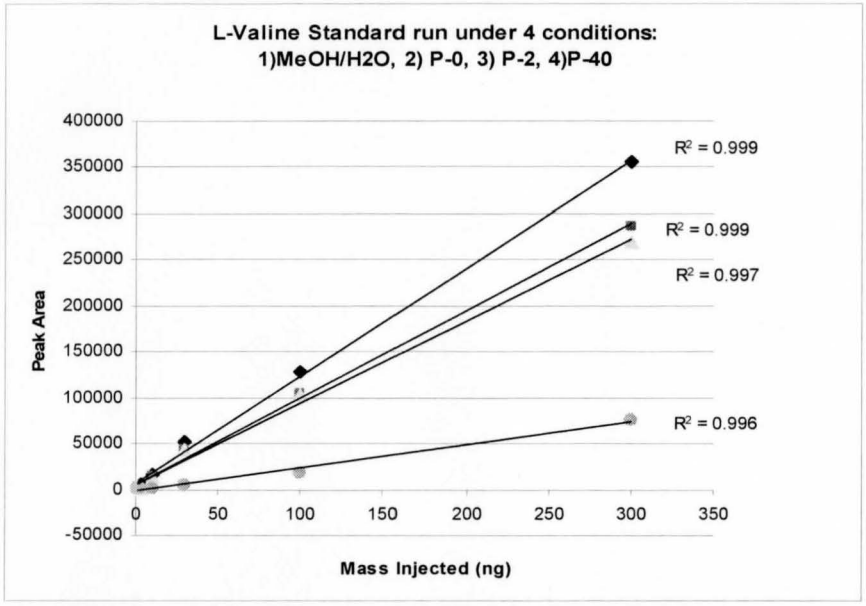

Figure 16: Calibration curve for a standard solution of L-valine by LC-MS/MS.